Transcription Factor Modulation in T-Cells to Improve Cancer Immunotherapy

Alec Baker Wilkens

A dissertation

submitted in partial fulfillment of the

requirements for the degree of

Doctor of Philosophy

University of Washington

2022

Reading Committee:

Stanley Riddell, Chair

Shivani Srivastava

Jarrod Dudakov

Program Authorized to Offer Degree:

Molecular and Cellular Biology

University of Washington

Abstract

Transcription Factor Modulation in T-Cells to Improve Cancer Immunotherapy

Alec Baker Wilkens

Chair of the Supervisory Committee:

Stanley Riddell

Department of Molecular and Cellular Biology

Adoptive transfer of T-cells expressing chimeric antigen receptors (CAR-T) effectively treats refractory hematologic malignancies in a subset of patients, but can be limited by the inability of *ex vivo* culture systems to expand T-cells sufficiently for effective dosing while producing highly active T-cell products. Less-differentiated T-cell states correlate with CAR-T capacity to proliferate and mediate anti-tumor responses *in vivo*, but signals induced by antigen stimulation and IL-2 supplementation during tumor-specific T-cell culture couple proliferation to differentiation, creating an inverse relationship between *ex vivo* expansion and anti-tumor fitness. Accordingly, interventions during culture that enhance T-cell potency and/or uncouple T-cell proliferation from loss of activity are of high clinical value. We investigated whether modulation of the activity of two transcription factors, NOTCH and the aryl hydrocarbon receptor (AhR), during CAR-T production could enhance immunotherapy efficacy.

NOTCH signaling controls both stem cell self-renewal and cellular differentiation across diverse tissues. NOTCH1 agonism restricted the differentiation of CAR-T derived from naïve

CD4+ T-cells, and upregulated expression of AhR and c-MAF, driving heightened production of IL-22, IL-10 and Granzyme B upon tumor encounter. NOTCH1-agonized CD4+ CAR-T demonstrated enhanced antigen responsiveness and proliferated to strikingly higher frequencies in mice bearing human lymphoma xenografts. NOTCH1-agonized CD4+ CAR-T also provided superior help to co-transferred CD8+ CAR-T, driving improved expansion and curative anti-tumor responses *in vivo* at low CAR-T doses.

AhR is a ligand-activated transcription factor upregulated in response to TCR ligation, and IL-2 signaling induces AhR-mediated upregulation of coinhibitory receptors and attenuation of cytokine production. AhR also participates in regulatory T-cell function and can limit autocrine IL-2 production. Independently of NOTCH1 agonism, AhR was expressed in T-cells under culture conditions conducive to efficient CAR-T production. AhRi culture induced strong autocrine IL-2 production, driving enhanced T-cell expansion even in absence of supplemental IL-2. However, AhRi-expanded T-cells did not display phenotypic evidence of expansion-associated differentiation, and proliferated robustly and produced elevated levels of T_H1/T_C1-associated cytokines upon *in vitro* restimulation with tumor. AhRi CAR-T further mediated superior tumor control in mice bearing human lymphoma xenografts.

Our data expand the mechanisms by which NOTCH can shape CD4+ T-cell behavior, and demonstrate that inducing NOTCH1 signaling during activation *ex vivo* is a viable strategy for enhancing the function of T-cells engineered with tumor-targeting receptors. Our findings also indicate that AhR activity constitutes a critical autoregulatory axis in human T-cells, and identify AhR inhibition during tumor-specific T-cell manufacturing as an easily-translatable strategy to improve both cell product yields and anti-tumor function. This work shows that modulation of transcription factor activity during *ex vivo* T-cell culture constitutes a valuable and efficacious strategy for enhancing cancer immunotherapy potency.

Table of Contents

List of Figures	6
List of Supplemental Tables	7
Acknowledgements	8
Chapter 1: Introduction	9
Chapter 2: NOTCH1 signaling alters differentiation and enhances antigen responses of CD4+ chimeric antigen receptor T cells	25
Chapter 3: *Ex vivo* inhibition of the aryl hydrocarbon receptor enhances production of chimeric antigen receptor T-cells exhibiting potent anti-tumor activity	55
Chapter 4: Concluding Remarks	85
Bibliography	91

List of Figures

1.1	TCR and CAR Structure	11
1.2	CAR-T production	12
1.3	Progressive T-cell differentiation	13
1.4	Modulation of activation-related pathways to attenuate T-cell differentiation	15
1.5	Physiologic CD4+ T-cell polarization	17
1.6	*Ex vivo* CD4+ T-cell polarization	18
1.7	Roles of NOTCH signaling	20
1.8	AhR signaling	22
1.9	Roles of AhR signaling	24
2.1	NOTCH1 agonism during CD4+ T_N activation results in a less-differentiated phenotype	33
2.2	NOTCH1 agonism during CD4+ T_N activation results in a less-differentiated transcriptome	34
2.3	Effects of NOTCH1 agonism during CD4+ T_{MEM} activation	35
2.4	NOTCH1 agonism alters cytokine production of CAR-T derived from CD4+ T_N	37
2.5	NOTCH1 agonism induces AhR and c-MAF activity	38
2.6	NOTCH1 agonism programs cytokine production via AhR	39
2.7	NOTCH1 agonism programs cytokine production via c-MAF	41
2.8	N1 CD4+ CAR-T proliferate more than control CD4+ CAR-T in response to CD19+ tumor	43
2.9	NOTCH1 agonism enhances CD4+ CAR-T proliferation and cytokine production in response to antigen	44
2.10	N1 CD4+ T-cells are more responsive to TCR ligation	46
2.11	NOTCH1 agonism enhances CD4+ CAR-T proliferation in mice bearing lymphoma xenografts	47
2.12	N1 CD4+ CAR-T strongly express proliferation- and T_H1-associated genes *in vivo*	49
2.13	N1 CD4+ CAR-T enhance CD8+ CAR-T proliferation and anti-tumor efficacy	51
3.1	AhR controls gene expression following T-cell activation	62
3.2	Gene sets controlled by AhR following T-cell activation	64
3.3	AhR inhibition enhances T-cell proliferation during *ex vivo* culture	65
3.4	AhR inhibition during T-cell culture preserves early T_{MEM} phenotypes	66
3.5	AhR inhibition alters IL-2 production and signaling kinetics in naïve T-cells	69
3.6	AhR inhibition alters IL-2 production and signaling kinetics in bulk T-cells	71
3.7	AhR inhibition supports robust bulk T-cell expansion in absence of exogenous IL-2	72
3.8	AhR inhibition augments T_H1 and T_C1 cytokine production by T_N-derived CAR-T	74
3.9	AhR inhibition does not substantially alter T_{MEM}-derived CAR-T cytokine production	76
3.10	AhR inhibition promotes robust CAR-T proliferation following antigen stimulation	78
3.11	AhRi CAR-T mediate potent anti-tumor effects	80

List of Supplemental Tables

1 Day 11 N1 and control CD4+ CAR-T gene expression

2 Day 3 N1 and control CD4+ CAR-T gene expression

3 +24hr restimulated N1 and control CD4+ CAR-T gene expression

4 Hallmark gene set enrichment analysis of +24hr restimulated N1 and control CD4+ CAR-T gene expression

5 N1 and control CD4+ CAR-T gene expression 8 days post-transfer into lymphoma-bearing NSG mice

6 Hallmark gene set enrichment analysis of N1 and control CD4+ CAR-T gene expression 8 days post-transfer into lymphoma-bearing NSG mice

7 Day 3 AhRi and control CD4+ CAR-T gene expression

8 Day 3 AhRi and control CD8+ CAR-T gene expression

Acknowledgments

Thank you to the current and past members of the Riddell lab, who are an uncommonly high-quality group of people and have made graduate school a hugely rewarding experience: Alex, for welcoming me to the lab and happily providing extensive support / Margot, for including me in the NOTCH project and teaching me about technique and experimental design / Gabby, for the hottest gossip and great friendship / Michelle, for your cheerfulness, helpfulness and hard work to keep us functioning / Isabel, for countless lab corner conversations and talking through ideas / Carla, for willingness to teach me techniques and puzzle over T-cell differentiation together / Yun, for sharing lab knowledge and cat enthusiasm / Sylvain, for your endless good nature and the late-night conversations / Bugos, for your general sanity, good humor and generously-shared blotting mastery / Anusha, for keeping me going with promises of tamarind rice at graduation / Rachel, for the smooth jams and excellent vibes / Tamer, for the weekend companionship and blink-hellos / Sylvia, for your skillful experimental help and hard work / Tommy, for the indelible image of Kiss running flow / Shivani, for your immense competence and patient mentoring / Josh, for the politics, memes, medicine and CD4+ arcana / Naina, for TC chats and your steadfast enthusiasm for science / Julia, for late-shift commiseration and consistent hilarity / Elena, for being my right hand, left hand and often my brain / Stan, for seeing that I didn't know how to do anything four years ago, taking me on anyway and teaching me how to be a good scientist.

Thank you to Matt and Irv for your efforts toward and enthusiasm for the NOTCH project, and for helping me learn to appreciate the vastness of the subject, and to Scott for the NOTCH and AhRi discussions, informatics help and helping me turn data around quickly. Many thanks to the Fred Hutch Flow Cytometry, Immune Monitoring, Genomics and CCEH cores, without whom I would have taken immeasurably longer to graduate.

Thank you to Nick for being a friend, a mentor, and equally helpful when trying to think or not think about science; to Patrick and Chris for your friendship and telling me to go outside; and to my parents and Claire, for raising me to work hard while reminding me that life is bigger than work.

Chapter 1

Introduction

Chimeric antigen receptor T-cell therapy for cancer

Cancer immunotherapy, the rapidly developing "fourth pillar" of cancer treatment, is predicated on the ability of immune cells to recognize tumor cells on the basis of differential protein expression or protein fragment presentation. In many cases, tumors can be distinguished from healthy tissues in the human body this way: cells recycle their proteins via proteasomal digestion and present peptide antigens on their surfaces via MHC molecules, permitting T-cell receptor (TCR) surveillance of their proteome for mutations acquired during oncogenesis that create foreign-appearing neoantigens, or aberrant expression of developmentally- or spatially-restricted proteins. Recognition of cognate peptide antigen leads to T-cell activation and killing of the tumor cell[1,2]. While T-cells' ability to specifically kill tumors expressing their cognate antigens has long held clinical promise, therapeutic efficacy has been limited by tumors' capacity to disrupt MHC antigen presentation[3,4], rendering cancer invisible to T-cells, and by the lack of costimulatory molecule expression on tumors that T-cells require to fully activate and mount an effective immune response[5].

To circumvent these barriers, chimeric antigen receptors (CARs) were developed: synthetic molecules featuring extracellular antigen recognition domains linked to intracellular T-cell receptor (CD3ζ) and costimulatory molecule (4-1BB, CD28, OX40, CD27, ICOS, etc) signaling machinery that enable T-cells to directly sense intact proteins expressed on tumor cell surfaces without need for MHC-assisted peptide presentation or separate cell-extrinsic costimulation[6]. The design of these CARs enables sensing of tumor cells based on differential protein expression and provides sufficient stimulation to activate T-cells, induce direct killing of the targeted tumor cell, and spur T-cell proliferation and cytokine production critical for amplifying the anti-tumor immune response.

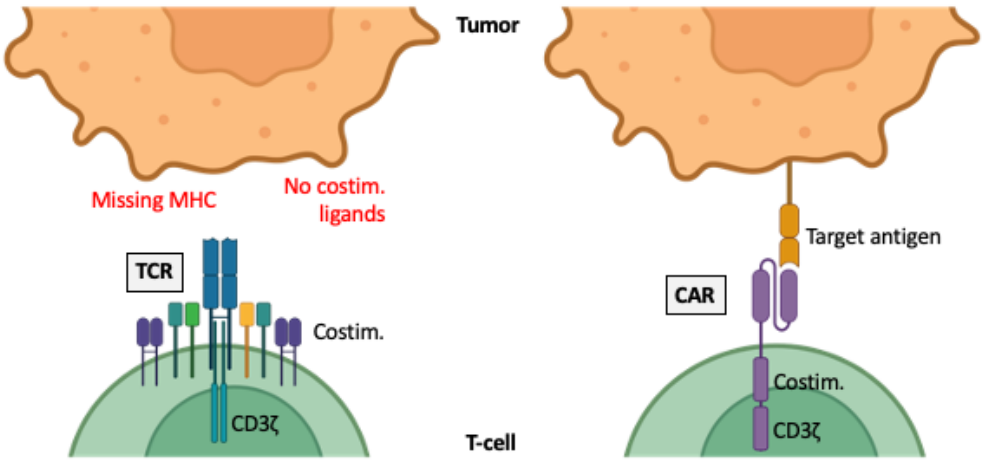

Figure 1.1. TCR and CAR Structure
TCRs (left) rely on MHC antigen presentation and costimulatory ligands to induce maximal function, while CARs (right) can elicit robust immune responses through direct target protein recognition.

The first clinical successes of this treatment modality were achieved in 2011, when B-cell malignancies were treated with CAR-T targeting the surface molecule CD19[7–9], and clinical trials using CAR-T to treat diverse hematologic cancers have rapidly expanded since[10–18]. Though significantly higher barriers confront CAR-T therapy in solid tumors, which can fail to clearly differentiate themselves by protein expression from healthy tissue, physically exclude T-cells, and generate immunosuppressive microenvironments that impair CAR-T function[2], the early successes of synthetic antigen receptor T-cell immunotherapy in hematologic malignancies represent a monumental step forward in cancer treatment and offer a strong platform from which to build.

To produce CAR-T for cancer immunotherapy, patient T-cells are obtained by leukapheresis, activated *ex vivo* (generally by ligation of CD3 and CD28 in the presence of exogenous IL-2, IL-7 and/or IL-15), transduced with lenti- or retroviral constructs encoding a CAR, expanded to high numbers, and then transfused back into patients[2,6]. However, therapeutic efficacy can be compromised if CAR-T fail to expand to sufficient dose numbers *ex vivo* or are unable to subsequently proliferate, persist or mediate effector functions *in vivo* [7,9,19–23]. Thus, understanding how to effectively produce CAR-T products and developing methods of programming efficacious behavior into CAR-T are of critical clinical importance.

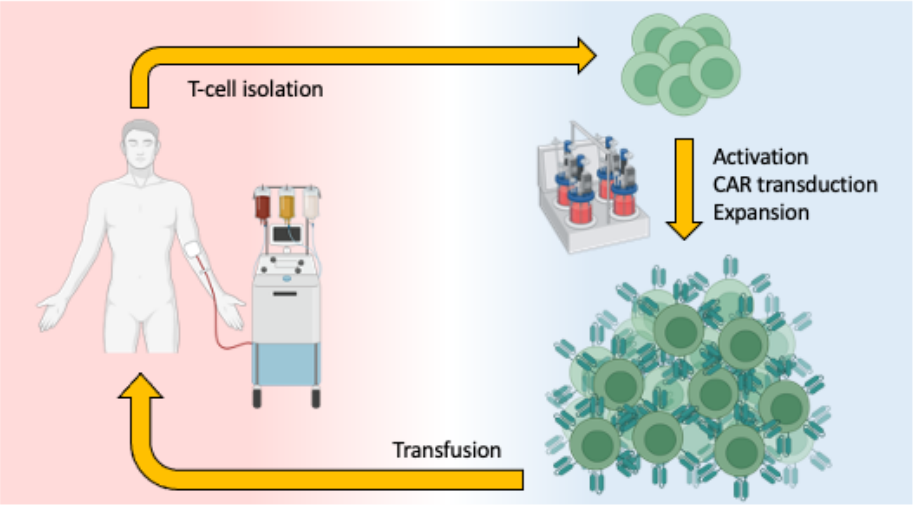

Figure 1.2. CAR-T production
CAR-T are produced from endogenous patient T-cells via activation, viral transduction and expansion.

Relationship between T-cell differentiation state and CAR-T therapeutic efficacy

Mature antigen-inexperienced naïve T-cells (T_N) develop from lymphocyte precursor cells in the thymus, and upon recognition of cognate antigen presented by antigen-presenting cells (APCs), activate, proliferate, and undergo differentiation that allows them to effectively respond to infection. Effector T-cells (T_{EFF}) expand to high frequencies during infection and produce abundant cytotoxic molecules that kill infected cells and pathogens but rapidly contract following clearance of inflammatory stimuli, while memory T-cells (T_{MEM}) survive in circulation and tissues after the resolution of infection and are capable of rapidly mounting new effector responses upon subsequent encounters with their cognate antigens[24]. Because T_N and T_{MEM} persist in the blood at steady state, these cells comprise the starting materials for CAR-T products.

While different models seek to explain how T_{EFF} and T_{MEM} develop from T_N, as well as whether and when these subsets can differentiate into each other[24–27], clear functional evidence supports a model of progressive T_{MEM} differentiation driven by antigen exposure, in which T_{MEM} gradually lose their capacities for lymphoid tissue homing, antigen-independent persistence and proliferation upon restimulation, and gradually gain cytotoxicity and effector functions[28,29]. These functional qualities correlate with patterns of surface protein expression

collectively termed “phenotype,” which can reciprocally be used to define T_{MEM} subsets that exhibit marked behavioral differences. For example, the most minimally-differentiated T_{MEM} subset, known as stem cell memory (T_{SCM}) and defined as CD45RA+ CD45RO- CD62L+ CCR7+ CD27+ CD28+ CD95+, exhibits stronger proliferative potential and weaker cytokine production capacity than more-differentiated central memory (T_{CM}) cells (CD45RA- CD45RO+ CD62L+ CCR7+ CD27+ CD28+ CD95+), which proliferate more and make less cytokine than more-differentiated effector memory (T_{EM}) cells (CD45RA- CD45RO+ CD62L- CCR7- CD27± CD28± CD95+)[29].

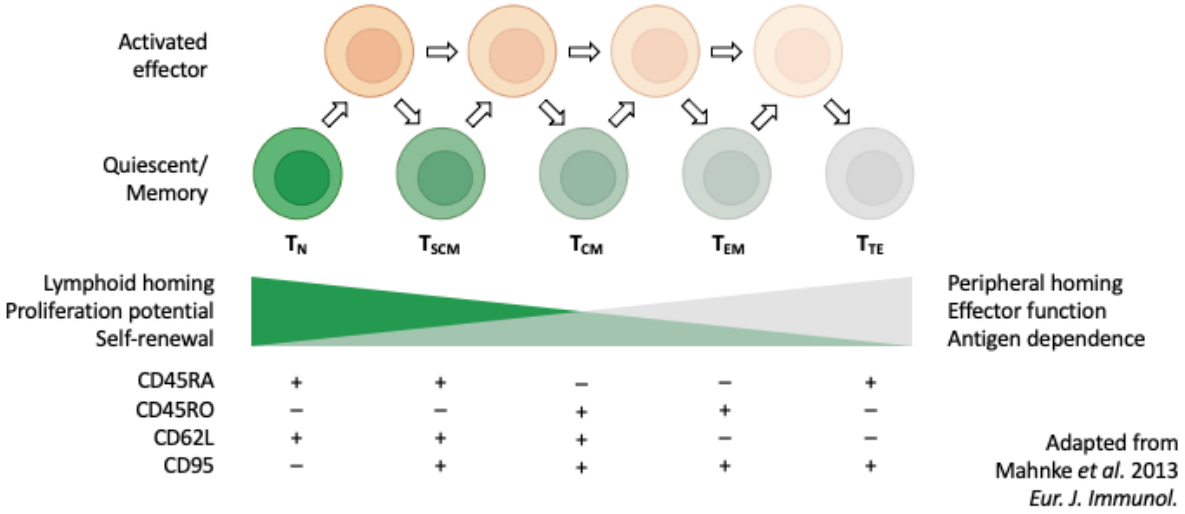

Figure 1.3. Progressive T-cell differentiation
T_{MEM} behavior and phenotype change in a correlated fashion as antigen exposure drives T-cell differentiation.

The differences between these subsets take on critical importance in cancer immunotherapy, as CAR-T anti-tumor activity correlates with the differentiation state of both the T-cells used to generate the CAR-T product and the CAR-T product administered. Adoptive transfer of T_N- and T_{CM}-derived human CD19-specific CAR-T into lymphoma-bearing NSG mice prolonged survival compared to T_{EM}-derived CAR-T[30], as did transfer of tumor-specific human CD8+ T-cells expressing a T_{SCM} phenotype into tumor-bearing mice compared to transfer of T_{CM} or T_{EM}[29]. These studies identified T_N and less-differentiated T_{MEM} as ideal substrates for producing effective CAR-T products.

Unfortunately, thymic involution with aging reduces T_N production, and prior chemotherapy often skews cancer patients' T-cells toward a more-differentiated T_{EM} phenotype[31–35]. Compounding this issue is further differentiation induced in T-cells by the stimulations and cytokines used to promote efficient transduction and T-cell expansion during the *ex vivo* culture process of making CAR-T[36]. These issues have prompted investigation into how T-cells might be cultured or engineered to differentiate less or otherwise retain function during *ex vivo* culture.

Cell culture regimens to enhance T-cell anti-tumor efficacy

T-cell studies have identified a wide variety of signaling pathways that activate downstream of TCR ligation and are crucial for the development of effector function, as well as regulatory pathways that maintain cellular quiescence and are silenced during T-cell activation to permit proliferation and effector responses. TCR signaling, CD28 ligation and IL-2 signaling can all activate phosphoinositide-3-kinase (PI3K), which generates PIP_3 from PIP_2 and leads to activation of AKT, which in turn drives mTORC1 to engage cell cycle, growth and survival pathways critical for T_{EFF} function[37]. Strong and prolonged activation of the PI3K-AKT pathway can drive T-cell differentiation, and conversely, inhibition of either of these two pathway members during T-cell culture has been found to preserve stem-like characteristics and produce more highly-active T-cell immunotherapy products[38–41]. Similarly, CRISPR screening of kinases active in T-cells following TCR stimulation identified P38 kinase as a target that, when pharmacologically inhibited during T-cell culture, enhanced T-cell proliferation while maintaining a memory phenotype and promoted effective anti-tumor responses upon transfer into tumor-bearing mice[42].

Conversely, studies in hematopoietic stem cells identified the Wnt signaling pathway as a key regulator of cellular proliferation and differentiation. Further investigation found that Wnt promoted a similar dynamic of memory conservation over effector differentiation in T-cells, and that T-cells expressing an early memory phenotype and exhibiting superior anti-tumor activity could be generated by activation of the Wnt signaling pathway during T-cell culture[43].

Downstream of the early transducers of activation signals, T-cells undergo numerous metabolic changes, including a transition to aerobic glycolysis, glutaminolysis, and mitochondrial biogenesis to support enhanced oxidative phosphorylation that enables rapid growth and proliferation[44]. Interventions that interfere with these bioenergetic changes (via inhibition of glycolysis[45] or enforcement of mitochondrial fusion[46]) have been reported to maintain early T_{MEM} phenotypes and improve T-cell anti-tumor function. Metabolic changes can be externally imposed as well: following the observation that tumor-infiltrating lymphocytes (TILs) can be arrested in stem-like states by high-K+ tumor microenvironments, it was found that culturing T-cells in high concentrations of extracellular K+ could induce T-cell autophagy, restrict differentiation and improve subsequent anti-tumor activity[47].

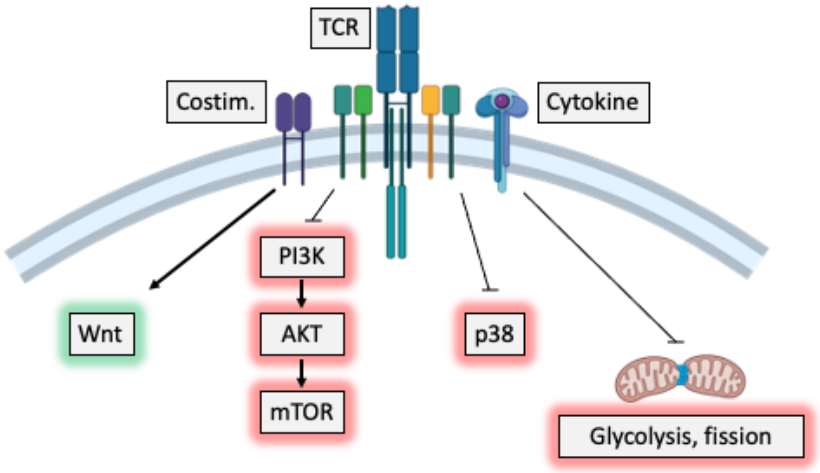

Figure 1.4. Modulation of activation-related pathways to attenuate T-cell differentiation
Activation of quiescence-associated pathways, inhibition of effector-associated pathways and restriction of effector-associated metabolic changes have all been shown to preserve early memory qualities and enhance T-cell immunotherapy.

Thus, cell culture interventions that accentuate features of quiescent T_{MEM} or attenuate cellular processes required for the development of T_{EFF} characteristics can be leveraged to improve T-cell anti-tumor activity by attenuating differentiation. Predictably, some of these strategies impair T-cell proliferation, working against the need to expand large numbers of T-cells *ex vivo* for effective dosing[29,48–50] and highlighting the need for additional strategies that support T-cell growth.

T-cells require signals through the TCR, costimulatory receptors and cytokine receptors to survive activation and proliferate robustly[51,52]. The cytokine IL-2 is commonly used to expand T-cells during CAR-T production due to its strong proliferation-inducing effects, but can also promote effector differentiation[36,53–57]. Use of other supportive cytokines that also signal through the common γ chain CD132 has achieved encouraging results: CD19-specific CAR-T produced with IL-7 and IL-15 displayed a less-differentiated memory phenotype compared to IL-2-expanded cells[58], and IL-15 culture enhanced CAR-T activity[59]. Similar results have been obtained using IL-21, which was reported to maintain early T_{MEM} phenotypes and improve anti-tumor activity[57,60,61]. While IL-2 remains a useful tool for expanding T-cells to large numbers for adoptive transfer, these encouraging results from alternative common γ chain cytokines indicate they can play helpful supportive roles in culture systems intended to produce minimally-differentiated T-cells.

CD4+ T-cell polarization in normal physiology and cancer immunotherapy

A completely distinct strategy for improving T-cell activity lies in polarization of CD4+ T-cells. Polarization is the process by which CD4+ T-cells adopt stereotyped expression patterns of transcription factors, chemokine receptors, cytokines and other effector molecules in response to signals from APCs in order to tailor their subsequent activity to most effectively combat the class of pathogen first sensed by the APC. When APCs detect pathogen invasion by sensing conserved molecular alarm signals, they migrate from sites of infection to lymph nodes, where they present pathogen-specific antigens and express costimulatory ligands and cytokines. CD4+ T_N integrate TCR, costimulatory and cytokine signals from these APCs to gauge the class of pathogen that activated the APC, and accordingly begin to differentiate, or polarize, into any of several distinct helper (T_H) identities[62].

Cytokine signals in particular drive T_H polarization: interferon-γ (IFNγ) and IL-12 signal through STAT1 and STAT4 to induce the subset-defining transcription factor (TF) T-bet and promote T_H1 polarization, IL-4 signals through STAT6 to induce GATA-3 and promote T_H2 differentiation, and IL-6 and TGFβ signal through STAT3 and SMAD3 to promote RORγt expression and T_H17 differentiation[63]. These distinct CD4+ T_H subsets go on to organize very

different immune responses: T_H1 cells produce abundant IFNγ, which activates phagocyte killing of ingested pathogens and drives CD8+ T-cell-dependent killing of intracellularly infected cells by upregulating antigen presentation; T_H2 cells produce IL-4, IL-5 and IL-13, which recruit and activate eosinophils, mast cells and plasma cells to promote mucosal barrier immunity against parasites; and T_H17 cells produce IL-17, which induces epithelial and stromal cells to recruit neutrophils to sites of bacterial and fungal invasion. T_H9 cells comprise a distinct subset induced by IL-4 and TGFβ, which drive PU.1 expression, anti-parasite immunity and allergic responses[62].

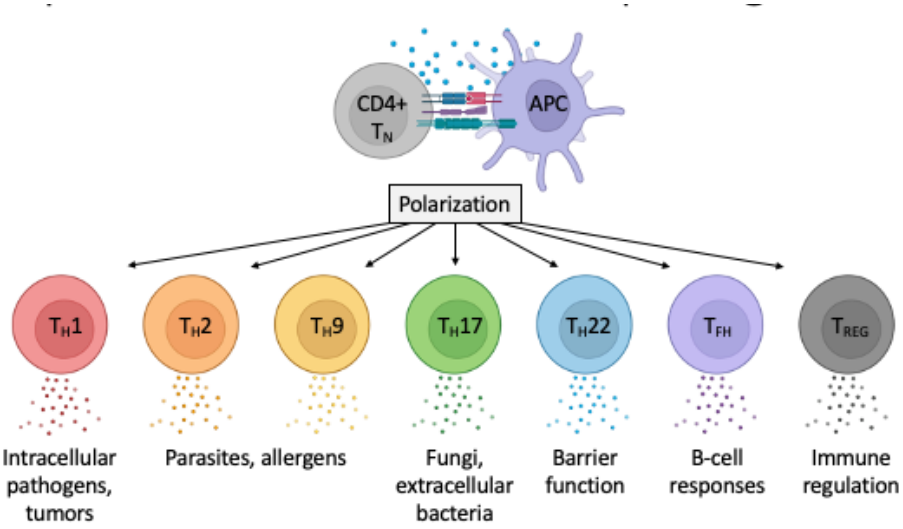

Figure 1.5. Physiologic CD4+ T-cell polarization
Naïve CD4+ T-cells can adopt stereotyped transcriptional and functional states in response to signals delivered by priming and inflammation to effectively respond to immune stimuli.

Activating CD4+ T_N in the presence of these polarizing cytokines (and/or neutralizing monoclonal antibodies [mAbs] against competing cytokine signals) can impart many of the distinct functional qualities of T_H subsets. Given that a primary mechanism of anti-tumor immunity is CD8+ T-cell recognition of mutated tumor cell antigens[64], effective CD4+ T-cell immunotherapy products should be able to efficiently promote CD8+ T-cell responses *in vivo*, and it was assumed that polarizing tumor-specific CD4+ T-cells toward a T_H1 phenotype during *ex vivo* culture would help impart this behavior. However, culture in IL-12 drives effector differentiation, and T_H1 polarization does not convincingly enhance T-cell anti-tumor immunity[65].

Intriguingly, polarization of CD4+ T-cells toward other T_H subsets has been shown to enhance anti-tumor efficacy. *Ex vivo* polarization of tumor-specific T-cells toward a T_H17 phenotype was shown to maintain stemness while efficiently expanding cells[66], and resulted in a T-cell product that mediated superior anti-tumor responses that were contingent on the acquisition of T_H1 function[67] and activation of CD8+ T-cells *in vivo*[68]. CD4+ T-cell polarization toward the T_H9 phenotype yielded similarly fascinating results, with T_H9 cells exhibiting long-lived effector features without evidence of enhanced activity in stemness-associated pathways, strong proliferative capabilities, and robust anti-tumor activity in absence of sustained T_H9 function, acquired T_H1 function or CD8+ T-cell interaction *in vivo*[69].

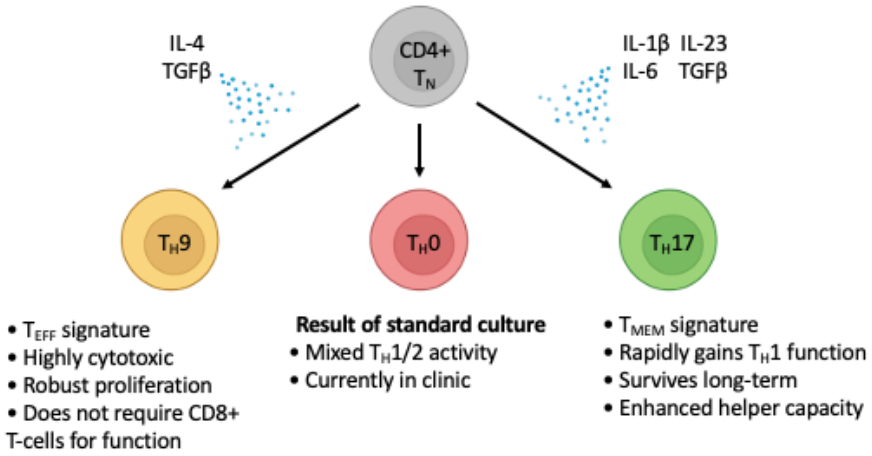

Figure 1.6. *Ex vivo* CD4+ T-cell polarization
T-cell polarization toward both T_H9 and T_H17 phenotypes has demonstrated to improve tumor-specific CD4+ T-cell efficacy in solid tumor models.

The study of these two CD4+ T_H subsets has demonstrated that restrictive cell culture interventions aimed at promoting T_{MEM} characteristics and attenuating the development of effector function are not the only viable strategy for enhancing tumor-specific T-cell efficacy: indeed, guiding T-cell differentiation toward particular cell states has yielded improvements in preclinical results just as impressive.

<u>NOTCH signaling in T-cell differentiation and stem cell quiescence</u>

The NOTCH signaling pathway lies at the nexus of cellular self-renewal and differentiation. The mammalian NOTCH family of surface receptors (NOTCH1, NOTCH2,

NOTCH3 and NOTCH4) can be engaged by ligands of the Delta-like (DLL1, DLL3, DLL4) and Jagged (Jagged1 and Jagged2) families. NOTCH signaling is triggered when ligands bind to NOTCH receptors, inducing conformational changes that enable proteolytic cleavage of the NOTCH intracellular domain (NICD) into the cytoplasm. The NICD translocates to the nucleus, where it regulates gene expression by assembling a transcriptional activator complex with the DNA-binding protein RBPJκ and MAML family proteins[70].

NOTCH signaling is critical for the differentiation of common lymphoid progenitors to T-cells in the thymus[71–73], but takes on a completely distinct role in mature T-cells, coordinating expression of effector genes in response to antigen stimulation. Murine T_N express low levels of NOTCH1 and NOTCH2 at rest, but rapidly upregulate expression of NOTCH1, NOTCH2 and NOTCH3 within 24hr of TCR ligation[74]. Activated APCs proffer NOTCH ligands during T-cell priming, engaging NOTCH receptors as T-cells express them and delivering NOTCH signal during activation.

NOTCH transcriptional activity is crucial for the differentiation of T_{EFF} from activated T_N: nearly half of genes upregulated in T_{EFF} compared to T_{MEM} depend on intact NOTCH signaling[75]. NOTCH enables secretion of key cytolytic molecules and cytokines by T_{EFF}[76–78], and immune responses to influenza virus, *listeria monocytogenes* and dendritic cell vaccination by T-cells lacking functional NOTCH1 and NOTCH2 exhibited marked reductions in T_{EFF} expansion[75,79]. In contrast, while NOTCH signaling has been demonstrated to support resting CD4+ T_{MEM} survival *in vivo*[80], the pathway is generally not required for the generation of T_{MEM} during immune responses[79].

NOTCH plays a similar role in CD4+ T_H immune responses: numerous studies document the requirement of NOTCH signaling for effective T_H1 responses to *leishmania major*[81,82] and in allogeneic bone marrow transplantation[83–85]; T_H2 responses to pulmonary allergens[86] and the parasite *trichuris muris*[87]; and T_H17 responses in experimental autoimmune disease[88–90]. Rather than imparting directionality to CD4+ T_H polarization (as was initially hypothesized), NOTCH has been shown in mechanistic studies to facilitate expression of distinct subset-defining transcription factors and cytokines that are further transcriptionally driven by polarizing cytokine signals[91].

In contrast to its role driving T_{EFF} differentiation from mature T_N, the NOTCH signaling pathway is also critical for stem cell self-renewal in many distinct tissues. NOTCH signaling inhibits hair follicle stem cell differentiation, and NOTCH1/NOTCH2-null mice lose hair due to excessive epidermal differentiation and disruption of follicle homeostasis[92–94]. NOTCH signaling induced in hematopoietic stem cells by trabecular bone osteoblasts and sinusoidal endothelial cells in the stem cell niche has similarly been shown to limit differentiation[95–99]. Intestinal stem and progenitor crypt cells rely on NOTCH signaling for maintenance; pharmacologic and genetic inhibition results in rapid differentiation into Goblet and endocrine cells incapable of further proliferation[100–103]. Neural stem cells also require NOTCH activity to maintain quiescence, and rapidly differentiate if it is interrupted[104–106]. Thus, the effects of NOTCH signaling are highly context-dependent, and the pathway can promote both differentiation and quiescence depending on the environment in which the signal is delivered.

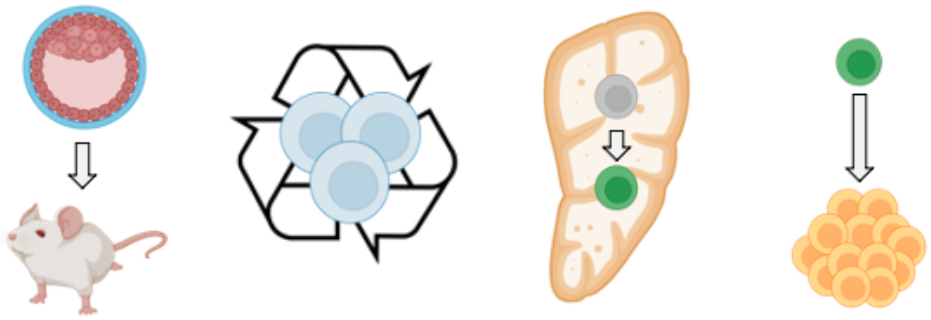

Figure 1.7. Roles of NOTCH signaling
NOTCH is essential for development and limb patterning, stem cell self-renewal, naïve T-cell generation from common lymphoid progenitors in the thymus, and T_{EFF} generation from T_N in response to activation.

<u>NOTCH signaling during tumor-specific T-cell culture</u>

The NOTCH pathway's roles in promoting both T_{EFF} differentiation and stem cell self-renewal suggest that its activation during CAR-T production might be utilized to either restrain differentiation and confer functional benefits associated with early T_{MEM} phenotypes, or to promote differentiation toward a highly functional cell state. One group of investigators co-cultured tumor-specific T-cells with OP9 stromal cells overexpressing DLL1 to induce NOTCH signaling, and found that the resulting T-cells exhibited a minimally-differentiated T_{SCM} surface

phenotype. Consistent with this induced phenotype, OP9/DLL1-exposed CD4+ T-cells exhibited robust proliferation in response to subsequent *ex vivo* antigen stimulation and homeostatic cytokine signals *in vivo*[107]. They observed similar effects in CD8+ T-cells, and identified activation of the FOXM1 pathway downstream of NOTCH as a contributing mechanism to the development of early memory characteristics in a subsequent report[108].

While these studies provided some support for the idea that NOTCH signaling during T-cell culture can enhance function during subsequent antigen encounter, the use of OP9 cells to deliver NOTCH signal may confound the results—indeed, some of the observed effects of OP9/DLL1 co-culture could be recapitulated simply by culturing T-cells in OP9/DLL1-conditioned culture medium[108]. Further, when the investigators performed tumor control experiments in mice, only T-cells that had been exposed to OP9/DLL1 were included, precluding evaluation of whether NOTCH signaling actually altered T-cell anti-tumor activity. The published studies also did not examine whether OP9/DLL1 co-culture altered CD4+ T-cell cytokine production or other T_H subset characteristics, which could underlie potential enhancements to anti-tumor efficacy.

Outstanding questions

Given the strong behavior-determining effects of NOTCH signaling and the clinical need for improvements to adoptive T-cell therapeutic potency, we developed a list of questions to answer experimentally:

- Can we devise a cell-free culture system capable of meeting GMP standards that can induce NOTCH signaling during human CD4+ CAR-T production?
- Can we deliver NOTCH signal in a manner that favorably alters CD4+ T-cell differentiation in culture settings amenable to CAR-T production?
- Does NOTCH signaling polarize CD4+ CAR-T function toward a particular T_H subset?
- What genes does NOTCH signaling induce during CD4+ CAR-T production? Do these genes control T-cell differentiation or function?
- Does NOTCH signaling alter subsequent CD4+ CAR-T antigen responses, proliferative capacity and/or helper function? If so, how do these changes alter *in vivo* anti-tumor efficacy?

The answers to these questions and the data supporting them comprise Chapter 2 of this dissertation.

Work on the NOTCH signaling pathway led to investigation of the role of another transcription factor, the aryl hydrocarbon receptor, in programming T-cell activity, and these studies are the focus of Chapter 3.

Aryl hydrocarbon receptor discovery and function in T_H differentiation

The aryl hydrocarbon receptor, or AhR, is a ligand-activated transcription factor maintained in the cytosol in complex with chaperone proteins. Upon AhR binding of activating ligands, the chaperone AIP/XAP2/ARA9 dissociates from the complex and exposes AhR's nuclear localization sequence[109]. AhR is then imported into the nucleus, where it associates with ARNT/HIF1β and sheds the remainder of the chaperone complex. The AhR-ARNT complex is recruited to xenobiotic response elements (XREs) in the genome containing the consensus sequence 5'-TNGCGTG-3', where it controls gene expression[110,111]. AhR has also been shown to associate with other transcription factors and regulate expression of genes not containing XREs[112–116].

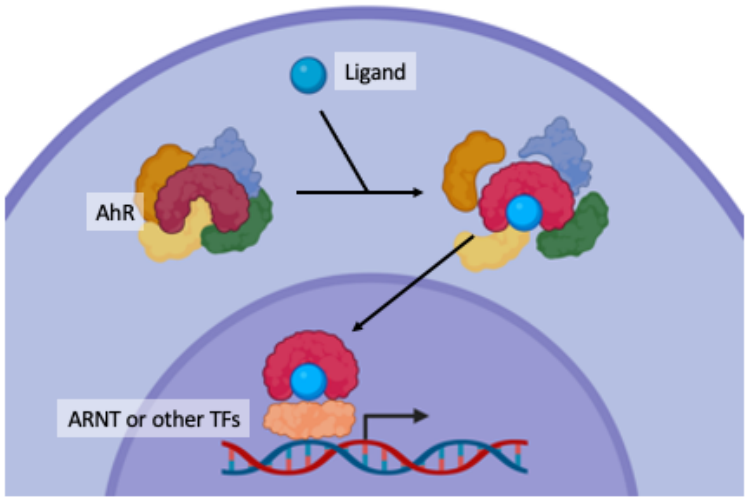

Figure 1.8. AhR signaling
AhR is maintained in the cytosol by chaperone proteins and translocates to the nucleus to regulate gene expression upon binding of activating ligands.

AhR was originally discovered in 1976 as a protein that bound the herbicide byproduct dioxin[117], and was subsequently found to mediate many of its toxic effects, which included suppression of T-cell immunity and elevated levels of regulatory T-cells[118–124]. Successive studies have found high levels of AhR expression in T_{REG} and T_R1 cells and defined important roles in their function, including driving expression of Foxp3 and CD39 and production of IL-10[118,119,125,126]. AhR was also found to be strongly expressed in T_H17 cells[127], to contribute to their development by reducing autocrine IL-2 production and signaling during activation[128,129], and to promote characteristic T_H17 cytokine production[126,130]. Differing strength and duration of signaling induced by individual AhR ligands, as well as subsequent cytokine signals received, may determine whether AhR signaling drives T_H17 or T_{REG}/T_R1 subset differentiation[126,131].

Metabolic drivers of AhR signaling in T-cells

While investigation of the effects of AhR activity in T-cells originally focused on environmental toxins, a wide variety of AhR-activating molecules are available within the human body. Cruciferous vegetables and gut microbes are abundant sources of AhR ligands and ligand precursors that may help prevent intestinal and central nervous system inflammation, and other ligands can form during heme breakdown or sun exposure in the skin[132].

Of particular note in cancer immunotherapy, tryptophan metabolism is a key source of AhR ligands. Tumors and tumor-associated myeloid cells expressing the enzymes IDO and TDO, which perform the rate-limiting step in the conversion of tryptophan to the AhR ligand kynurenine, are able to both deplete the local environment of tryptophan and activate AhR in infiltrating lymphocytes, generating regulatory signals and metabolically impairing T-cell function[133–135]. IL-2 signaling in T-cells increases production of the AhR ligand 5-HTP from tryptophan by upregulating the enzyme tryptophan hydroxylase 1; 5-HTP in turn signals through AhR to drive features of exhaustion, including coinhibitory marker expression and reduced cytokine production[136]. Encouragingly, T-cell anti-tumor activity is improved when pharmacologic AhR inhibition is provided in settings of tumor-driven ligand production[133] and when STAT5 activity is attenuated in settings of strong IL-2 signaling[136].

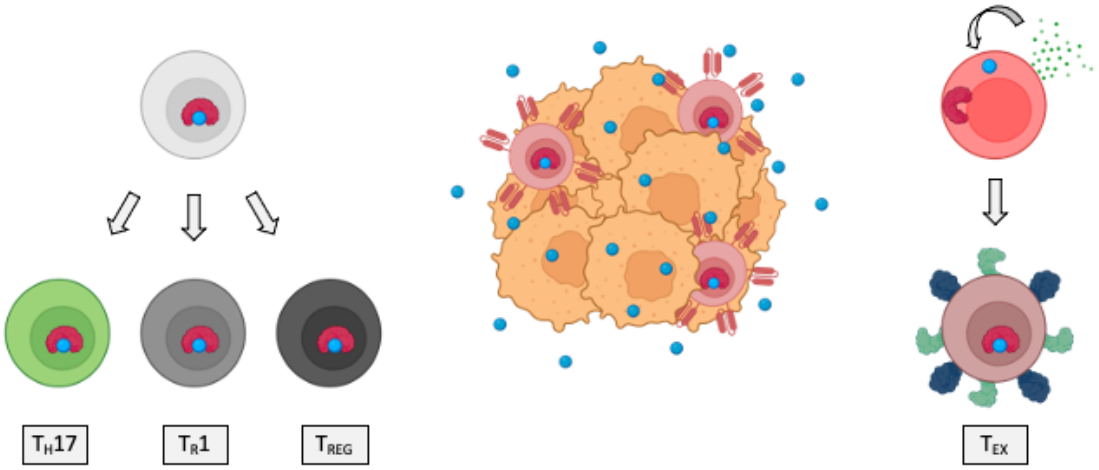

Figure 1.9. Roles of AhR signaling
AhR is involved in T_H17 and regulatory T cell development and function, tumor control of immune responses, and T-cell autoregulation following activation.

Outstanding Questions

While AhR is increasingly gaining attention as an immune checkpoint target *in vivo*, its expression and activity during CAR-T production *ex vivo* have not been explored. Given the strong regulatory effects AhR has on T-cell differentiation and activity during immune responses, we developed a second set of questions to explore:

- Is AhR expressed under culture conditions conducive to CAR-T production?
- Does AhR inhibition (AhRi) alter gene expression in during CAR-T production?
- Does AhRi during *ex vivo* T-cell culture affect growth or differentiation? If so, how?
- Does AhRi alter CD4+ CAR-T polarization?
- How does AhRi during primary T-cell activation alter subsequent antigen responses?

Chapter 2

NOTCH1 signaling alters differentiation and enhances antigen responses of CD4+ chimeric antigen receptor T cells

Abstract

Adoptive transfer of T-cells expressing chimeric antigen receptors (CAR-T) effectively treats refractory hematologic malignancies in a subset of patients, but can be limited by poor T-cell expansion and persistence in vivo. Less-differentiated T-cell states correlate with CAR-T capacity to proliferate and mediate anti-tumor responses, and interventions that limit tumor-specific T-cell differentiation during ex vivo manufacturing enhance therapeutic efficacy. NOTCH signaling is involved in fate decisions across diverse cell lineages, and in memory CD8+ T-cells was reported to upregulate the transcription factor FOXM1, attenuate differentiation and enhance proliferation and anti-tumor efficacy in vivo. Here, we used a cell-free culture system to provide an agonistic NOTCH1 signal during naïve CD4+ T-cell activation and CAR production, and studied the effects on differentiation, transcription factor expression, cytokine production and responses to tumor. NOTCH1 agonism efficiently induced a stem cell memory phenotype in CAR-T derived from naïve but not memory CD4+ T-cells, and upregulated expression of AhR and c-MAF, driving heightened production of IL-22, IL-10 and Granzyme B. NOTCH1-agonized CD4+ CAR-T demonstrated enhanced antigen responsiveness and proliferated to strikingly higher frequencies in mice bearing human lymphoma xenografts. NOTCH1-agonized CD4+ CAR-T also provided superior help to co-transferred CD8+ CAR-T, driving improved expansion and curative anti-tumor responses in vivo at low CAR-T doses. Our data expand the mechanisms by which NOTCH can shape CD4+ T-cell behavior, and demonstrate that activating NOTCH1 signaling during genetic modification ex vivo is a potential strategy for enhancing the function of T-cells engineered with tumor-targeting receptors.

Introduction

The NOTCH pathway plays context-dependent roles in cell differentiation and stem cell self-renewal[137,138]. NOTCH instructs the differentiation of T-cells throughout their lifespan, coordinating thymic T-cell development from common lymphoid progenitors[71–73], facilitating gene expression critical for effector function[75,79,91], and promoting memory CD4+ T-cell (T_{MEM}) survival following infection[80]. Naïve T-cells (T_N) upregulate NOTCH receptors after T-cell receptor (TCR) ligation and receive signals from antigen-presenting cells (APCs) expressing various NOTCH ligands[74,76,139]. In activated CD4+ T-cells, NOTCH signaling promotes T helper (T_H) subset-defining transcription factor (TF) and cytokine gene expression irrespective of polarizing cytokine signals, broadly enabling effector responses[88,91,140–144]. Depending on experimental context, NOTCH signaling has also been reported to skew differentiation toward various CD4+ T_H subsets[82,140–142,145,146]. In contrast to NOTCH's roles in facilitating T-cell effector function, one study reported that co-culturing previously-activated T_{MEM} with OP9 stromal cells overexpressing the NOTCH ligand DLL1 (OP9/DLL1) induced a less-differentiated T-cell surface phenotype and enhanced T-cell proliferation upon restimulation[107]. These diverse effects suggest that manipulation of NOTCH signaling could be used to improve T-cell cancer immunotherapy.

Treatment of advanced hematologic malignancies with T-cells engineered to express chimeric antigen receptors (CARs) targeting tumor-associated molecules is effective, but responses are often incomplete[23,147]. Both CD4+ and CD8+ CAR-T contribute to anti-tumor activity through direct tumor killing and host immune cell activation in the tumor microenvironment[30,148]. In preclinical models, CAR-T derived from less-differentiated subsets mediate superior anti-tumor responses[30], and limiting tumor-specific T-cell differentiation during *ex vivo* manufacturing can enhance efficacy[39,40,42,43,45–47]. *Ex vivo* polarization of CD4+ T-cell differentiation toward particular T_H subsets has also been shown to improve anti-tumor responses *in vivo*[67,149]. These findings suggest that NOTCH signaling, whether delivered in contexts that restrict CD4+ differentiation or promote acquisition of particular T_H subset behavior, could improve CAR-T therapy.

The effects of NOTCH signaling in CD4+ T-cells can vary with induction method, as soluble NOTCH ligands, NOTCH-specific monoclonal antibodies (mAbs) and overexpression of transcriptionally active NOTCH intracellular domains in T-cells provide signals of different quality, strength and duration[150]. Additional membrane-bound and soluble signals available to T-cells during cell-based delivery of NOTCH ligands further complicates interpretation—indeed, culturing CD8+ T-cells in OP9/DLL1-conditioned medium was sufficient to induce phenotypic changes reported to be NOTCH-specific[108]. To avoid use of cell lines, we developed a culture system using αCD3/CD28 mAb-coated beads and plate-coated αNOTCH mAb to simultaneously activate CD4+ T-cells and engage NOTCH receptors, and used this method to study the effects of NOTCH1 signaling on CD4+ CAR-T gene expression, differentiation and responses to tumor.

Methods

Cell Lines

Lenti-X cells (Takara) were cultured as described[151]. Raji and K562 cells (ATCC) were cultured and stably transfected with full-length human CD19 or BCMA cDNA as described[151,152].

Primary T-Cells

Peripheral blood was obtained from healthy donors following informed consent on research protocols approved by the Fred Hutchinson Cancer Research Center Institutional Review Board (FHCRC, Seattle, WA). Peripheral blood mononuclear cells were isolated by density gradient centrifugation, and T-cell subsets were isolated as described using EasySep CD4+ Naïve, CD8+ Naïve and CD4+ Memory T-cell negative selection kits (STEMCELL).

Lentiviral Vectors and Lentivirus Production

CAR vectors encoding the CD19-specific FMC63 scFv and EGFRt transduction marker or the ROR1-specific R12 scFv and truncated CD19 (tCD19) transduction marker were previously generated[16,153]. GFP was removed from the SGEP plasmid (#111170, Addgene) and replaced with a selectable truncated CD34 (tCD34) marker. *Maf*-targeting short hairpin RNAs (shRNAs)

were designed using SplashRNA and cloned into SGEP-tCD34 as described[154]. Lentivirus was generated as described[151].

T-Cell Culture

Non-tissue culture (TC)-coated plates were coated overnight at 4˚C with PBS+5μg/ml RetroNectin (Takara) and either 2.5μg/ml Ultra-LEAF-Purified αNOTCH1 mAb (MHN1-519, BioLegend) for NOTCH1 (N1) culture or 2.5μg/ml mouse IgG1κ isotype (BioLegend) for control culture. Coating solution was aspirated and plates washed twice with PBS before T-cell plating. On day 0, $2x10^5$ T-cells and $6x10^5$ Human T-Activator CD3/CD28 Dynabeads (ThermoFisher) in 1ml T-cell culture medium including IL-2[151] were plated per N1/control 24-well. On day 1, T-cells were transduced with CAR or shRNA lentivirus[151]. On day 3, cells from each N1/control 24-well were split into two N1/control 12-wells. On day 5, cells from each N1/control 12-well were incubated on magnets to remove Dynabeads, then transferred to a N1/control 6-well. Cells were transferred from each N1/control 6-well to a vented TC-coated $25cm^2$ flask on day 7, and were analyzed on day 11. Prior to some analyses, EGFRt+ CAR-T were enriched by biotinylated cetuximab[151] staining followed by biotin microbead positive selection (Miltenyi). tCD34+ T-cells were enriched by CD34 microbead positive selection (Miltenyi).

Flow Cytometry

For surface markers, T-cells were stained with fluorochrome-conjugated mAbs for 20min at 4˚C in PBS with 2% FBS and 3.6mM EDTA. For intracellular cytokines, CD19-specific CAR-T were stimulated by Cell Stimulation Cocktail containing PMA/ionomycin (eBioscience) or CD19+ Raji cell co-culture for 5-8hr with GolgiPlug (BD), stained for viability, fixed/permeabilized in Cytofix/Cytoperm buffer (BD) for 20min at 4˚C and stained with cytokine-specific mAbs for 30min at 4˚C. For TFs, cells were stained for viability, fixed/permeabilized in Foxp3 Fix/Perm buffer (eBioscience) for 30min at 22˚C and stained for TFs for 30min at 22˚C. For phosphoproteins, CAR-T were fixed in Phosflow Fix Buffer I (BD) for 10min at 37˚C, permeabilized in Phosflow Perm Buffer III (BD) for 30min on ice and stained for 30min at 4˚C. Cells were analyzed on FACSymphony or FACelesta flow cytometers (BD). For CAR

expression quantification, CD19- or ROR1-specific CAR-T were stained with biotinylated rhCD19 or recombinant human ROR1 for 20min at 4˚C in PBS with 2% FBS and 3.6mM EDTA, washed twice, stained with fluorochrome-conjugated streptavidin for 20min at 4˚C, washed twice and analyzed.

RNA Sequencing (RNAseq)

300 CD4+ EGFRt+ CAR-T cells were FACS-sorted into SMART-Seq HT lysis buffer (Takara). cDNA was generated using 13 amplification cycles and purified using AMPure XP beads (Agencourt). Libraries were prepared using the Nextera XT kit (Illumina) and sequenced in an SP flow cell on a NovaSeq 6000 (Illumina) to read depths >$10x10^6$/sample. Transcripts were aligned using STAR[155] and analyzed for differential expression using DESeq2[156] and gene set enrichment analysis (GSEA)[157].

In Vitro Restimulation Assays

For co-cultures, tumors were irradiated (10,000rad) and plated at $1.25x10^4$ cells/well in a 96-well U-bottom plate. For assays with recombinant human CD19 (rhCD19), 100µl PBS+10µg/ml avidin (Fisher) was added per well of a 96-well flat-bottom non-TC-coated plate, incubated overnight at 4˚C, washed with PBS, blocked 1hr with PBS+2% bovine serum albumin and washed again. 100µl PBS+biotinylated rhCD19 at the indicated concentrations was added per well, incubated 30min at 4˚ and washed again. For assays with OKT3, 100µl PBS+OKT3 at the indicated concentrations was added per well, incubated overnight at 4˚C and washed with PBS.

For proliferation analyses, CAR-T were labeled in 0.25µM carboxyfluorescein succinimidyl ester (CFSE) or CellTrace Violet (CTV) (ThermoFisher). $2.5x10^4$ or $7.5x10^4$ CAR-T were added to wells containing tumor cells or plate-bound rhCD19/OKT3 respectively. 24hr post-plating, culture medium was harvested and analyzed for CAR-T cytokine production by Luminex, and CAR-T were fixed/permeabilized and stained for IL-2R and phosphoproteins, or FACS-sorted for RNAseq. Separately, CFSE-labeled CAR-T were analyzed by flow cytometry for CFSE dilution after 72hr co-culture with tumor. CTV-labeled CAR-T were transferred from

rhCD19/OKT3-coated plates to uncoated 96-well U-bottom plates after 24hr stimulation and analyzed by flow cytometry for CTV dilution 48hr later.

NSG Mouse Experiments

6- to 8-week-old NOD.Cg-Prkdc^{scid}Il2rg^{tm1Wjl}/SzJ (NSG) mice were engrafted intravenously with 5x10^5 CD19+/GFP+/firefly luciferase+ Raji lymphoma. One week later, mice were treated intravenously with specified doses of CD19-specific CAR-T. For CD4+-only experiments, CAR-T cultures were depleted of any contaminating CD8+ T-cells by positive selection using CD8+ microbeads (Miltenyi) immediately prior to injection. CAR-T quantification in peripheral blood and tumor imaging were performed as described[151,153].

Luminex

Samples and cytokine standards were incubated with multiplexed microbeads coated with cytokine-specific mAbs (capture reagents). Beads were then washed, stained for 1hr with biotinylated αcytokine mAbs (detection reagents), washed again, stained for 30min with PE-conjugated streptavidin (Agilent), washed and analyzed on a Luminex 200 instrument. Sample concentrations were calculated from logistic curves generated from each cytokine standard. Limit of detection was established as the lowest standard value with a coefficient of variance <20% of the measured value, and thus varied between assays.

Statistical Analysis

Indicated statistical tests were performed using Prism software (GraphPad).

Results

αNOTCH1 mAb induces NOTCH signaling during T-cell activation

We measured NOTCH receptor surface expression in human CD4+ T_N at rest and after activation with αCD3/CD28 mAb-coated beads and IL-2. Initial experiments were performed using CD4+ T_N to avoid potential differences introduced by variable T_N and T_{MEM} frequencies between donors. Unstimulated CD4+ T_N expressed low levels of NOTCH1 and no detectable

NOTCH2, 3 or 4. Following activation, NOTCH1 was rapidly and uniformly upregulated and durably expressed, while NOTCH2 and NOTCH3 were upregulated more slowly and expressed transiently on a smaller fraction of cells [Figure 2.1A]. These data suggested that NOTCH1 ligation would most uniformly induce NOTCH signaling early during *in vitro* activation.

We then evaluated the effects of using plate-coated αNOTCH1 mAb to engage NOTCH1 during αCD3/CD28 stimulation of CD4+ T_N. T-cells were cultured at low density on RetroNectin-coated plates to promote cell adhesion and provide mechanical stress required to induce NOTCH signaling[158,159]. This method also allowed efficient lentiviral transduction of a CD19-specific CAR [Figure 2.1B]. The NOTCH target genes *Hes1* and *Dtx1* were induced after CD4+ T_N activation with plate-coated αNOTCH1, and their expression was increased by the addition of RetroNectin [Figure 2.1C]. NOTCH1-induced *Hes1* upregulation was abrogated by γ-secretase inhibition, indicating the effect was NOTCH-dependent [Figure 2.1D]. T-cells cultured on RetroNectin and αNOTCH1 mAb (hereafter "N1") exhibited equivalent fold expansion and viability and a higher lentiviral transduction rate compared to cells cultured on RetroNectin and IgG1κ isotype (hereafter "control") [Figure 2.1E].

NOTCH signaling during CD4+ T_N activation promotes a less-differentiated phenotype

Co-culture of previously-activated murine OVA-specific and human EBV-specific T-cells with OP9/DLL1 to activate NOTCH resulted induced a less-differentiated stem cell memory (T_{SCM}) phenotype[107]. We evaluated the phenotype of N1 and control CAR-T derived from CD4+ T_N at the end of culture. More N1 CD4+ CAR-T expressed CD45RA and CD62L and fewer expressed CD45RO than control cells, consistent with the T_{SCM} phenotype [Figure 2.1F,G]. N1 and control cells expressed similar levels of other memory-associated molecules including CCR7, CD27, CD28, CD95 and TCF1 [Figure 2.1G]. Fewer N1 cells expressed the chemokine receptors CXCR3 or CCR4, which are associated with T_H1 and T_H2 differentiation respectively and are expressed by CD4+ T_{SCM} less frequently than by central (T_{CM}) or effector memory (T_{EM}) cells [Figure 2.1H][160,161].

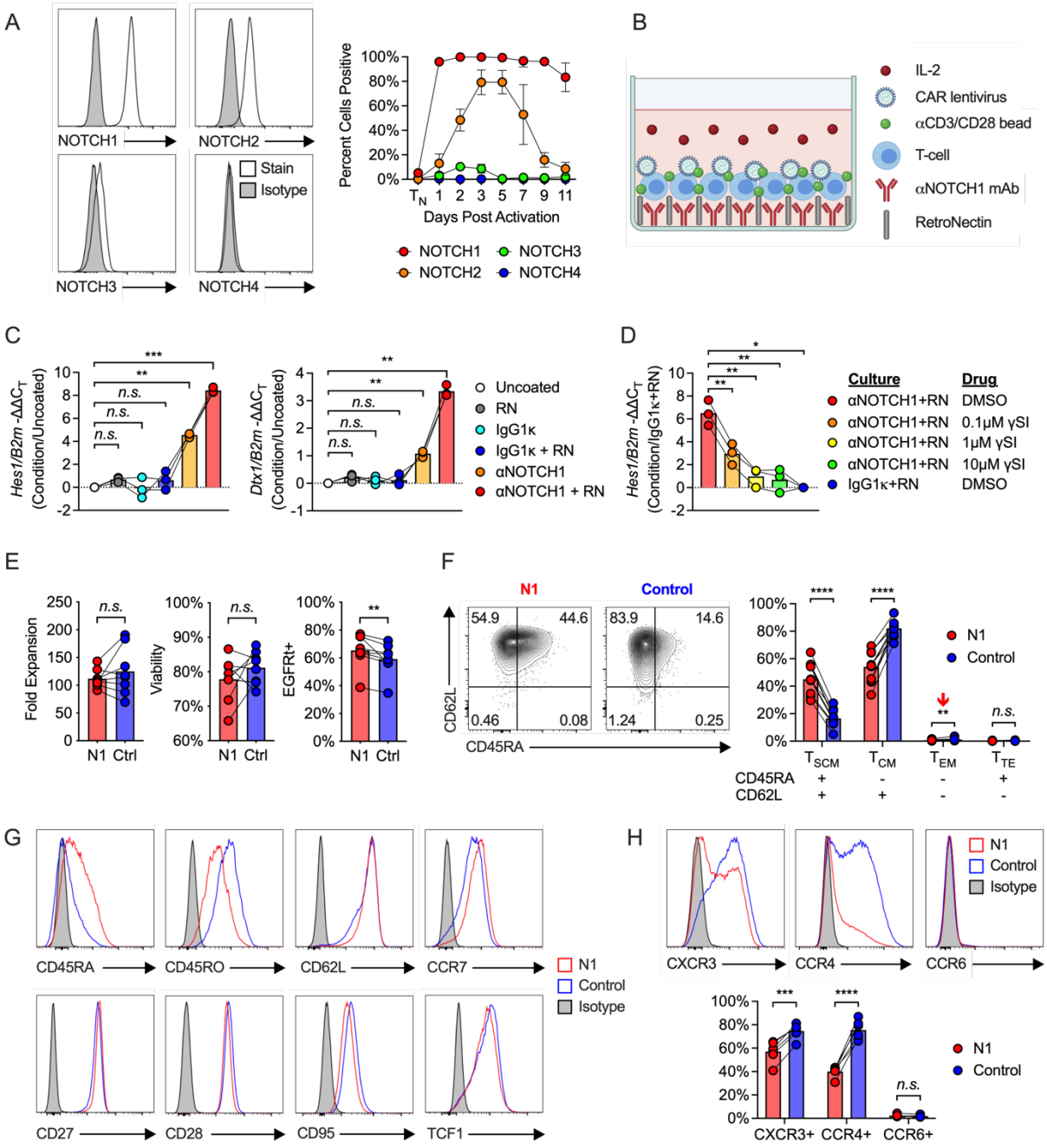

Figure 2.1. NOTCH1 agonism during CD4+ T_N activation results in a less-differentiated phenotype
(A) Left: Flow cytometry of NOTCH receptor expression compared to isotype in human CD4+ T_N 3 days after activation with αCD3/CD28 mAb-coated beads and IL-2. Histograms show one representative donor. Right: percent of CD4+ T_N expressing each NOTCH receptor at rest over time after activation. N=6 donors.
(B) Schematic of the N1 culture method using αNOTCH1 mAb- and RetroNectin-coated plates.
(C) RTqPCR evaluation of *Hes1* (left) and *Dtx1* (right) expression relative to *B2m* in activated CD4+ T_N after 48 hours of culture on plates coated with different combinations of αNOTCH1 mAb, M IgG1κ

and RetroNectin. N=3 donors. One-way ANOVA with Dunnett's multiple comparisons test. **p<0.01, ***p<0.005.
(D) Expression of *Hes1* relative to *B2m* in activated CD4+ T_N after 48 hours of N1 culture in the presence of various doses of RO4929097 γ-secretase inhibitor (γSI). N=3 donors. One-way ANOVA with Dunnett's multiple comparisons test. *p<0.05, **p<0.01.
(E) Fold expansion of N1 and control CD4+ T-cells, viability assessed by propidium iodide exclusion, and CAR lentivirus transduction rate measured after 11 days of culture. N=8 donors. Ratio paired two-tailed student's T test. **p<0.01.
(F) CD45RA and CD62L expression on N1 and control CD4+ CAR-T at day 11. Left: representative flow cytometry plots. Right: frequencies of N1 and control CD4+ CAR-T with T_{SCM}, T_{CM}, T_{EM} and T_{TE} phenotypes across 11 donors. Ratio paired two-tailed student's T test. **p<0.01, ****p<0.001.
(G) Cell surface phenotype of N1 and control CD4+ CAR-T on day 11 of culture. Histogram plots are representative of 11 donors.
(H) Chemokine receptor expression of N1 and control CD4+ CAR-T on day 11 of culture. Representative plots of 6 donors. Ratio-paired two-tailed student's T test. ***p<0.005, ****p<0.001.

Endogenous CD4+ T_{SCM} express lower levels of transcripts associated with T_H1, T_H2 and T_H17 effector responses than T_{CM} and T_{EM}[161]. To investigate whether NOTCH-induced phenotypic changes were reflected at the transcriptomic level, we performed RNAseq of N1 and control CAR-T at the end of culture. GSEA showed that N1 CD4+ CAR-T expressed lower levels of T_H1-, T_H2- and T_H17-characteristic genes compared to control CD4+ CAR-T[162] [Figure 2.2A, Supplemental Table 1]. Together, the enriched T_{SCM} phenotype and lower expression of genes associated with commitment to specific CD4+ T_H effector subsets indicate that NOTCH1 agonism during CD4+ T_N activation delays effector differentiation.

A

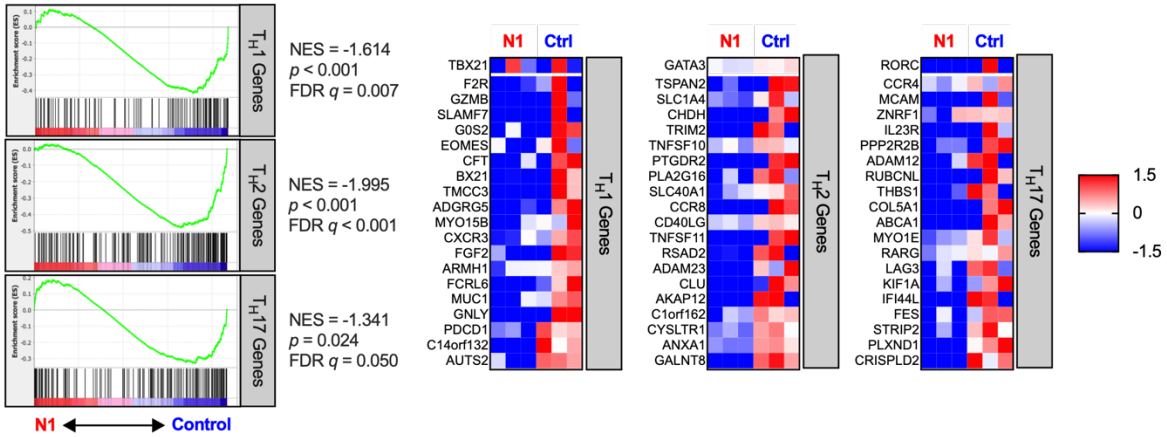

Figure 2.2. NOTCH1 agonism during CD4+ T_N activation results in a less-differentiated transcriptome
(A) Left: GSEA of RNAseq data from day 11 N1 and control CD4+ CAR-T. Right: Heatmaps depict log_2(normalized count/global average) for master regulator TFs and selected leading edge genes with a cutoff at 1.5-fold change. Significance was established at *p* and *q* both <0.05 after correction for multiple hypothesis testing. See also **Supplemental Table 1**.

To examine whether early NOTCH1 agonism mediated similar changes in CD4+ T_{MEM}, we isolated CD45RA- CD4+ T_{MEM} and evaluated NOTCH receptor expression at rest and following activation. CD4+ T_{MEM} activation induced uniform and persistent NOTCH1 expression similar to CD4+ T_N [Figure 2.3A], but N1 culture of CD4+ T_{MEM} induced only a minor population expressing a T_{SCM} phenotype and little change in chemokine receptor expression [Figure 2.3B,C]. We therefore focused further experiments on the effects of NOTCH1 signaling on CD4+ T_N.

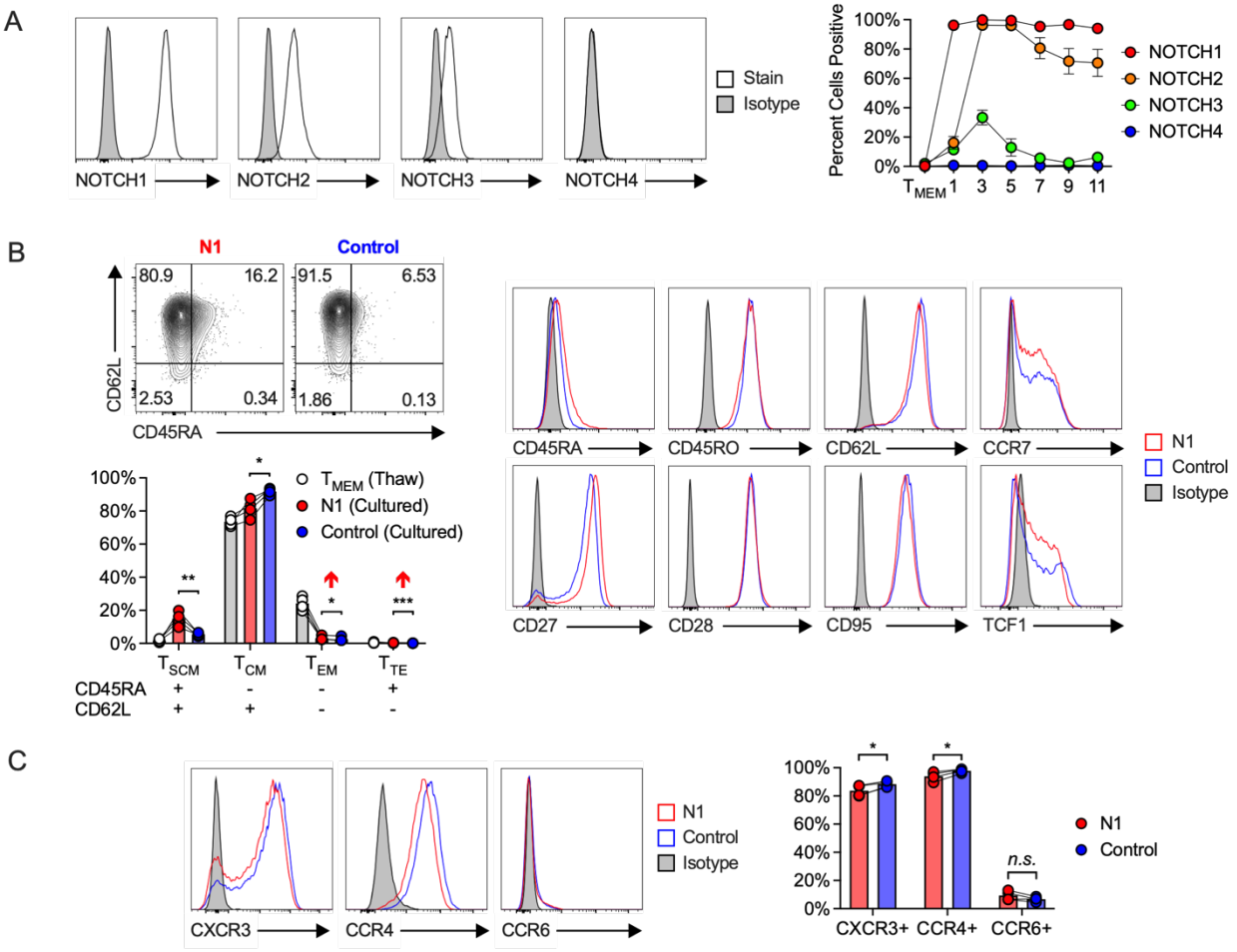

Figure 2.3. Effects of NOTCH1 agonism during CD4+ T_{MEM} activation
(A) Left: Flow cytometry of NOTCH receptor expression in human CD4+ T_{MEM} 3 days after activation with CD3/CD28 mAb-coated beads and IL-2. Histograms show one representative donor. Right:

percent of CD4+ T_{MEM} expressing each NOTCH receptor at rest over time after activation. N=4 donors.
(B) Phenotype of N1 and control CAR-T grown from CD4+ T_{MEM} at day 11. Top left: representative flow cytometry plots of CD45RA and CD62L expression. Bottom left: frequencies of N1 and control CD4+ CAR-T expressing T_{SCM}, T_{CM}, T_{EM} and T_{TE} phenotypes. Right: representative histograms of 4 donors. Ratio paired two-tailed student's T test. *p<0.05, **p<0.01, ***p<0.005.
(C) Chemokine receptor expression of N1 and control CD4+ CAR-T on day 11 of culture. Representative plots of 6 donors. Ratio-paired two-tailed student's T test. ***p<0.005, ****p<0.001.

NOTCH signaling alters CD4+ CAR-T cytokine production by inducing AhR and c-MAF

Prior work in murine models showed that NOTCH signaling can both direct production of specific cytokines[76,163] and facilitate expression of master regulator TFs that drive T_H effector cytokine production[91]. In response to restimulation with tumor, N1 CD4+ CAR-T produced more granzyme B (GzmB) and interferon-γ (IFNγ) than control CAR-T, similar TNFα, variable amounts of IL-2 and GM-CSF depending on tumor stimulus, and less IL-5 and IL-13 [Figure 2.4A]. N1 cells produced markedly more IL-10 than control cells, and, uniquely, produced IL-22 [Figure 2.4A]. N1 and control cells produced similar amounts of IL-4, IL-9, IL-17 and IL-21 [Figure 2.4A]. To determine whether IL-22 and IFNγ were produced by the same cells, we performed intracellular staining of N1 and control CD4+ CAR-T after restimulation with PMA/ionomycin or Raji tumor. IL-22 was expressed only by N1 cells and was produced by a population distinct from those making IFNγ [Figure 2.4B]. N1 primary culture supernatants contained higher levels of IFNγ, GzmB, IL-10 and IL-22 than control cultures after 3 days, indicating that NOTCH1 agonism imparted a functional program early in activation that endured upon restimulation [Figure 2.4C].

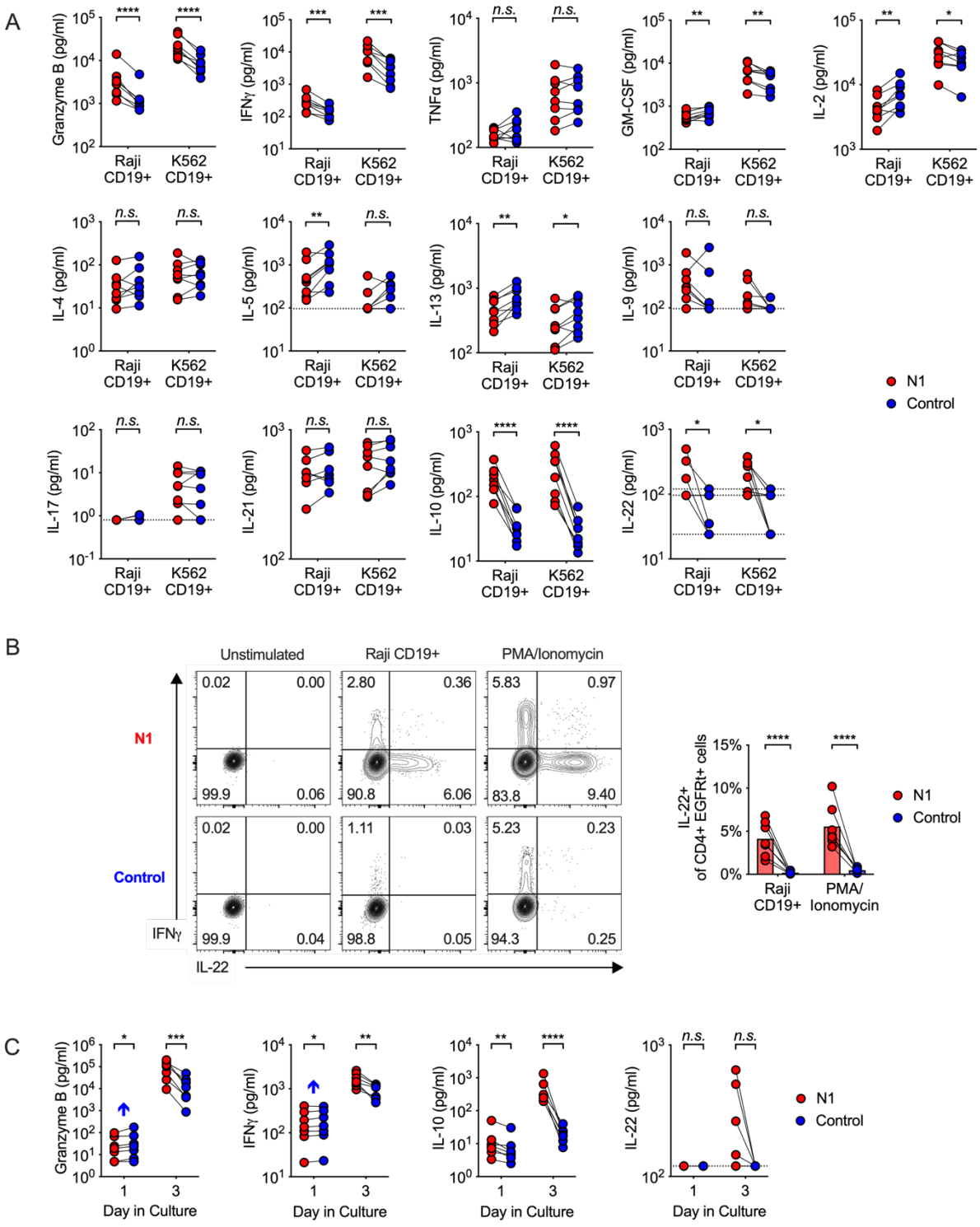

Figure 2.4. NOTCH1 agonism alters cytokine production of CAR-T derived from CD4+ T_N
(A) Luminex quantification of cytokines in culture medium after 24 hours of co-culture of N1 and control CD4+ CAR-T with irradiated CD19+ Raji or K562 tumor cells. Dotted lines indicate limits of detection. N=8 donors. Ratio paired two-tailed student's T test. *p<0.05, **p<0.01, ***p<0.005 and ****p<0.001.

(B) Intracellular staining for IL-22 and IFNγ after restimulation of N1 and control CD4+ CAR-T for 5-8 hours with PMA/ionomycin or CD19+ Raji tumor. Left: plots depict 1 donor representative of 7. Right: quantification of IL-22+ cell frequencies. Ratio paired two-tailed student's T test. ****p<0.001.
(C) Luminex quantification of cytokines in culture medium sampled on days 1 and 3 from primary N1 and control CD4+ T cell cultures. N=7 donors. Ratio paired two-tailed student's T test. *p<0.05, **p<0.01, ***p<0.005 and ****p<0.001.

Differences in CD4+ T-cell cytokine production can be driven by altered expression of TFs, particularly T_H subset-defining master regulators[164]. To profile TF and target gene expression, we performed RNAseq on N1 and control CD4+ CAR-T 3 days after activation, when cytokine differences were evident. At this early time, N1 CD4+ CAR-T were enriched for 18 genes, including the transcription factor *Maf* (c-MAF) [Figure 2.5A, Supplemental Table 2]. Though the differences did not rise to statistical significance, N1 CD4+ CAR-T also expressed more *Ahr* (aryl hydrocarbon receptor, or AhR), less *Gata3* (GATA-3) and equivalent *Tbx21* (T-bet) transcripts [Figure 2.5A]. Intracellular staining confirmed these differences at the protein level [Figure 2.5B]. Consistent with these findings, N1 cells expressed higher levels of AhR- and c-MAF-driven genes than control cells [Figure 2.5C][165–167].

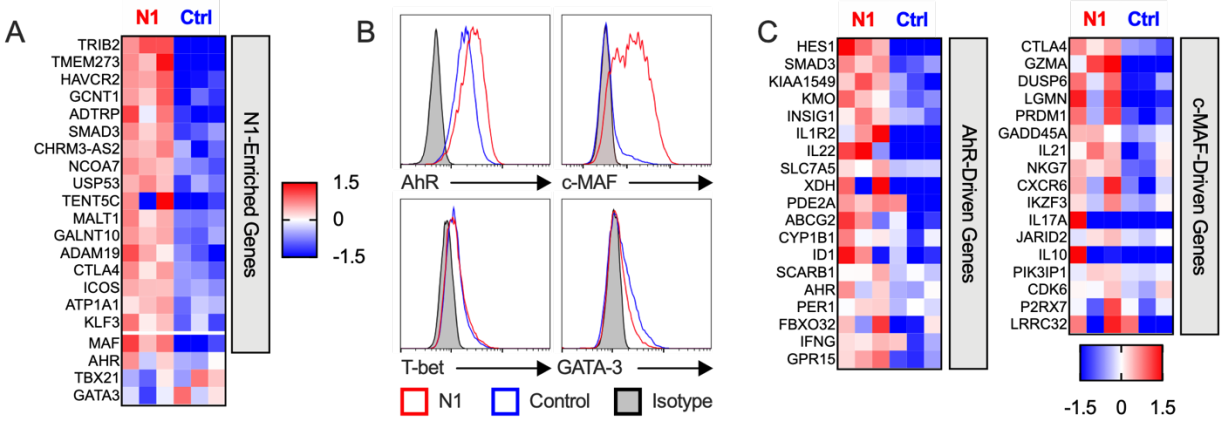

Figure 2.5. NOTCH1 agonism induces AhR and c-MAF activity
(A) Genes enriched in N1 compared to control CD4+ CAR-T at day 3 of culture. Heatmaps depict $\log_2$(normalized count/global average) with a cutoff at 1.5-fold change. N=3 donors per group. Significance was established as a minimum fold change of 1.5 and p<0.05. See also **Supplemental Table 2**.
(B) Intracellular staining for AhR, c-MAF, T-bet and GATA-3 in N1 and control CD4+ CAR-T at day 3 of culture. Histograms are representative of 5 donors.

(C) Expression of AhR- and c-MAF-driven genes in N1 and control CD4+ CAR-T quantified by RNAseq on day 3 of culture. Heatmaps depict log_2(normalized count/global average) with a cutoff at 1.5-fold change. N=3 donors per group.

We next evaluated how AhR and c-MAF might influence N1 CD4+ CAR-T cytokine production in response to tumor. The role of AhR was assessed by growing N1 CD4+ CAR-T cultures in the continuous presence an AhR inhibitor (CH-223191), then restimulating cells by co-culture with CD19+ tumor or PMA/ionomycin and assaying cytokine production in supernatants by Luminex or by intracellular staining. AhR inhibition abolished IL-22 production by N1 CD4+ CAR-T and reduced IL-10 and GzmB, but enhanced production of other cytokines including IFNγ, TNFα, GM-CSF, IL-2, IL-4, IL-13, IL-9 and IL-17 [Figure 2.6A-C]. These data indicate a dual role for AhR, both driving IL-22, IL-10 and GzmB secretion and restricting production of other cytokines induced in CD4+ T_N during activation in the presence of NOTCH signal.

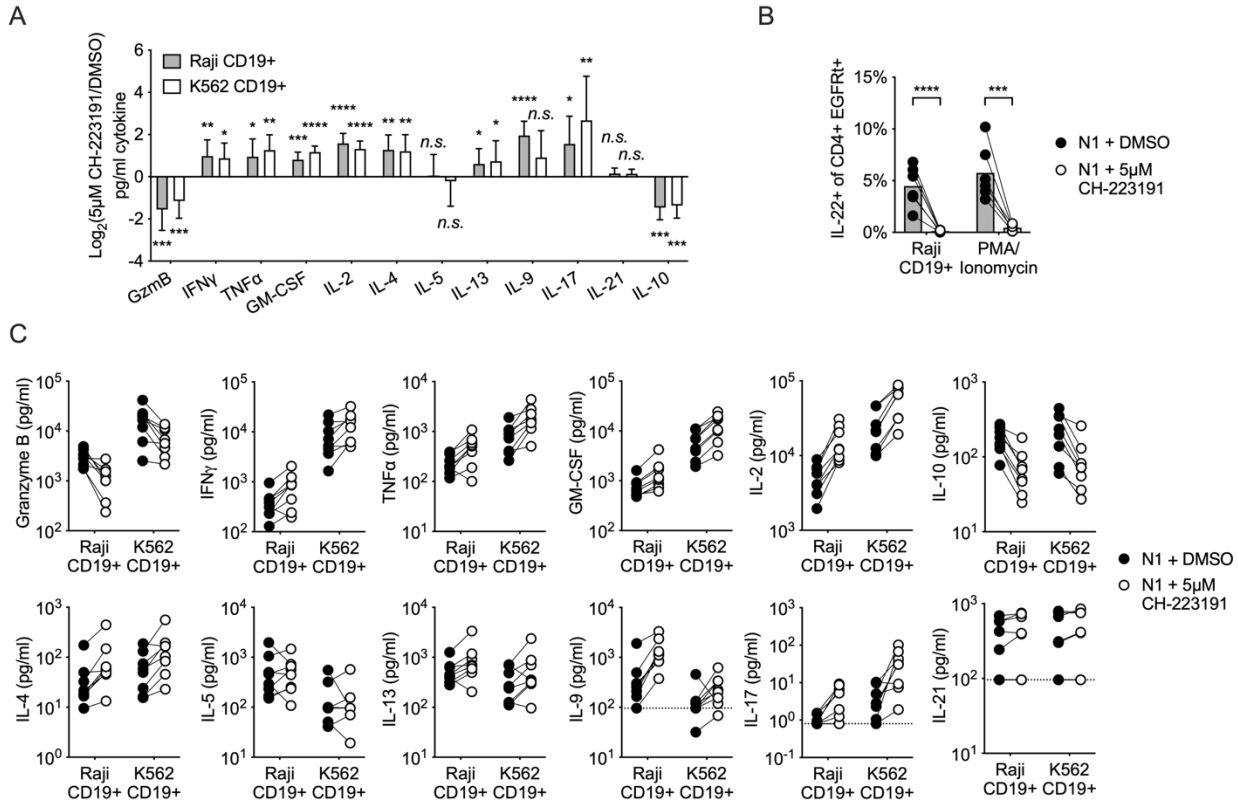

Figure 2.6. NOTCH1 agonism programs cytokine production via AhR
(A,C) Luminex quantification of cytokine production by CD19-specific N1 CD4+ CAR-T grown in DMSO or 5μM CH-223191 after 24 hours of co-culture with irradiated CD19+ Raji or K562 tumor in

absence of drug. (A) shows mean and standard deviation of relative sample values from 8 donors. Ratio paired two-tailed student's T test. *p<0.05, **p<0.01, ***p<0.005 and ****p<0.001. (B) Intracellular staining for IL-22 in N1 CD4+ CAR-T grown in DMSO or 5μM CH-223191 after restimulation for 5-8 hours with PMA/ionomycin or CD19+ Raji tumor. N=6 donors. Ratio paired two-tailed student's T test. ***p<0.005, ****p<0.001.

To evaluate the contributions of c-MAF, N1 CD4+ T-cells were transduced with a lentiviral vector encoding tCD34 and an shRNA either containing a scrambled sequence or targeting *Maf*. Two *Maf*-specific shRNAs both reduced c-MAF expression in N1 cells by half [Figure 2.7A]. Scrambled and *Maf*-targeted N1 cells were isolated by magnetic bead positive selection, rested overnight, then restimulated with PMA/ionomycin. c-MAF knockdown inhibited N1 cell IL-10 production to an even greater extent than AhR inhibition, but had no effect on GzmB, IFNγ or IL-22 production [Figure 2.7B-D]. These data indicate that c-MAF, together with AhR, promotes IL-10 production in the setting of NOTCH signaling, but does not limit IFNγ or IL-2 production as observed in other contexts[167,168].

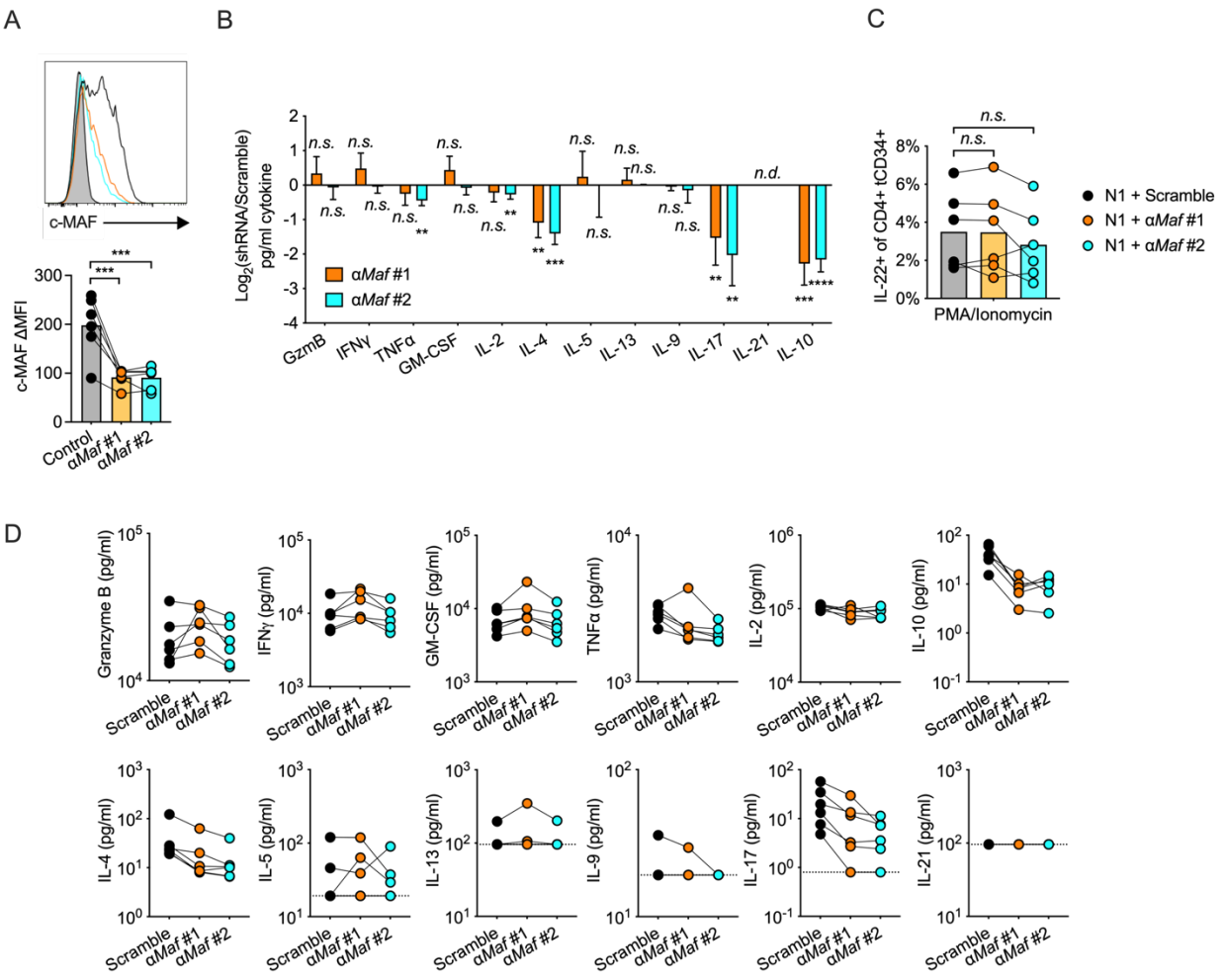

Figure 2.7. NOTCH1 agonism programs cytokine production via c-MAF

(A) Intracellular staining for c-MAF at day 3 of culture in N1 CD4+ T cells transduced with scrambled (black histogram) or one of two different *Maf*-targeting (orange, aqua) shRNA constructs relative to isotype (gray filled). Plot depicts 1 donor representative of 6. One-way ANOVA with Dunnett's multiple comparisons test. ***p<0.005.

(B,D) Luminex quantification of cytokine production by N1 CD4+ T cells transduced with a scrambled or *Maf*-targeting shRNA after 24 hours of stimulation with PMA and ionomycin. (B) shows mean and standard deviation of relative sample values from 6 donors. One-way ANOVA of log-transformed pg/ml values with Dunnett's multiple comparison testing. **p<0.01, ***p<0.005, ****p<0.001.

(C) Intracellular staining for IL-22 in N1 CD4+ T cells transduced with a scrambled or *Maf*-targeting shRNA after restimulation for 5-8 hours with PMA/ionomycin. N=6 donors. One-way ANOVA of log-transformed pg/ml data with Dunnett's multiple comparison testing.

<u>NOTCH1 agonism enhances CD4+ CAR-T proliferation and antigen sensitivity</u>

Less-differentiated tumor-specific T-cell phenotypes are linked to proliferation capacity and anti-tumor efficacy *in vivo*[29,30]. To assess whether NOTCH1 agonism altered CD4+ CAR-T

proliferation in response to tumor, CFSE-labeled CD19-specific N1 and control CD4+ CAR-T were co-cultured with CD19+ tumors and evaluated by flow cytometry over time. More N1 than control CD4+ CAR-T divided after 30 hours of stimulation, and this early proliferation advantage persisted over 3 days [Figure 2.8A]. ROR1-specific N1 CD4+ 4-1BB/CD3ζ or CD28/CD3ζ CAR-T also proliferated more than control CD4+ CAR-T after co-culture with ROR1+ tumor [Figure 2.8B], indicating the effect of NOTCH1 agonism on CD4+ CAR-T proliferation was independent of target antigen or costimulatory domain.

Activated T-cells produce IL-2 and upregulate IL-2 receptor (IL-2R) expression, enabling signaling through STAT3 and STAT5 that drives proliferation[169]. We measured IL-2R chain expression and STAT3 and STAT5 activation in N1 and control CD4+ CAR-T by flow cytometry after 24 hours of co-culture with CD19+ or CD19- K562 cells. N1 CD4+ CAR-T upregulated CD25, CD122 and CD132 expression and phosphorylated STAT3 Y705 and STAT5 Y694 to greater extents than control CAR-T in response to CD19+ but not CD19- tumor [Figure 2.8C]. RNAseq of N1 and control CAR-T co-cultured with CD19+ K562 showed that N1 cells were strongly enriched for expression of genes involved in c-Myc, E2F and mTORC1 activity and progression from G2 to mitosis compared to control cells[157,170] [Figure 2.8D, Supplemental Tables S3,S4]. Together, these data indicated NOTCH1 agonism during CD4+ T_N activation conferred a cell state capable of an enhanced proliferative response to subsequent antigen encounter.

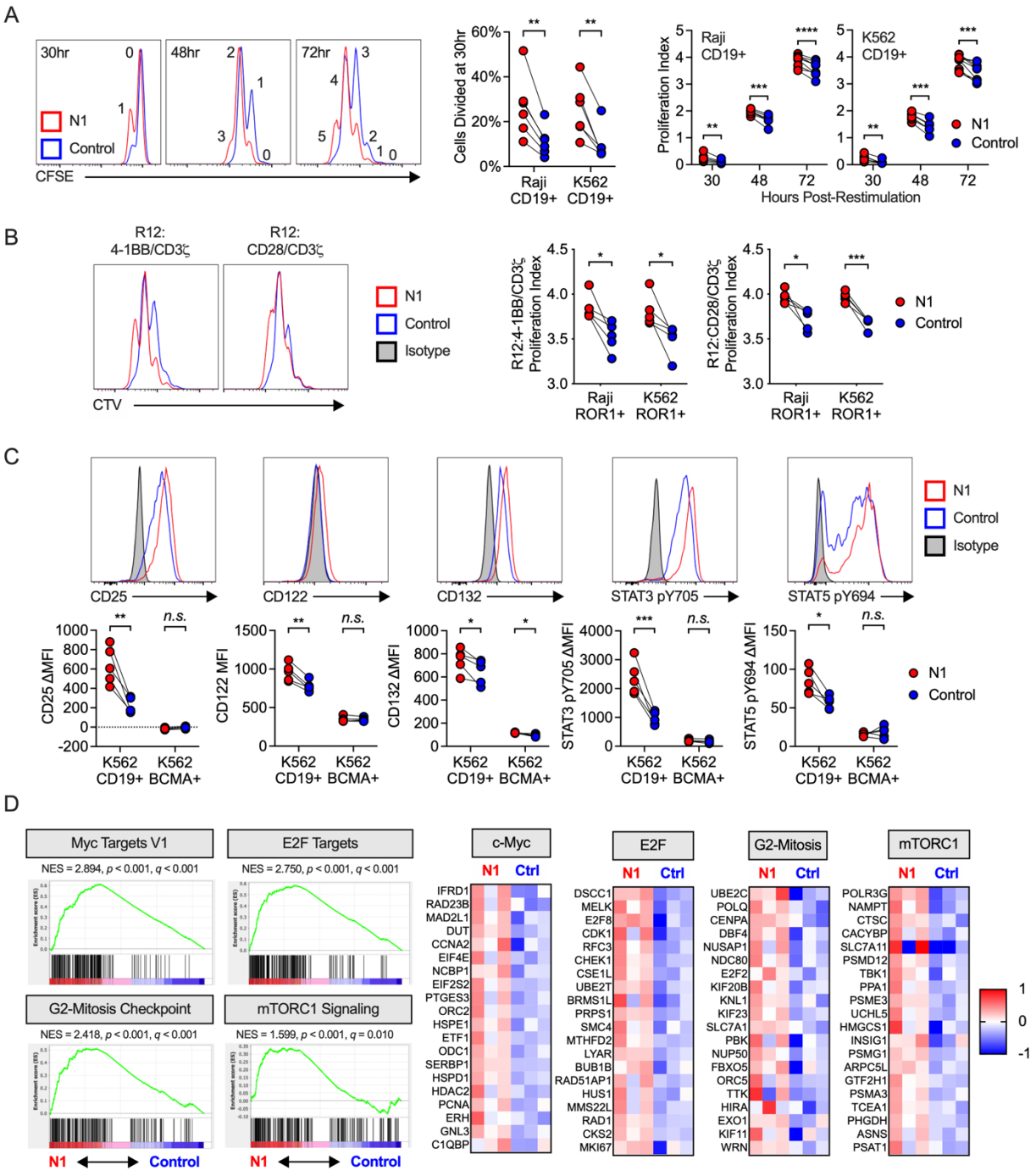

Figure 2.8. N1 CD4+ CAR-T proliferate more than control CD4+ CAR-T in response to tumor
(A) CFSE dilution by CD19-specific N1 and control CD4+ CAR-T after co-culture with irradiated CD19+ Raji or K562 tumor cells. Left: flow cytometry plots are representative of 6-9 donors per timepoint. Percent cells divided (middle) and proliferation index (average number of divisions) at various timepoints after stimulation (right) are shown for individual donors. Paired student's two-tailed T test. ***p*<0.01, ****p*<0.005, *****p*<0.001.

(B) CTV dilution by ROR1-specific N1 and control CD4+ CAR-T after 72 hours of co-culture with irradiated ROR1+ Raji or K562 tumor cells. Left: histograms of 1 donor representative of 5. Right: proliferation indices for 5 donors. Paired student's two-tailed T test. *p<0.05, ***p<0.005.
(C) Expression of IL-2R chains, STAT3 pY705 and STAT5 pY694 in CD19-specific N1 and control CD4+ CAR-T after 24 hours of co-culture with CD19+ or CD19-/BCMA+ K562 tumor cells. Top: histograms depict expression following CD19+ K562 restimulation representative of 5 donors. Bottom: IL-2R and phosphoSTAT expression in CAR-T following co-culture with CD19+ or CD19- BCMA+ tumor cells. Ratio paired student's two-tailed T test. *p<0.05, **p<0.01, ***p<0.005.
(D) Left: GSEA of RNAseq data generated from FACS-isolated CD19-specific N1 and control CD4+ CAR-T after 24 hours of co-culture with CD19+ K562 tumor cells. Right: Heatmaps depict $\log_2$(normalized count/global average) for leading edge genes. Significance was established at p and q both <0.05 after correction for multiple hypothesis testing. See also **Supplemental Tables 3,4**.

The increased proliferation of NOTCH1-agonized CD4+ CAR-T in response to tumor could result from enhanced antigen recognition. To test this, CTV-labeled CD19-specific N1 and control CD4+ CAR-T were restimulated on plates coated with titrated rhCD19. At low rhCD19 densities, more N1 than control CD4+ CAR-T had divided after 72 hours, and N1 cells proliferated more on average than control cells [Figure 2.9A]. N1 CD4+ CAR-T also produced more IFNγ, TNFα and IL-2, upregulated IL-2R chains and phosphorylated STAT3 to a greater extent than control CD4+ CAR-T at low antigen densities [Figure 2.9B,C].

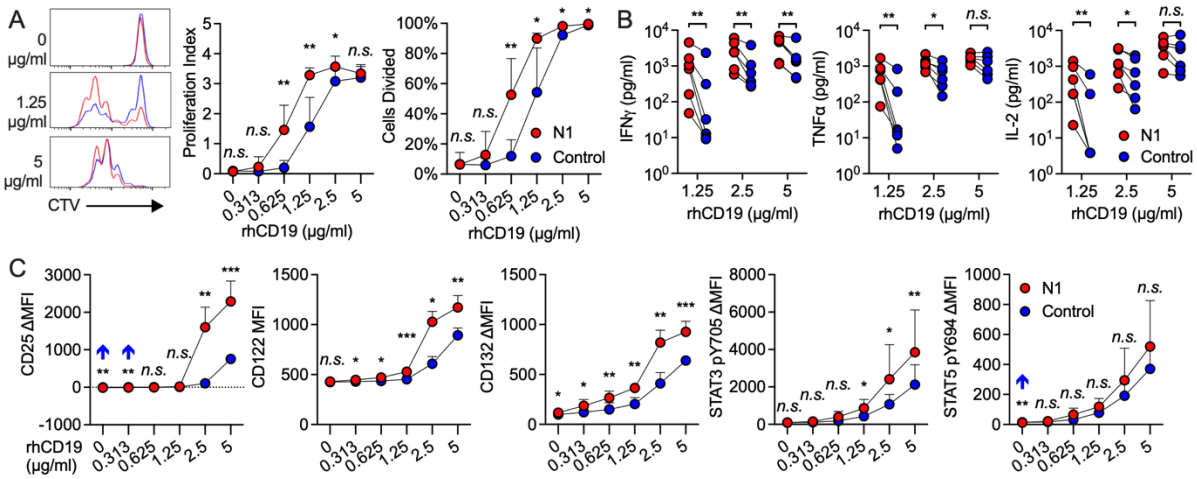

Figure 2.9. NOTCH1 agonism enhances CD4+ CAR-T proliferation and cytokine production in response to antigen
(A) CTV dilution by CD19-specific N1 and control CD4+ CAR-T 72 hours after restimulation on plates coated with various concentrations of rhCD19. Left: histograms of 1 donor representative of 6. Right: percent CAR-T divided and proliferation index at 72 hours. Paired two-tailed student's T test. *p<0.05, **p<0.01.

(B) Luminex quantification of cytokine production by CD19-specific N1 or control CD4+ CAR-T after 24 hours restimulation on plate-coated rhCD19. N=6 donors. Ratio paired two-tailed student's T test. *p<0.05, **p<0.01.
(C) Flow cytometry analysis of IL-2R chain, STAT3 pY705 and STAT5 pY694 expression by CD19-specific N1 or control CD4+ CAR-T after 24 hours restimulation on plate-coated rhCD19. N=5 donors. Ratio paired two-tailed student's T test. *p<0.05, **p<0.01, ***p<0.005.

Although N1 and control culture yielded similar transduction efficiencies, N1 CD4+ CAR-T expressed higher levels of CARs and transduction markers than control CAR-T [Figure 2.10A], providing a possible explanation for heightened N1 CD4+ CAR-T antigen sensitivity. N1 and control CD4+ T-cells expressed equivalent levels of CD3 at the end of culture [Figure 2.10B], allowing comparison of N1 and control T-cell responsiveness to plate-bound αCD3 mAb (OKT3). Mirroring responses to low rhCD19 levels, untransduced N1 CD4+ T-cells stimulated over a range of αCD3 concentrations exhibited greater proliferation, IFNγ and TNFα production, IL-2R chain upregulation and STAT3 Y705 phosphorylation than observed in control CD4+ T-cells [Figure 2.10C-E]. Thus, NOTCH1-agonized CD4+ T-cells are intrinsically capable of heightened responses to low antigen levels via both CAR and TCR signaling.

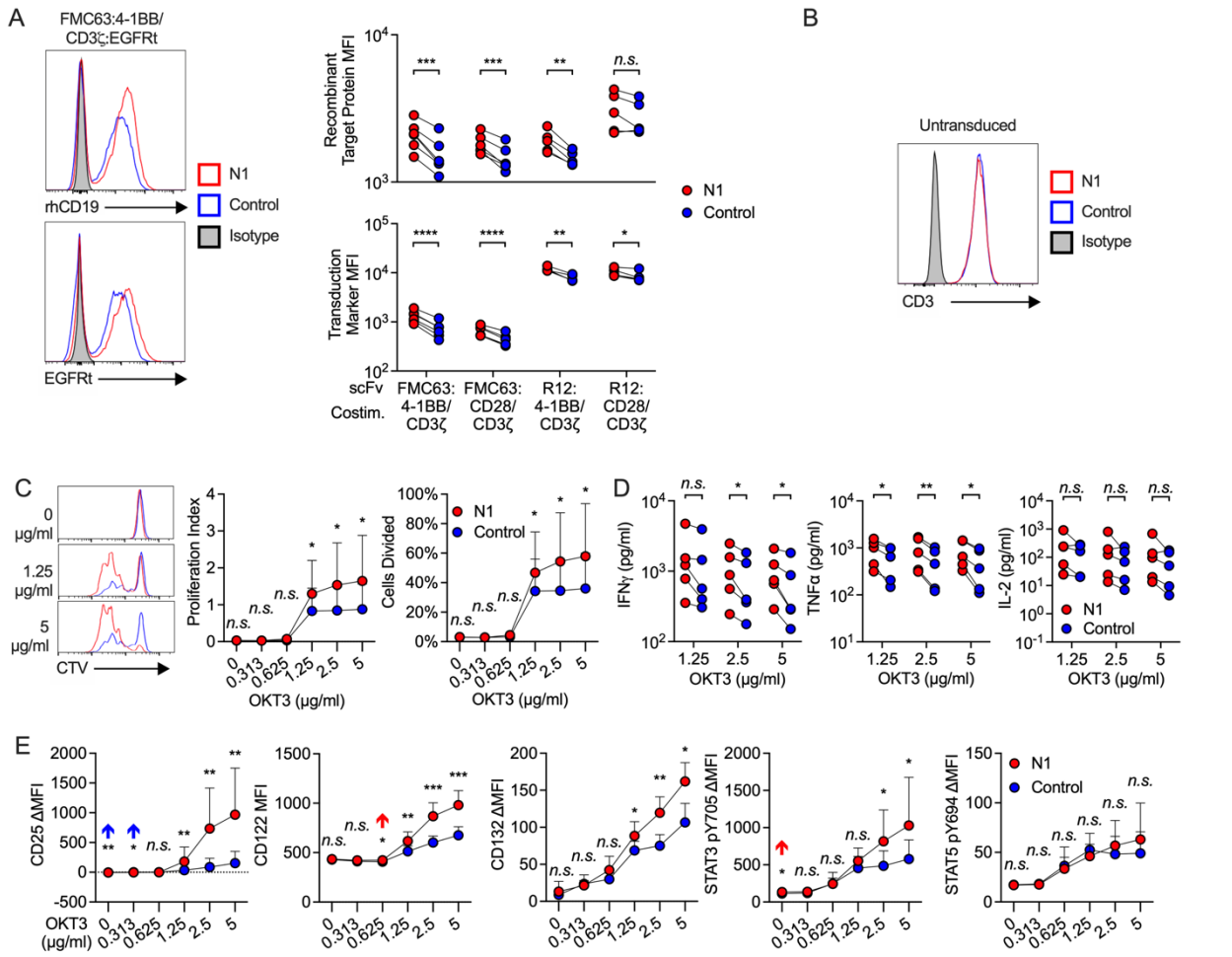

Figure 2.10. N1 CD4+ T-cells are more responsive to TCR ligation

(A) CAR and transduction marker expression on day 11 of culture in N1 and control CD4+ T-cells transduced with CAR constructs targeting CD19 or ROR1 with 4-1BB/CD3 or CD28/CD3 signaling domains. Top: representative histograms depicting CAR and transduction marker expression of N1 and control CD4+ CAR-T. Bottom: MFI quantification of CAR and transduction marker expression by N1 and control CD4+ CAR-T. N=5-6 donors per construct. Ratio paired two-tailed student's T test. **p*<0.05, ***p*<0.01, ****p*<0.005, *****p*<0.001.

(B) Flow cytometry of CD3 expression by N1 and control CD4+ CAR-T on day 11 of culture. Histogram shows 1 donor representative of 6.

(C) CTV dilution by untransduced N1 and control CD4+ T cells after 24 hours restimulation on plate-coated agonistic αCD3 mAb (OKT3) followed by 48 hours culture on uncoated plates. Representative plots of 5 donors. Paired two-tailed student's T test. **p*<0.05.

(D) Luminex quantification of cytokine production by untransduced N1 and control CD4+ T cells after 24 hours restimulation on plate-coated OKT3. N=5 donors. Ratio paired two-tailed student's T test. **p*<0.05, ***p*<0.01.

(E) Flow cytometry analysis of IL-2R chain, STAT3 pY705 and STAT5 pY694 expression by untransduced N1 and control CD4+ T cells after 24 hours restimulation on plate-coated OKT3. N=6 donors. Ratio paired two-tailed student's T test. **p*<0.05, ***p*<0.01, ****p*<0.005.

NOTCH1 agonism enhances CD4+ CAR-T proliferation in mice bearing lymphoma xenografts

The phenotypic and functional characteristics imparted by NOTCH1 agonism suggested that N1 CD4+ CAR-T might exhibit superior anti-tumor activity *in vivo*. NSG mice were engrafted with disseminated CD19+ Raji lymphoma, treated 7 days later with CD19-targeting N1 or control CD4+ CAR-T, and monitored for CAR-T expansion and changes in tumor burden [Figure 2.11A]. N1 CD4+ CAR-T rose to markedly higher peak frequencies in the blood than control CAR-T, and analysis of paired blood, splenocytes and bone marrow demonstrated higher N1 CD4+ CAR-T numbers at all sites [Figure 2.11B-D]. Neither N1 nor control CD4+ CAR-T expanded in non-tumor-bearing mice, indicating tumor recognition drove T-cell expansion [Figure 2.11E].

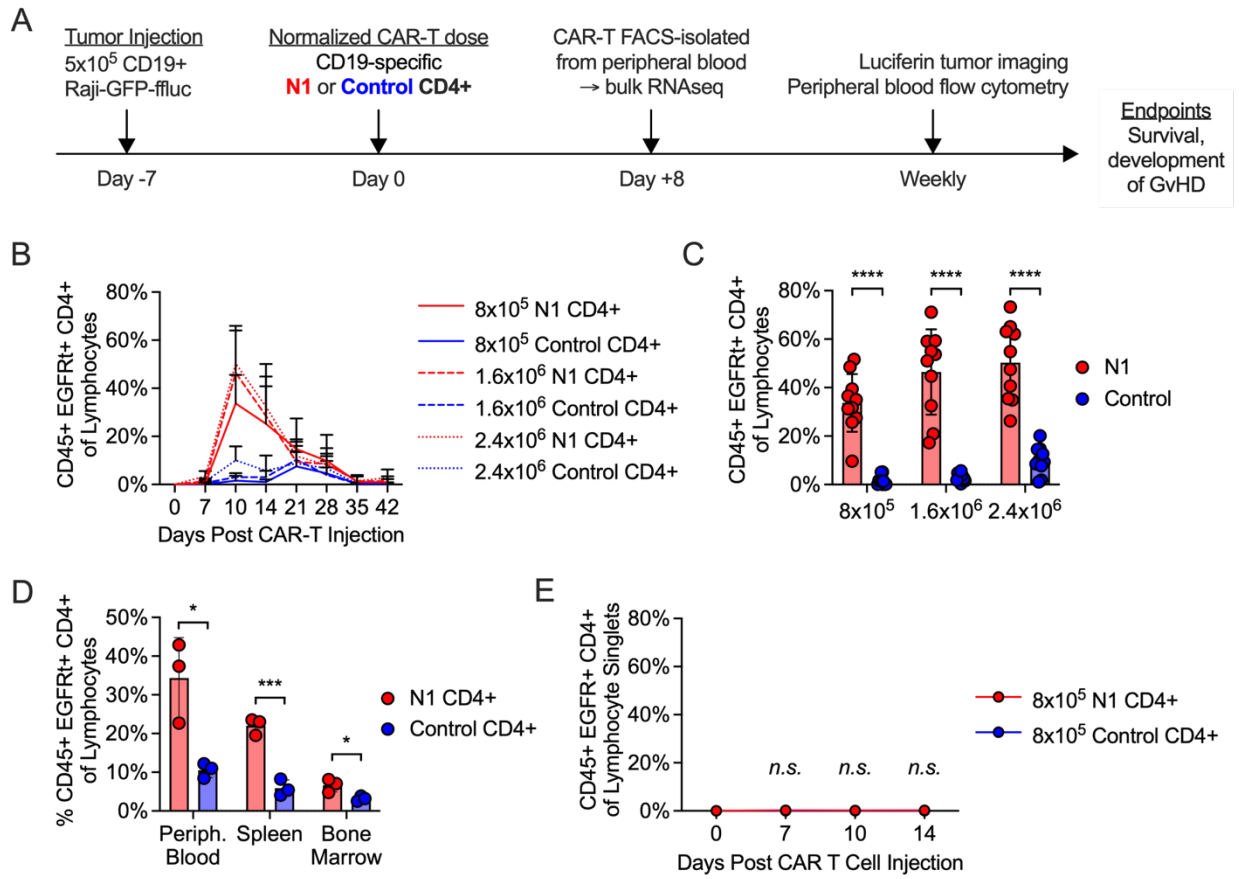

Figure 2.11. NOTCH1 agonism enhances CD4+ CAR-T proliferation in mice bearing lymphoma xenografts

(A) Experimental schematic for the xenograft model.

(B) Frequencies of N1 and control CD4+ CAR-T in peripheral blood over time following injection into tumor-bearing mice. N=10 mice per group, 2 donors.

(C) Frequencies of N1 and control CD4+ CAR-T at peak expansion 10 days post-transfer into tumor-bearing mice. N=10 mice per group, 2 donors. Unpaired two-tailed student's T test. ****p<0.001.

(D) Frequencies of N1 and control CD4+ CAR-T in peripheral blood, spleen and bone marrow of tumor-bearing mice treated with $1.6x10^6$ N1 or control CD4+ CAR-T 14 days post-treatment. N=3 mice per group, 1 donor. Unpaired two-tailed student's T test. *p<0.05, ***p<0.005.
(E) N1 and control CD4+ CAR-T frequencies in peripheral blood over time following injection into non-tumor-bearing mice. N=3 mice per group, 1 donor.

RNAseq of N1 and control CD4+ CAR-T isolated from the blood of tumor-bearing mice 8 days after transfer showed that N1 cells expressed higher levels of genes associated with T-cell cytotoxicity, including *Gzmb, Gnly, Prf1* and *Nkg7* [Figure 2.12A, Supplemental Table 5]. N1 cells were also strongly enriched for gene signatures of cell cycle progression and c-Myc, E2F and mTORC1 activity compared to control cells, similar to transcriptional differences observed after tumor recognition *in vitro* [Figure 2.12B, Supplemental Table 6]. GSEA further revealed strong skewing of N1 CD4+ CAR-T toward T_H1-like and away from T_H2-like gene expression relative to control CAR-T [Figure 2.12C]. In line with these transcriptomic findings, a higher fraction of N1 CD4+ CAR-T harvested from marrow and restimulated with PMA/ionomycin produced IFNγ [Figure 2.12D]. The pronounced T_H1-like N1 CD4+ CAR-T effector response was accompanied by transiently enhanced tumor regression compared to control cells [Figure 2.12E]. These data demonstrate that NOTCH1 agonism strikingly improves CD4+ CAR-T proliferative potential, skews cells toward a T_H1-like fate and accelerates tumor control *in vivo*.

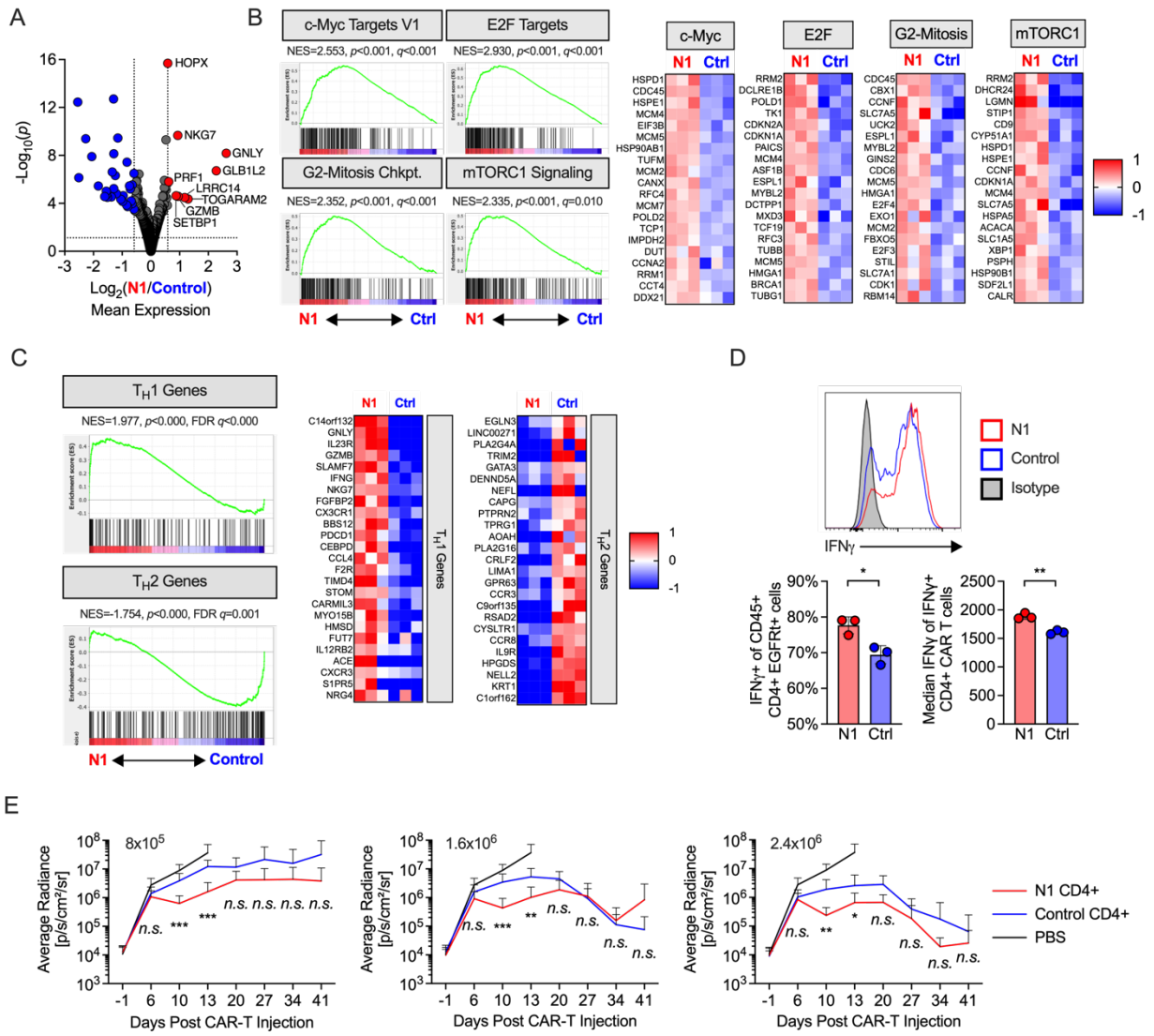

Figure 2.12. N1 CD4+ CAR-T strongly express proliferation- and T_H1-associated genes *in vivo*

(A) Gene expression by RNAseq of N1 and control CD4+ CAR-T FACS-isolated from peripheral blood 8 days post-transfer into tumor-bearing mice. N=3 mice per group, 1 donor. Significance was established at $p<0.05$ and fold change>1.5. See also **Supplemental Table 5**.

(B) Left: GSEA of RNAseq generated from N1 and control CD4+ CAR-T FACS-isolated from peripheral blood 8 days post-transfer into tumor-bearing mice. N=3 mice per group, 1 donor. Right: heatmaps depict $\log_2$(normalized count/global average) for selected leading edge genes with a cutoff at 1. Significance was established at p and q both <0.05 after correction for multiple hypothesis testing.

(C) Left: GSEA of RNAseq generated from N1 and control CD4+ CAR-T FACS-isolated from peripheral blood 8 days post-transfer into tumor-bearing mice. N=3 mice per group, 1 donor. Right: heatmaps depict $\log_2$(normalized count/global average) for selected leading edge genes with a cutoff at 1. Significance was established at p and q both <0.05 after correction for multiple hypothesis testing.

(D) Flow cytometry evaluation of IFNγ production by N1 and control CD4+ CAR-T after hind limb marrow harvest, T cell enrichment by CD4 microbead positive selection, restimulation with

PMA/ionomycin and brefeldin A for 5 hours and intracellular staining. N=3 mice per group, 1 experiment. Unpaired two-tailed student's T test. *p<0.05, **p<0.01.
(E) Tumor burden over time in mice treated with N1 or control CD4+ CAR-T, evaluated by intraperitoneal luciferin injection and bioluminescent imaging. N=10 mice per group, 2 donors. Mann-Whitney U test. *p<0.05, **p<0.01, ***p<0.005. See also **Supplemental Table 6**.

N1 CD4+ CAR-T markedly enhance CD8+ CAR-T proliferation and anti-tumor efficacy

While CD8+ T-cells are thought to be the primary mediators of anti-tumor responses, CD4+ T-cells can enhance (and in some cases are required for) CD8+ T-cell anti-tumor efficacy[16,30,148,171–173]. The striking difference in expansion between N1 and control CD4+ CAR-T in tumor-bearing mice suggested that NOTCH1 agonism might also improve the ability of CD4+ CAR-T to support CD8+ CAR-T proliferation and function. To test this hypothesis, NSG mice bearing Raji lymphoma were treated with $3x10^5$ control CD8+ CAR-T and either $3x10^5$ N1 or $3x10^5$ control CD4+ CAR-T [Figure 2.13A]. N1 CD4+ CAR-T rose to higher peak frequencies in the peripheral blood than control CD4+ CAR-T and promoted much greater expansion of control CD8+ CAR-T [Figure 2.13B,C]. The enhanced CAR-T expansion in mice treated with N1 CD4+ and control CD8+ CAR-T drove rapid and complete tumor regression in all mice, while half of mice treated with control CD4+ and CD8+ CAR-T failed to regress tumor [Figure 2.13D]. Thus, NOTCH1 agonism during *ex vivo* culture enhanced the capacity of CD4+ CAR-T to support CD8+ CAR-T proliferation and anti-tumor function *in vivo*.

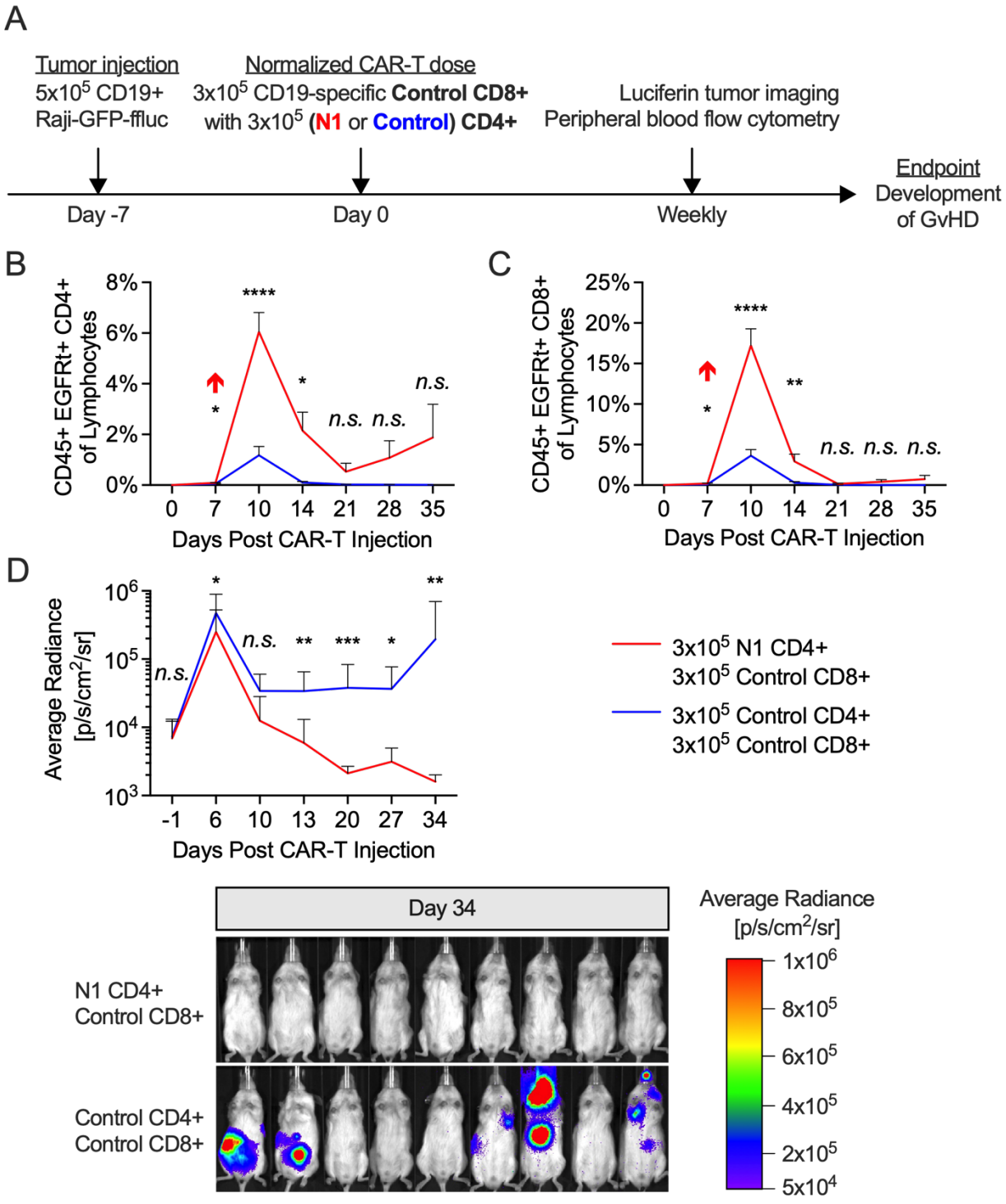

Figure 2.13. N1 CD4+ CAR-T enhance CD8+ CAR-T proliferation and anti-tumor efficacy
(A) Experiment schematic for the xenograft model.
(B,C) Flow cytometry quantification of (B) CD4+ and (C) CD8+ CAR-T frequencies in peripheral blood over time following injection into tumor-bearing mice. N=10 mice per group, 2 experiments. Unpaired two-tailed student's T test. *p<0.05, **p<0.01, ****p<0.001.

(D) Flow cytometry quantification of CD4+, CD8+ and total CAR-T frequencies at peak expansion 10 days post-transfer into tumor-bearing mice. N=10 mice per group, 2 experiments. Unpaired two-tailed student's T test. ****p<0.001.
(E) Tumor burden over time in mice treated with control CD8+ and either N1 or control CD4+ CAR-T, measured by intraperitoneal luciferin injection. N=10 mice per group, 2 experiments. Mann-Whitney U test. *p<0.05, **p<0.01, ***p<0.005.

Discussion

CAR-T therapy is effective in treating refractory hematologic malignancies[147], but patient responses can vary depending on CAR-T differentiation state, expansion and persistence *in vivo*[7,9,19–23]. NOTCH signaling induced by co-culture of previously-activated human CD8+ CAR-T with OP9/DLL1 and IL-7 induced a T_{SCM} phenotype and improved anti-tumor activity, in part by inducing FOXM1[108]. Whether NOTCH signaling alters human CD4+ T-cell phenotype and function via a similar axis has not been reported. To address this, we developed a cell-free culture system to simultaneously activate T-cells and induce NOTCH signaling during CAR-T production. In contrast to prior work[107], early NOTCH1 agonism efficiently induced a T_{SCM} phenotype in CAR-T grown from CD4+ T_N but not T_{MEM}, indicating that the mechanisms by which NOTCH signaling alters T-cell differentiation may be context- and T-cell subset-dependent.

NOTCH signaling during CD4+ T_N priming facilitates cytokine and master regulator TF gene expression, amplifying other polarizing signals[91]. Under stimulation conditions conducive to efficient CAR-T production, NOTCH1 agonism enhanced IFNγ, GzmB, IL-10 and IL-22 production. Different populations of N1 CD4+ T-cells produced IFNγ and IL-22, indicating that NOTCH signaling permitted distinct cell fates and might be used to generate diverse T_H subsets for different applications in adoptive cellular therapy. The effects of NOTCH signaling on CD4+ T-cell cytokine production have often been studied through the lens of master regulator TFs; here, we observed that NOTCH instead controls cytokine production primarily by inducing AhR and c-MAF. AhR drove N1 CD4+ CAR-T production of IL-22, IL-10 and GzmB, in agreement with studies documenting its role transactivating these genes[125,126,130]. Moreover, AhR antagonism during N1 culture disinhibited production of other CD4+ effector cytokines, suggesting that NOTCH-induced AhR restrains overexpression of inflammatory cytokines during CD4+ T_H responses. In conjunction with recent findings that attenuation of AhR activation can improve

CD8+ T-cell anti-tumor activity[136], our data invite further inquiry into whether manipulating AhR activity might improve T-cell function in cancer immunotherapy.

NOTCH-induced c-MAF also contributed to IL-10 production, consistent with its described role in cooperating with AhR to program T_R1 characteristics[119,174,175]. N1 CD4+ CAR-T did not exhibit regulatory activity in the xenogeneic lymphoma model used here, instead providing robust help to CD8+ CAR-T and promoting curative anti-tumor responses. N1 cells lacked key T_R1 traits, including CD49b and LAG3 coexpression, IL-21 secretion and reduced IL-2 production[119,175,176]. However, it is possible that NOTCH1-agonized CD4+ T-cells could mediate T_R1-like regulatory effects in an immunocompetent syngeneic setting, in which APCs play critical roles in T-cell anti-tumor responses. Our findings add to the known pathways through which NOTCH can alter CD4+ T-cell function and indicate that unbiased profiling strategies might identify additional novel behavior-determining axes initiated by NOTCH in other activation settings.

Unexpectedly, NOTCH1 agonism during CD4+ T_N activation rendered T-cells more responsive to subsequent activation through the CAR or TCR. Restimulated N1 CD4+ T-cells upregulated IL-2R chain expression more, contained higher levels of activated signal transducers and were enriched for genes associated with T-cell activation and proliferation. These differences translated into improved proliferation, T_H1 function and transiently improved tumor regression *in vivo*. While N1 CD4+ CAR-T did not control tumor more effectively on their own at later timepoints, they provided markedly better help to co-transferred CD8+ CAR-T, supporting CD8+ expansion to higher frequencies *in vivo* and driving uniformly curative anti-tumor responses. N1 CD4+ CAR-T enabled potent CD8+ CAR-T anti-tumor responses at low doses, suggesting NOTCH activation during CD4+ CAR-T production might be leveraged to improve both therapeutic efficacy and safety.

In summary, NOTCH1 signaling provided concurrently with CD3/CD28 stimulation restricted differentiation during CAR-T production from human CD4+ T_N, generating a cell product that activated strongly in response to low levels of antigen, proliferated robustly and provided superior help to co-transferred CD8+ CAR-T. We identified AhR and c-MAF as transcriptional mediators of NOTCH-induced changes to CD4+ T-cell cytokine production,

expanding the mechanisms by which NOTCH can shape T_H behavior beyond modulation of master regulator TF expression. Our data demonstrate that short-term cell-free NOTCH1 agonism during *ex vivo* culture is a viable strategy for enhancing tumor-specific T-cell performance.

Chapter 3

Ex vivo inhibition of the aryl hydrocarbon receptor enhances production of chimeric antigen receptor T-cells exhibiting potent anti-tumor activity

Abstract

Chimeric antigen receptor (CAR) T-cell therapy has demonstrated early clinical success in hematologic malignancies, but efficacy can be limited by the inability of *ex vivo* culture systems to expand T-cells sufficiently for effective dosing while producing highly active T-cell products. Indeed, signals induced by antigen stimulation and IL-2 supplementation during tumor-specific T-cell expansion couple proliferation to differentiation, creating an inverse relationship between *ex vivo* proliferation and anti-tumor fitness. Accordingly, interventions that uncouple T-cell proliferation from loss of stemness are of high clinical value. The aryl hydrocarbon receptor (AhR) is a ligand-activated transcription factor upregulated in response to TCR ligation, and IL-2 signaling drives T-cell-intrinsic production of tryptophan metabolite ligands that induce AhR-mediated upregulation of coinhibitory receptors and attenuate cytokine production. AhR also participates in regulatory T-cell function and can promote T_H17 polarization by limiting autocrine IL-2 production. Here, we observed AhR expression in T-cells under culture conditions conducive to efficient expansion, and studied the effects of AhR inhibition (AhRi) during CAR-T production on T-cell transcription, proliferation, differentiation and subsequent antigen responses to tumor. Activated AhRi T-cells expressed lower levels of many effector-associated transcripts compared to control cells. AhRi culture of T-cells induced strong autocrine IL-2 production, driving enhanced expansion even in absence of supplemental IL-2. However, AhRi-expanded T-cells did not display phenotypic evidence of proliferation-associated differentiation, and proliferated robustly and produced elevated levels of T_H1/T_C1-associated cytokines upon *in vitro* restimulation with tumor. AhRi CAR-T further mediated superior tumor control in mice bearing human lymphoma xenografts. Together, these findings confirm that AhR activity constitutes a critical autoregulatory axis in human T-cells, and indicate that AhR inhibition during tumor-specific T-cell manufacturing can both improve cell product yields and anti-tumor function.

Introduction

The aryl hydrocarbon receptor (AhR) is a ligand-activated transcription factor (TF) broadly expressed in immune cells. AhR nuclear translocation and transcriptional activity can be induced by a variety of ligands, including xenobiotic toxins, compounds available through the diet and gut microbiota, and tryptophan metabolites produced by tumors or by cell-intrinsic metabolism[132].

AhR was originally identified as the mediator of immunosuppression caused by the herbicide byproduct dioxin[117], and was subsequently found to promote CD4+ T_{REG} development and function by driving the expression of Foxp3, CD39 and IL-10[118,119,122,125,126]. AhR also participates in murine T_H17 development by inducing AIOLOS to limit autocrine IL-2 production and signaling[128,129], and promotes murine T_H17 cytokine production and pathogenicity[126,127,130]; in contrast, pharmacologic AhR activation drives IL-22 but attenuates IL-17 secretion in human T_H17[177,178].

More recently, AhR signaling was shown to constitute an autoregulatory axis: TCR ligation induces AhR expression in CD8+ T-cells, and IL-2-driven AhR activation upregulates coinhibitory receptors and inhibits cytokine production[136]. These observations align with reports of T-cell dysfunction driven by AhR ligands produced by tumor and tumor-associated macrophage tryptophan metabolism[133–135,165,179–183], and invite further inquiry into how cell-intrinsic AhR activity regulates T-cell gene expression and behavior.

T-cells engineered to express chimeric antigen receptors (CARs) targeting tumor-expressed proteins have shown great clinical promise in hematologic malignancies[147], but efficacy can be hampered by inability of *ex vivo* culture systems to expand T-cells sufficiently for effective dosing while producing T-cell products able to mediate potent anti-tumor effects[6,23]. Cell culture and engineering strategies that enhance T-cell activity and/or augment T-cell expansion *ex vivo*[38,40–43,45–48,66,67,69] are accordingly of high clinical value in the production of adoptive tumor-specific T-cell therapies.

We hypothesized that AhR expression and activity would be induced in T-cells under *ex vivo* culture conditions amenable to efficient CAR-T generation, which generally include TCR ligation and expansion with IL-2[6]. To study the effects of relieving AhR signaling during CAR-T

production, we grew T-cell cultures with pharmacologic AhR inhibitors and examined effects on T-cell transcription, growth, differentiation and subsequent antigen responses to tumors.

Methods

Primary T-Cells

Peripheral blood was obtained from healthy donors following informed consent on research protocols approved by the Fred Hutchinson Cancer Research Center Institutional Review Board (FHCRC, Seattle, WA). Peripheral blood mononuclear cells were isolated by density gradient centrifugation, and T-cell subsets were isolated as described using EasySep CD4+ Naïve, CD8+ Naïve and CD4+ Memory T-cell negative selection kits (STEMCELL).

Lentiviral Vectors and Lentivirus Production

The CAR vector encoding the CD19-specific FMC63 scFv, 4-1BB/CD3ζ costimulatory domains and EGFRt transduction marker was previously generated. Lentivirus was generated as described[38].

T-Cell Culture

Non-tissue culture (TC)-coated plates were coated overnight at 4˚C with PBS+5µg/ml RetroNectin (Takara). Coating solution was aspirated and plates washed twice with PBS before T-cell plating. On day 0, $2x10^5$ T-cells and $6x10^5$ Human T-Activator CD3/CD28 Dynabeads (ThermoFisher) in 1ml T-cell culture medium with 50IU/ml recombinant human IL-2 and either vehicle DMSO (1:1000), 5µM CH-223191 or 5µM StemRegenin 1 were plated per RN-coated 24-well. On day 1, T-cells were transduced with CAR lentivirus. On day 3, cells from each 24-well were split into two RN-coated 12-wells. On day 5, cells from each 12-well were incubated on magnets to remove Dynabeads, then transferred to a RN-coated 6-well. Cells were transferred from each 6-well to a vented TC-coated $25cm^2$ flask on day 7, and were analyzed on day 11. Fresh DMSO, CH-223191 or StemRegenin 1 was added to all new media added to cultures.

Flow Cytometry

For surface markers, T-cells were stained with fluorochrome-conjugated mAbs for 20min at 4˚C in PBS with 2% FBS and 3.6mM EDTA. For intracellular IL-2, T-cells were incubated for 5hr with GolgiPlug (BD), stained for viability, fixed/permeabilized in Cytofix/Cytoperm buffer (BD) for 20min at 4˚C and stained with IL-2-specific mAb for 30min at 4˚C. For transcription factors, cells were stained for viability, fixed/permeabilized in Foxp3 Fix/Perm buffer (eBioscience) for 30min at 22˚C and stained for TFs for 30min at 22˚C. For phosphoproteins, CAR-T were fixed in Phosflow Fix Buffer I (BD) for 10min at 37˚C, permeabilized in Phosflow Perm Buffer III (BD) for 30min on ice and stained for 30min at 4˚C. Cells were analyzed on FACSymphony or FACelesta flow cytometers (BD).

RNA Sequencing (RNAseq)

300 (CD4+ or CD8+) EGFRt+ CAR-T cells were FACS-sorted into SMART-Seq HT lysis buffer (Takara). cDNA was generated using 13 amplification cycles and purified using AMPure XP beads (Agencourt). Libraries were prepared using the Nextera XT kit (Illumina) and sequenced in an SP flow cell on a NovaSeq 6000 (Illumina) to read depths 10-30x10^6/sample. Transcripts were aligned using STAR and analyzed for differential expression using DESeq2 and gene set enrichment analysis (GSEA).

In Vitro Restimulation Assays

For co-cultures, tumors were irradiated (10,000rad) and plated at 1.25x10^4 cells/well in a 96-well U-bottom plate. For proliferation analyses, CAR-T were labeled in 0.25µM carboxyfluorescein succinimidyl ester (CFSE) or CellTrace Violet (CTV) (ThermoFisher). 2.5x10^4 CAR-T were added to wells containing tumor cells. 24hr post-plating, culture medium was harvested and analyzed for CAR-T cytokine production by Luminex. RNAseq. CFSE-labeled CAR-T were analyzed by flow cytometry for CFSE dilution after 72hr co-culture with tumor.

Luminex

Samples and cytokine standards were incubated with multiplexed microbeads coated with cytokine-specific mAbs (capture reagents). Beads were then washed, stained for 1hr with

biotinylated αcytokine mAbs (detection reagents), washed again, stained for 30min with PE-conjugated streptavidin (Agilent), washed and analyzed on a Luminex 200 instrument. Sample concentrations were calculated from logistic curves generated from each cytokine standard. Limit of detection was established as the lowest standard value with a coefficient of variance <20% of the measured value, and thus varied between assays.

NSG Mouse Experiments

6- to 8-week-old NOD.Cg-Prkdc^{scid}Il2rg^{tm1Wjl}/SzJ (NSG) mice were engrafted intravenously with 5x10^5 CD19+/GFP+/firefly luciferase+ Raji lymphoma cells. One week later, mice were treated intravenously with specified doses of either DMSO- or CH-223191-cultured CD4+, CD8+, or CD4+ and CD8+ CD19-specific CAR-T. For CD4+-only experiments, CAR-T cultures were depleted of any contaminating CD8+ T-cells by positive selection using CD8+ microbeads (Miltenyi) immediately prior to injection. CAR-T quantification in peripheral blood and tumor imaging were performed as described.

Statistical Analysis

Indicated statistical tests were performed using Prism software (GraphPad).

Results

AhRi alters gene expression in T-cells after αCD3/CD28 activation.

We first characterized AhR expression in CD4+ and CD8+ T_N and T_{MEM} at rest and following activation with αCD3/CD28 beads in the presence of IL-2. Intracellular staining demonstrated that all subsets upregulated AhR expression within 24hr of activation, reached peak expression in nearly all cells after 72hr, and maintained expression in varying percentages of cells for the duration of culture [Figure 3.1A].

While AhR expression is well-described in T_H17 and T_R1 CD4+ T_H subsets, its transcriptional activity in unpolarized CD4+ and CD8+ T_N has not been explored. To examine potential gene regulation by AhR, we activated CD4+ and CD8+ T_N with αCD3/CD28 beads and IL-2 in the continuous presence of 5μM CH-223191 (an AhR inhibitor, hereafter "CH") or vehicle

DMSO for 72hr and performed RNAseq [Figure 3.1B]. GSEA using a universal AhR signature[165] demonstrated that culture with CH downregulated T-cell expression of known AhR target genes, confirming effective AhR inhibition [Figure 3.1C].

AhR-inhibited (AhRi) CD4+ T-cells were enriched for expression of 6 genes relative to control cells, including the stemness-associated TF *Tcf7* [Figure 3.1D, Supplemental Table 7]. RNAseq of activated control and AhRi CD8+ T_N identified substantially more differentially-expressed genes, likely due to greater sequencing depth and inclusion of an additional biologic replicate. Mirroring AhRi CD4+ T-cells, AhRi CD8+ T-cells expressed higher levels of *Tcf7* and *C1orf162* transcripts compared to control cells, and additionally expressed higher levels of transcripts encoding proteins that limit reactive oxygen species levels (*Ucp2*, *Ucp3* and *Gsta4*), several solute and ion channels (*Slc43a2, Kcng1*, *Atpb8b2, Slc41a1, Atp6v0a1, Slc25a37*, *Kcnq3*), and transcription factors both positively (*Znf683*) and negatively (*Aff3*) correlated with T_{RM} identity [Figure 3.1D, Supplemental Table 8].

Control CD4+ T-cells were enriched for 29 genes relative to AhRi cells, including the canonical AhR target genes *Cyp1b1*, *Ahrr* and *Tiparp*, the effector molecules *Gnly* and *Il3*, genes associated with the development and function of T_H2 (*Il4*, *Tprg1*, *Asb2*) and T_{RM} and T_{REG} (*Il10, Prdm1*, *Hic1*, *Gpr15*, *Cd226*, *Myof*, *Samsn1*) subsets, and a variety of genes involved in T-cell activation (*Fut8*), trafficking (*S1pr1*) and cell signaling (*Nptx1*, *Ralb*, *Ptprk*) [Figure 3.1D, Supplemental Table 7]. Control CD8+ T-cells were enriched for many of the same genes relative to AhRi cells, as well as several effector-associated molecules (*Klrc1, Cxcr6, Ccl5*, *Gzmk*, *Gzma*), drivers of glycolytic metabolism (*Dusp6, Igf1*), molecules involved in TGFβ signaling transduction and regulation (*Smad3, Tgif1, Cd109*), and the integrins *Itga1, Itgax* and *Itgb7* [Figure 3.1D, Supplemental Table 8].

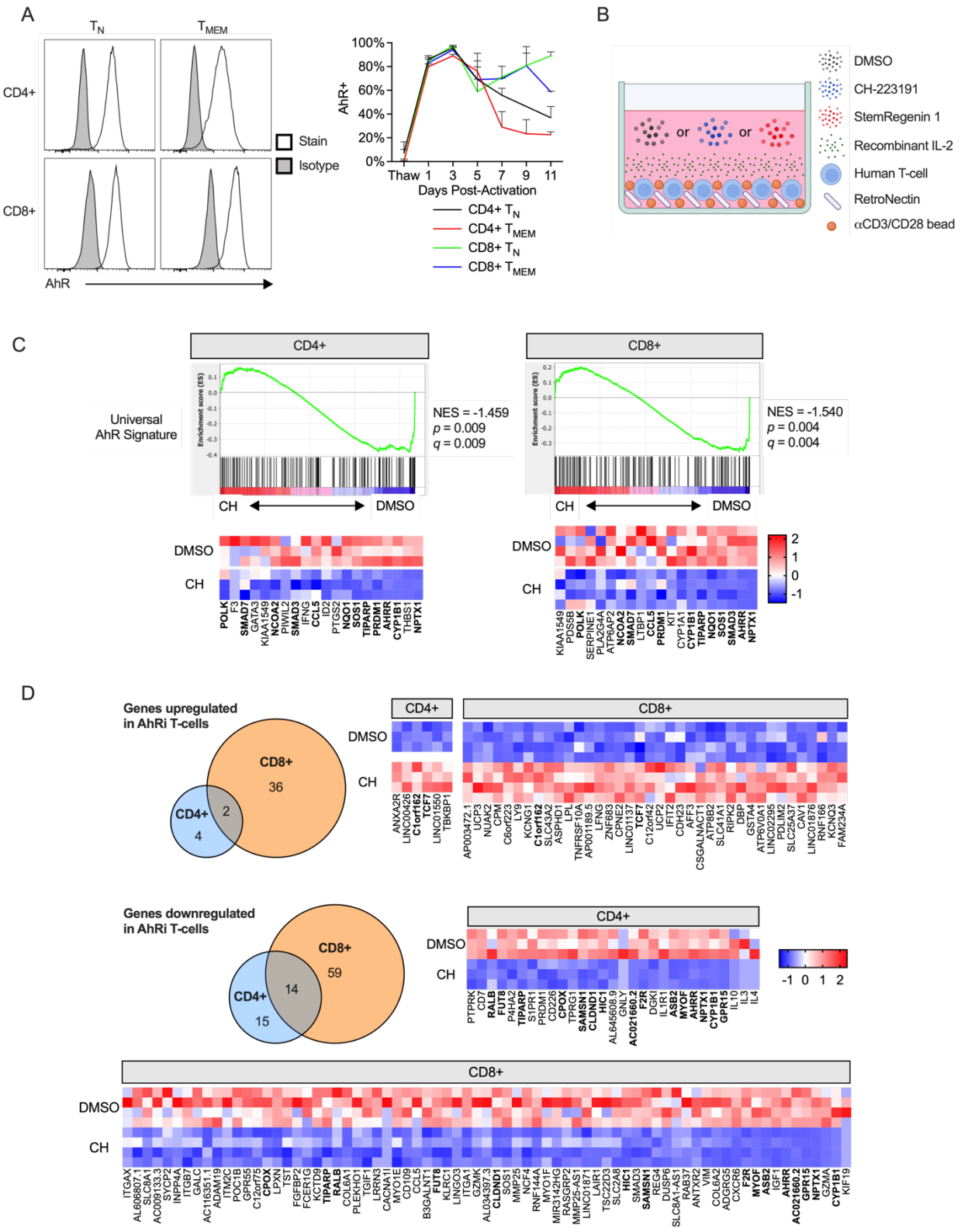

Figure 3.1. AhR controls gene expression following T-cell activation

(A) Left: Flow cytometry of AhR expression in human CD4+ and CD8+ T_N and T_{MEM} 3 days after activation with αCD3/CD28 mAb-coated beads and IL-2. Histograms show one representative donor. Right: percent of T-cells expressing AhR at rest and over time after activation. N=3-6 donors per T-cell subset.
(B) Schematic of T-cell activation with vehicle DMSO, CH-223191 or StemRegenin 1.
(C) GSEA of RNAseq data generated from CD4+ and CD8+ T_N 3 days after activation with αCD3/CD28 beads and IL-2 in the presence of DMSO or 5μm CH-223191. Significance was established as *p* and FDR *q* both <0.05. Top: running enrichment score plots. Bottom: heatmaps depicting Z-scores of normalized counts for the top 20 leading edge genes. Bolded genes were found in the top 20 leading edge genes of both CD4+ and CD8+ datasets.
(D) Differentially-expressed genes quantified by RNAseq among CD4+ and CD8+ T_N activated with αCD3/CD28 beads and IL-2 in the presence of DMSO or 5μm CH-223191. N=3 for CD4+ and 4 for CD8+ T-cell samples. Significance was established as a minimum fold change of 1.5 and $p<0.05$. Top left: Venn diagram depicting numbers of CD4+ and CD8+ shared and individual differentially-expressed genes enriched in AhRi compared to control T-cells. Top right: heatmap depicting differentially-expressed genes enriched in AhRi CD4+ and CD8+ compared to control T-cells; bolded genes were differentially expressed in both CD4+ and CD8+ T-cells. Bottom left: Venn diagram depicting numbers of CD4+ and CD8+ shared and individual differentially-expressed genes enriched in control compared to AhRi T-cells. Bottom right: heatmap depicting differentially-expressed genes enriched in control CD4+ and CD8+ compared to AhRi T-cells; bolded genes were differentially expressed in both CD4+ and CD8+ T-cells. Heatmaps depict Z-scores of normalized transcript counts. See also **Supplemental Tables 7 and 8**.

GSEA using the Hallmark gene sets demonstrated enrichment of c-MYC target genes, genes involved in the Wnt/β-catenin and NOTCH signaling pathways, and IFNα response genes in AhRi CD8+ T-cells relative to control CD8+ T-cells. AhRi CD4+ T-cells were not statistically significantly enriched for any pathways, though similar trends were observed for the Wnt/β-catenin, NOTCH and IFNα signaling gene sets [Figure 3.2A]. Control CD4+ and CD8+ T-cells both bordered on significant enrichment for the TGFβ signaling gene set relative to AhRi T-cells [Figure 3.2A]. Thus, AhR inhibition alters expression of many genes in distinct transcriptional pathways that play roles in T-cell differentiation and behavior.

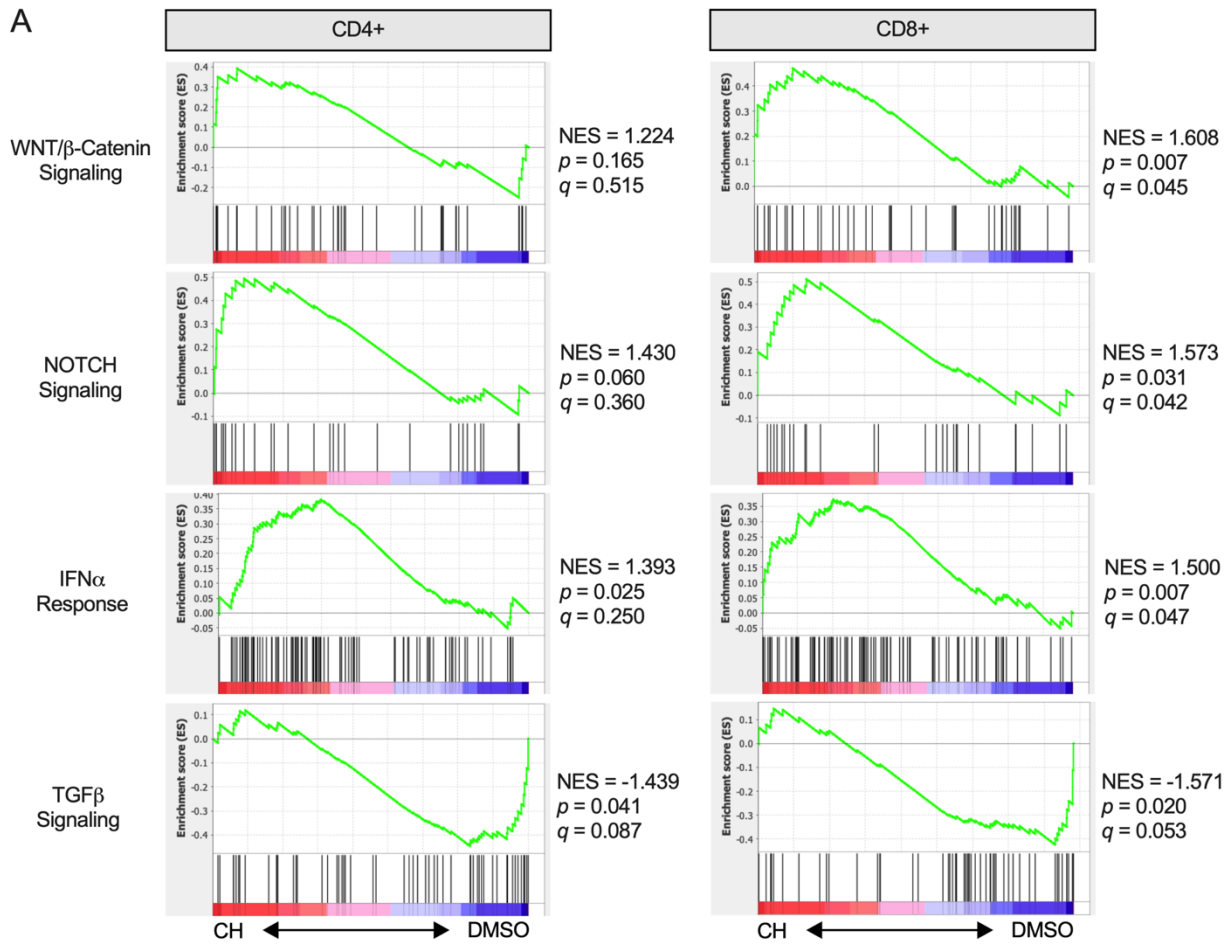

Figure 3.2. Gene sets controlled by AhR following T-cell activation
(A) GSEA of RNAseq data generated from CD4+ and CD8+ T_N 3 days after activation with αCD3/CD28 beads and IL-2 in the presence of DMSO or 5μm CH-223191. Significance was established as *p* and FDR *q* both <0.05.

AhRi enhances T-cell proliferation without driving differentiation.

Given the significant changes to activated T-cell gene expression mediated by AhR inhibition, we sought to further characterize the effects of AhRi on T-cell growth and differentiation. Bulk CD4+ and CD8+ T-cells cultured under control and AhRi conditions demonstrated similar expansion over the first 7 days of culture, after which control T-cell numbers plateaued and AhRi T-cell numbers continued to rise [Figure 3.3A]. Minimal differences in cell viability were observed between control and AhRi cultures [Figure 3.3B], suggesting differential survival did not significantly contribute to altered expansion. Cell cycle profiling on day 7 revealed that fewer AhRi T-cells were in G0/G1 phase and more were in S

phase compared to control T-cells, indicating that AhRi prolonged proliferation [Figure 3.3C]. AhRi similarly enhanced expansion of CD4+ and CD8+ T_N and T_{MEM}, demonstrating that the observed effect was not subset-specific [Figure 3.3D].

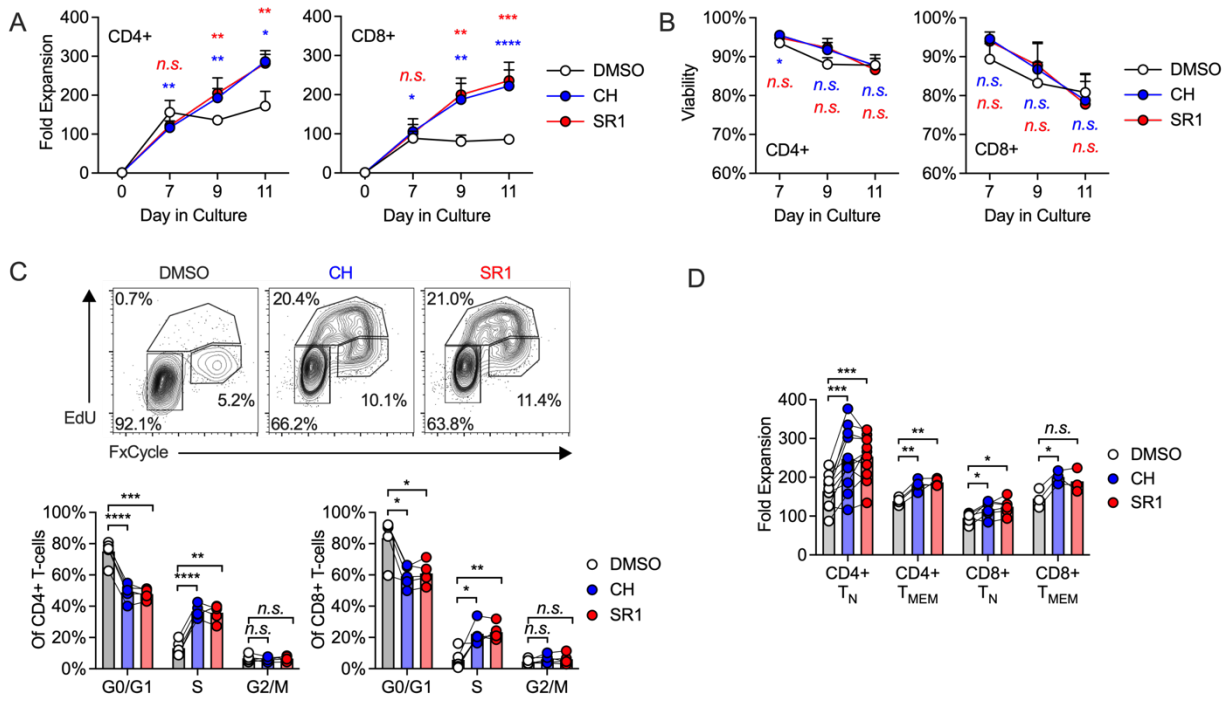

Figure 3.3. AhR inhibition enhances T-cell proliferation during *ex vivo* culture

(A-C) Bulk CD4+ and CD8+ T-cells were activated with αCD3/CD28 beads and IL-2 and grown in the continuous presence of vehicle DMSO, 5μM CH-223191 or 5μM StemRegenin 1. N=5 donors per subset.

(A) T-cell fold expansion over time. One-way ANOVA with Dunnett's test comparing CH and SR1 against DMSO; *p<0.05, **p<0.01, ***p<0.005.

(B) Viability assessed by propidium iodide exclusion over time. One-way ANOVA with Dunnett's test comparing CH and SR1 against DMSO; *p<0.05.

(C) Intracellular staining for EdU incorporation over 2 hours and total DNA content at day 7 after activation. Left: representative flow plots. Right: quantification of cells in Edu^{Low} $FxCycle^{Low}$ (G0/G1), Edu^{High} (S) and Edu^{Int} $FxCycle^{High}$ (G2/M) gates. One-way ANOVA with Dunnett's test comparing CH and SR1 against DMSO; *p<0.05, **p<0.01, ***p<0.005, ****p<0.001.

(D) Day 11 fold expansion of CD4+ and CD8+ T_N and T_{MEM} 11 days after activation with αCD3/CD28 beads and IL-2 in the continuous presence of vehicle DMSO, 5μM CH-223191 or 5μM StemRegenin 1. One-way ANOVA with Dunnett's test comparing CH and SR1 against DMSO; *p<0.05, **p<0.01, ***p<0.005, ****p<0.001. N=11 donors for CD4+ T_N, 4 donors for CD4+ T_{MEM}, 6 donors for CD8+ T_N and 3 donors for CD8+ T_{MEM}.

T-cell proliferation can be accompanied by changes to phenotypic markers correlated with progressive differentiation[184]. To evaluate whether AhR inhibition altered T-cell differentiation, we examined the phenotypes of control and AhRi CD4+ and CD8+ T_N and T_{MEM} cultures on day 11. AhRi modestly increased the fractions of CD4+ T-cells expressing a CD45RA+ CD62L+ stem cell memory (T_{SCM}) phenotype, but did not alter frequencies of CD8+ T-cells expressing T_{SCM}, CD45RA- CD62L+ central memory (T_{CM}) or CD45RA- CD62L- effector memory (T_{EM}) phenotypes [Figure 3.4A]. AhRi T_N-derived CD4+ and CD8+ T-cells expressed higher levels of TCF1 compared to control cultures, and all subsets exhibited striking elevation of CD62L [Figure 3.4B]. All cells in all cultures uniformly expressed CD95, indicating differentiation from T_N [Figure 3.4B]. Thus, AhR inhibition prolonged T-cell proliferation without overtly driving T-cell differentiation.

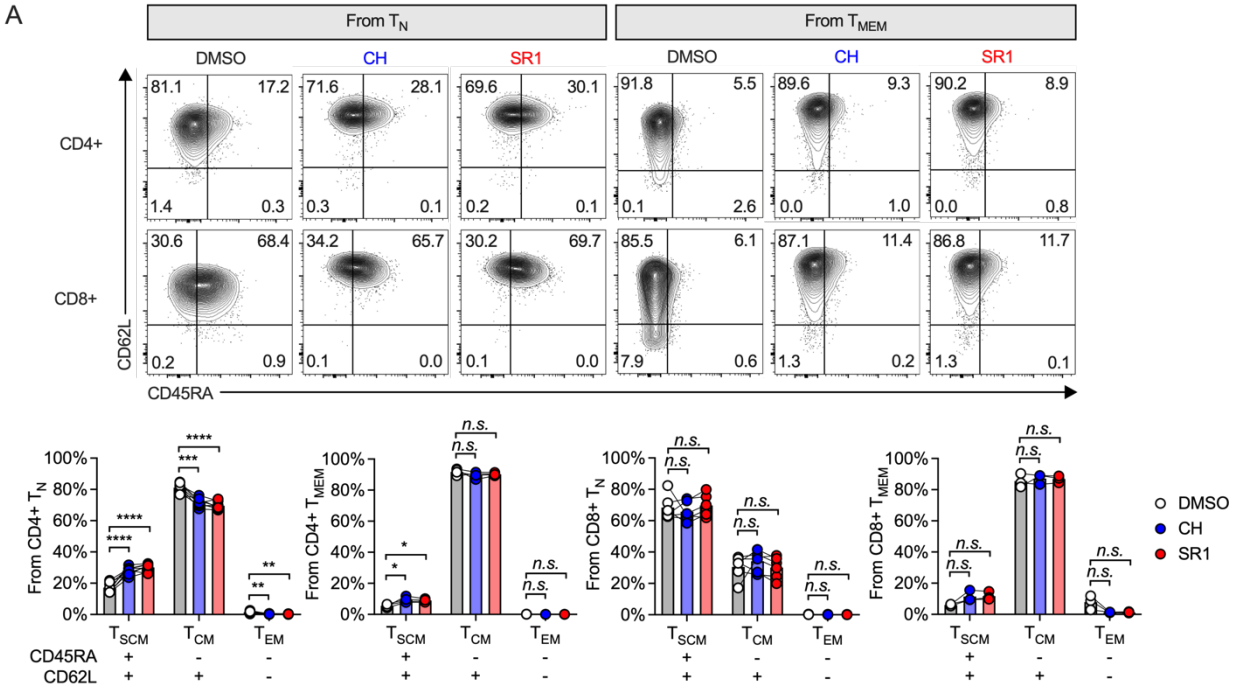

Figure 3.4. AhR inhibition during T-cell culture preserves early T_{MEM} phenotypes
(A) CD45RA and CD62L expression in CD4+ and CD8+ T_N and T_{MEM} 11 days after activation with αCD3/CD28 beads and IL-2 in the continuous presence of vehicle DMSO, 5μM CH-223191 or 5μM StemRegenin 1. Top: representative flow plots. Bottom: quantification of CD45RA and CD62L coexpression. One-way ANOVA with Dunnett's test comparing CH and SR1 against DMSO; *p<0.05, **p<0.01, ***p<0.005, ****p<0.001. N=8 donors for CD4+ T_N, 4 donors for CD4+ T_{MEM}, 6 donors for CD8+ T_N and 3 donors for CD8+ T_{MEM}.

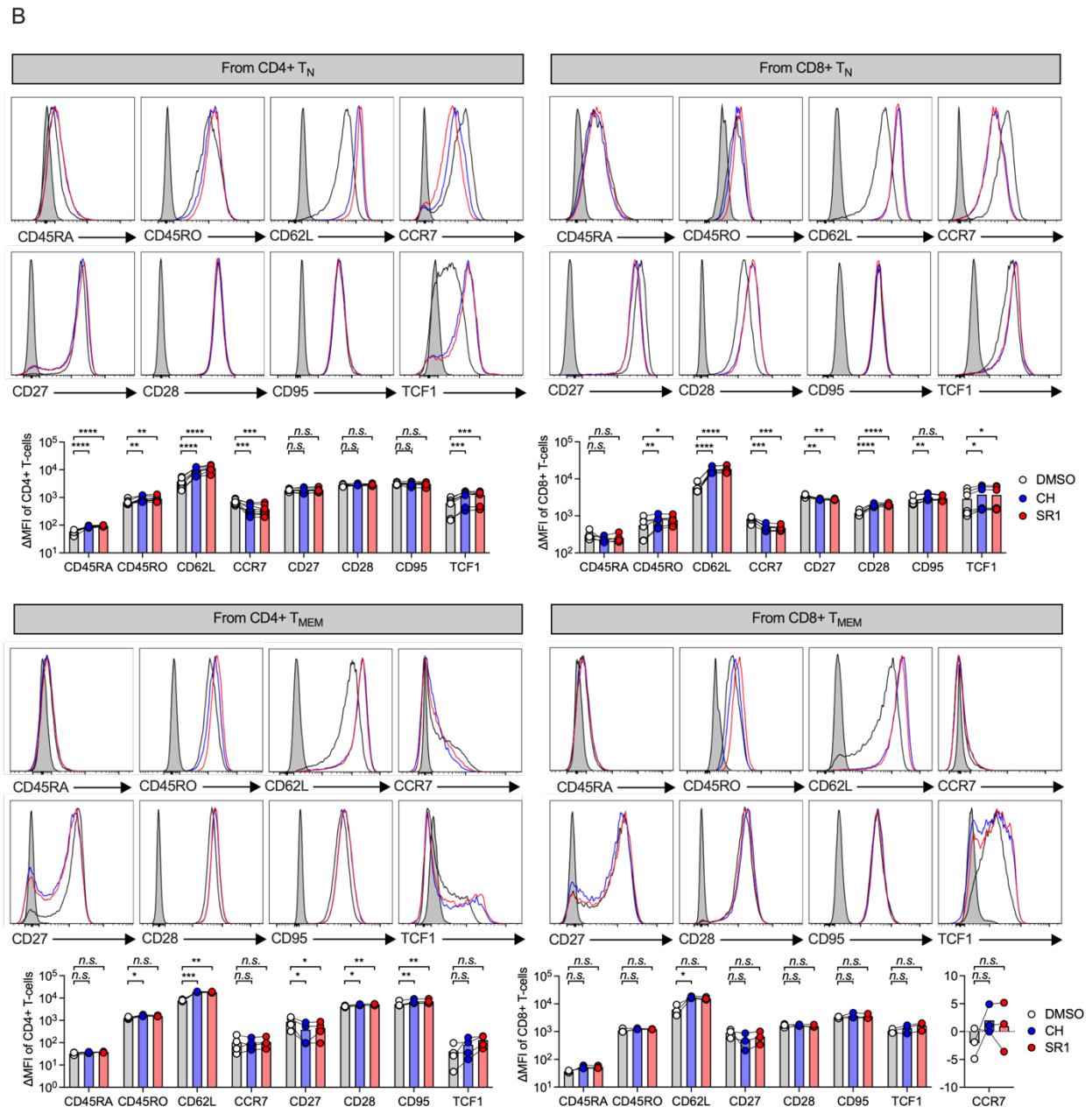

Figure 3.4 (continued). AhR inhibition during culture preserves early T_{MEM} phenotypes

(B) Representative histograms and quantification of surface and intracellular staining for phenotypic markers in CD4+ and CD8+ T_N and T_{MEM} 11 days after activation with αCD3/CD28 beads and IL-2 in the continuous presence of vehicle DMSO, 5μM CH-223191 or 5μM StemRegenin 1. One-way ANOVA with Dunnett's test comparing CH and SR1 against DMSO; *p<0.05, **p<0.01, ***p<0.005, ****p<0.001. N=8 donors for CD4+ T_N, 4 donors for CD4+ T_{MEM}, 6 donors for CD8+ T_N and 3 donors for CD8+ T_{MEM}.

AhRi disinhibits IL-2 production and alters the kinetics of IL-2 signaling.

AhR activity helps limit *Il2* transcription during murine T_H17 induction[129]. We hypothesized that AhRi might disinhibit IL-2 secretion during *in vitro* T-cell activation, leading to the enhanced proliferation observed. To examine potential changes to the IL-2 pathway, we grew CD4+ and CD8+ T_N cultures without supplemental IL-2, and observed that AhRi strikingly increased the amount of IL-2 produced by T-cells in culture medium [Figure 3.5A]. Intracellular staining 72hr after activation demonstrated a higher frequency of IL-2+ T-cells in AhRi than control cultures [Figure 3.5B], and RTqPCR showed elevated levels of *Il2* transcript in AhRi compared to control T-cells [Figure 3.5C], indicating that AhRi enhanced IL-2 production by increasing *Il2* transcription. We did not detect AIOLOS protein expression in either control or AhRi T-cells, suggesting AhRi enhanced IL-2 production directly via AhR or through an alternative pathway.

To confirm that AhRi T-cells displayed evidence of stronger IL-2 signaling, we performed staining for IL-2 receptors and signal transducers at days 3 and 7 of culture. Surprisingly, AhRi T-cells expressed lower levels of the IL-2 receptor chain CD25 and active phosphorylated STAT3 and STAT5 than control T-cells at day 3, while active STAT1 and AKT levels were similar [Figure 3.5D]. Consistent with transcriptomic data, AhRi T-cells also maintained higher levels of TCF1 expression at D3 [Figure 3.5D]. However, at day 7 of culture, AhRi T-cells expressed higher levels of active phosphorylated STAT1, STAT3, STAT5 and AKT [Figure 3.5E], indicating that IL-2 signaling pathways were more active at a timepoint when AhRi T-cells remained actively proliferating.

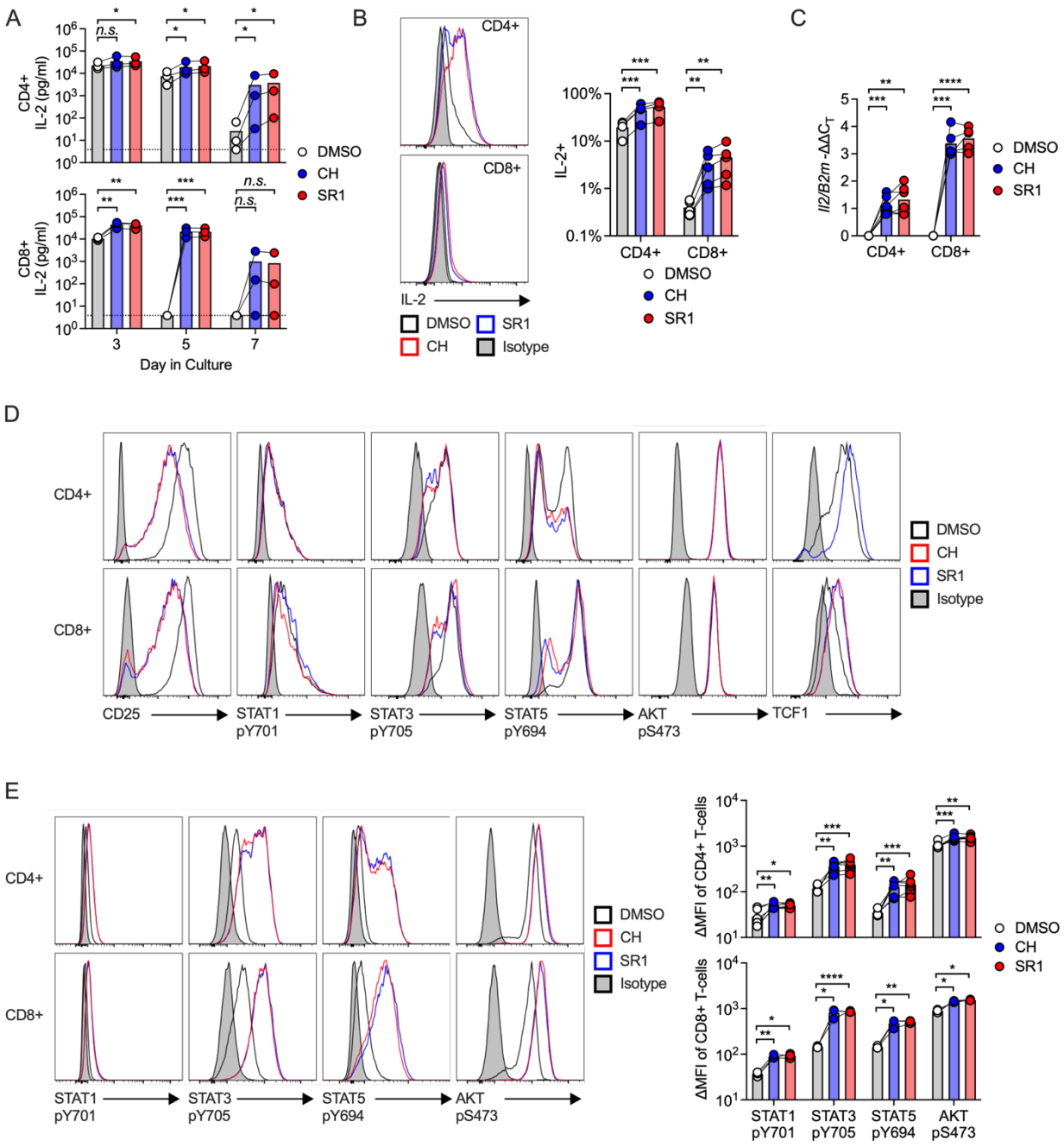

Figure 3.5. AhR inhibition alters IL-2 production and signaling kinetics in naïve T-cells

(A-E) CD4+ and CD8+ T_N were activated with αCD3/CD28 beads without supplemental IL-2 and grown in the continuous presence of vehicle DMSO, 5μM CH-223191 or 5μM StemRegenin 1.

(A) IL-2 in culture medium supernatants harvested over time after activation at day 0. One-way ANOVA of log-transformed pg/ml values with Dunnett's test comparing CH and SR1 against DMSO; *p<0.05, **p<0.01, ***p<0.005. N=3 donors.

(B) Intracellular staining for IL-2 5 hours after addition of GolgiPlug to culture medium on day 3 after activation. Left: representative histograms. Right: IL-2+ cell frequencies quantified. One-way ANOVA

of log-transformed pg/ml values with Dunnett's test comparing CH and SR1 against DMSO; **p<0.01, ***p<0.005. N=4 donors for CD4+ T_N and 5 donors for CD8+ T_N.
(C) RTqPCR for *Il2* gene expression relative to *B2m* on day 3 after activation. One-way ANOVA with Dunnett's test comparing CH and SR1 against DMSO; **p<0.01, ***p<0.005, ****p<0.001.
(D) Surface and intracellular staining for CD25, phosphorylated IL-2 signal transducers and TCF1 expression on day 3 after activation. Representative histograms are shown. N=1 donor for CD4+ TCF1; N≥3 donors for all other analytes.
(E) Intracellular staining for phosphorylated IL-2 signal transducers on day 7 after activation. Left: representative histograms. Right: quantification of mean fluorescence intensity. One-way ANOVA of log-transformed pg/ml values with Dunnett's test comparing CH and SR1 against DMSO; *p<0.05, **p<0.01, ***p<0.005, ****p<0.001. N=6 donors for CD4+ T_N and 3 donors for CD8+ T_N.

IL-2 production and signaling kinetics were similarly altered in AhRi bulk T-cell cultures grown without supplemental IL-2 [Figure 3.6A-E].

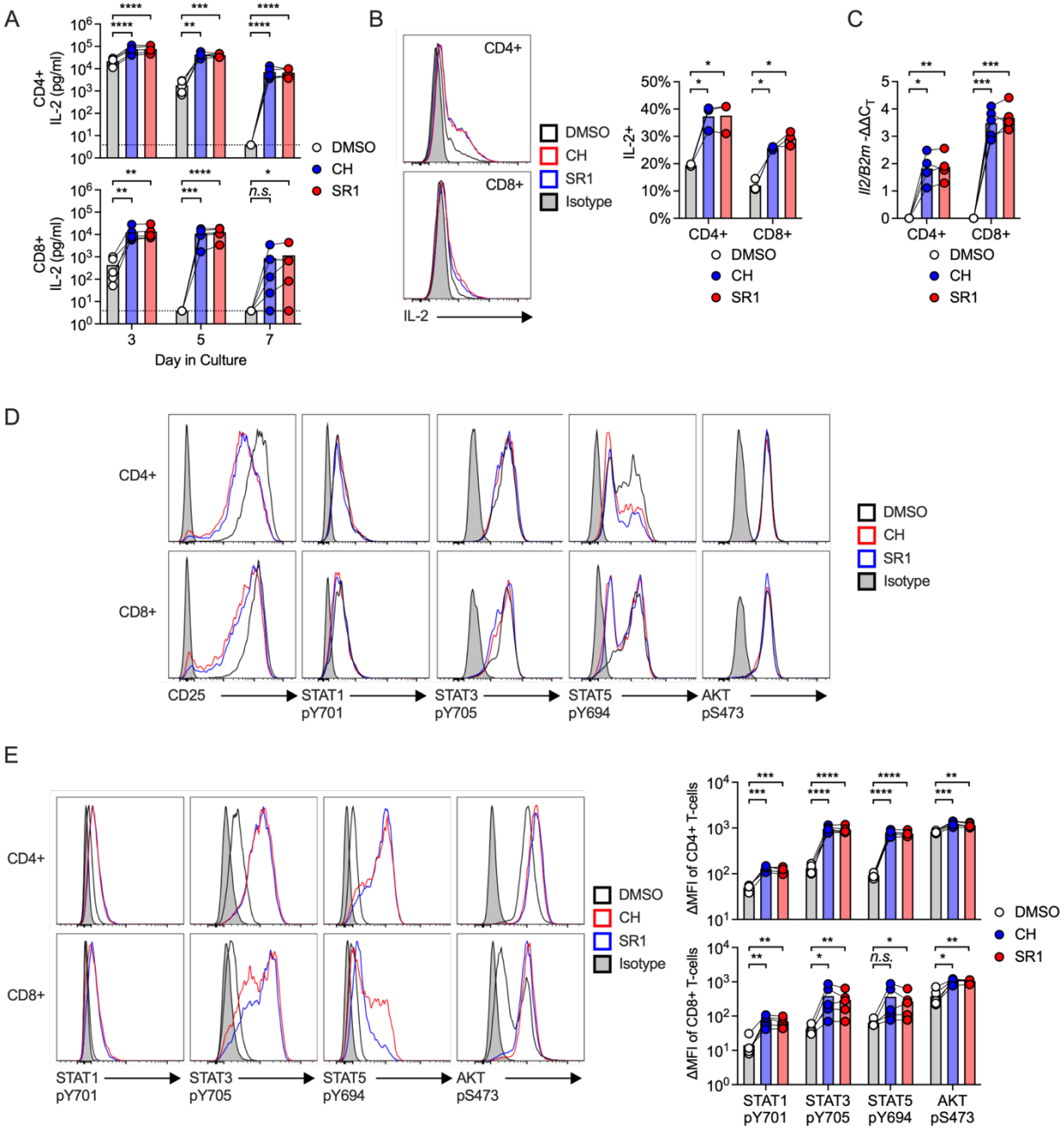

Figure 3.6. AhR inhibition alters IL-2 production and signaling kinetics in bulk T-cells
(A-E) Bulk CD4+ and CD8+ T-cells were activated with αCD3/CD28 beads without supplemental IL-2 and grown in the continuous presence of vehicle DMSO, 5μM CH-223191 or 5μM StemRegenin 1. N=5 donors per subset.

(A) IL-2 in culture medium supernatants harvested over time after activation at day 0. One-way ANOVA of log-transformed pg/ml values with Dunnett's test comparing CH and SR1 against DMSO; *p<0.05, **p<0.01, ***p<0.005, ****p<0.001.
(B) Intracellular staining for IL-2 5 hours after addition of GolgiPlug to culture medium on day 3 after activation. Left: representative histograms. Right: IL-2+ cell frequencies quantified. One-way ANOVA with Dunnett's test comparing CH and SR1 against DMSO; *p<0.05.
(C) RTqPCR for *Il2* gene expression relative to *B2m* on day 3 after activation. One-way ANOVA with Dunnett's test comparing CH and SR1 against DMSO; *p<0.05, **p<0.01, ***p<0.005.
(D) Surface and intracellular staining for CD25 and phosphorylated IL-2 signal transducer expression on day 3 after activation. Representative histograms are shown.
(E) Intracellular staining for phosphorylated IL-2 signal transducers on day 7 after activation. Left: representative histograms. Right: quantification of mean fluorescence intensity. One-way ANOVA of log-transformed pg/ml values with Dunnett's test comparing CH and SR1 against DMSO; *p<0.05, ****p<0.001.

The strong IL-2 production and signaling induced by AhRi further led us to ask whether AhRi could support T-cell expansion in absence of supplemental IL-2. While control bulk CD4+ T-cells expanded healthily without added IL-2, unsupplemented control bulk CD8+ T-cells exhibited low viability by day 7 of culture and could not be expanded further [Figure 3.7A]. In contrast, AhRi T-cells grown without IL-2 expanded as much or more than control T-cells grown with IL-2 [Figure 3.7A], indicating AhRi could supplant exogenous IL-2 in settings where robust T-cell expansion is required. In summary, AhRi enhances IL-2 production while delaying signaling in T-cells, driving enhanced proliferation following activation.

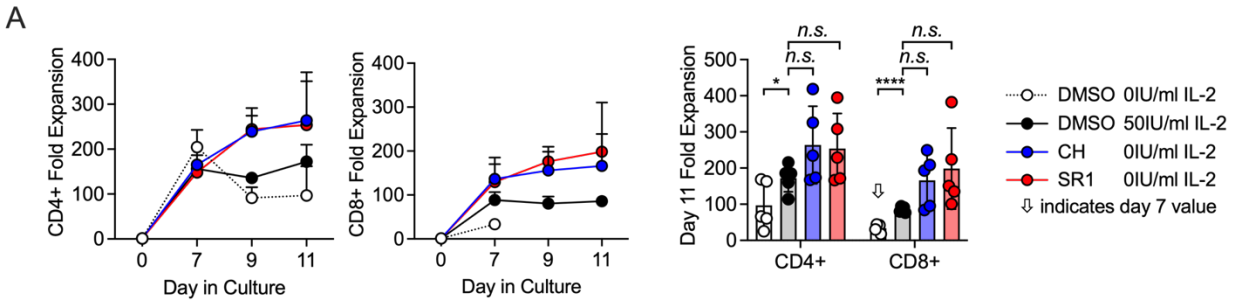

Figure 3.7. AhR inhibition supports robust bulk T-cell expansion in absence of exogenous IL-2
(A) Fold expansion of activated bulk CD4+ and CD8+ T-cells grown in vehicle DMSO with or without IL-2, in 5µM CH-223191 without IL-2, or in 5µM StemRegenin 1 without IL-2. Left: average fold expansion over time. Right: individual expansion 11 days after activation. One-way ANOVA with Dunnett's test comparing CH and SR1 against DMSO; *p<0.05, **p<0.01, ***p<0.005, ****p<0.001. N=5 donors per subset.

AhRi induces T_H1 polarization in CD4+ T_N and augments CD8+ T_N cytokine production.

Given AhR's known roles promoting T_H17, T_H22 and T_R1 development and cytokine production[118,119,122,125–130,177,178], we investigated whether AhRi altered CD4+ T_N polarization. We activated CD4+ T_N in the presence or absence of AhR inhibitors, transduced the cells with a CD19-specific CAR, and evaluated expression of T_H subset-defining TFs at day 3, chemokine receptors at day 11 and cytokines upon restimulation.

AhRi T-cells expressed markedly higher levels of the T_H1-associated TF T-bet, lower levels of T_H2-associated GATA-3 and equivalent levels of T_H17-associated RORγt compared to control T-cells [Figure 3.8A]. We found that AhRi CD4+ T-cells also expressed significantly higher levels of T_H1-associated CXCR3 and lower levels of T_H2-associated CCR4 than control cells at day 11 [Figure 3.8B]. Neither control nor AhRi T-cells expressed T_H17-associated CCR6 [Figure 3.8B]. To assay cytokine production, we restimulated CD19-specific control and AhRi CD4+ CAR-T by co-culture with irradiated CD19+ Raji or K562 tumor cells and measured cytokine levels in culture supernatants by Luminex. AhRi T-cells produced more IFNγ, IL-2 and IL-17, and less IL-4, IL-5 and IL-10 than control T-cells [Figure 3.8C]. Restimulation of control-cultured CAR-T in the presence of AhR inhibitor did not elevate IFNγ or IL-2 secretion, indicating that enhanced T_H1 cytokine production was not an artifact of drug carryover from primary culture [Figure 3.8D]. Together, these data demonstrate that AhRi during activation strongly polarizes CD4+ T_N toward a T_H1 phenotype.

To determine whether AhRi mediated similar changes to CD8+ T-cell cytokine production, we generated CD19-specific control and AhRi CAR-T from CD8+ T_N and restimulated them by co-culture with irradiated CD19+ Raji or K562 tumor cells. Luminex analysis of culture supernatants demonstrated that AhRi CAR-T derived from CD8+ T_N produced more IFNγ, TNFα and IL-2 and less Granzyme B than control CAR-T [Figure 3.8E], indicating that AhRi during primary CD8+ T_N activation enhances T_C1 function during subsequent antigen responses.

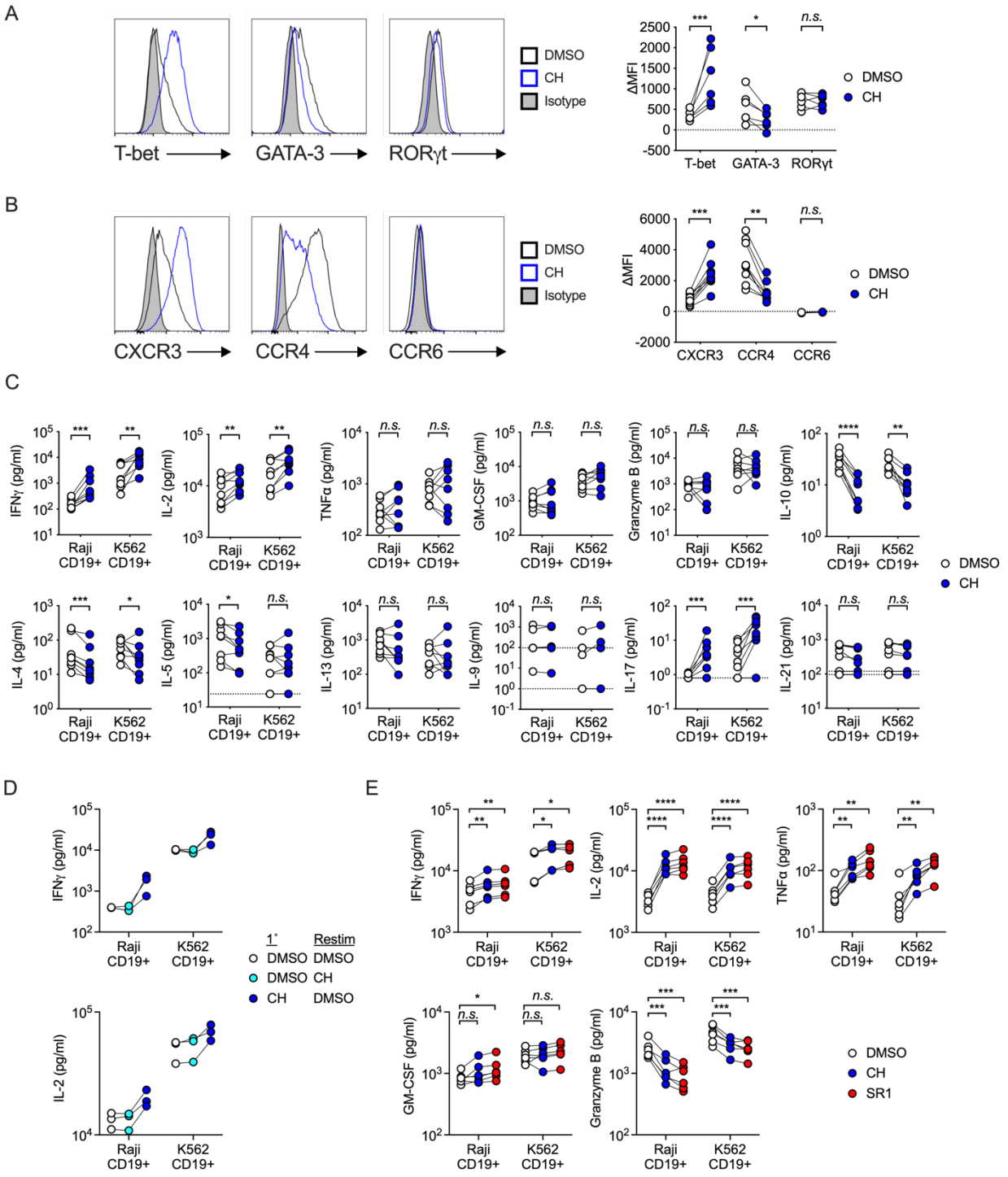

Figure 3.8. AhR inhibition augments T_H1 and T_C1 cytokine production by T_N-derived CAR-T
(A-E) CD4+ and CD8+ T_N were activated with αCD3/CD28 beads with IL-2, transduced with a CD19-specific CAR and grown in the continuous presence of vehicle DMSO, 5μM CH-223191 or 5μM StemRegenin 1.

(A) Intracellular staining of CD4+ T-cells for T_H master regulator transcription factors on day 3. Left: representative histograms. Right: quantification of mean fluorescence intensity. Ratio-paired (T-bet, RORγt) or paired (GATA-3) two-tailed student's T-test; *p<0.05, ***p<0.005. N=6 donors.
(B) Staining of CD4+ T-cells for T_H subset-characteristic chemokine receptors on day 11. Left: representative histograms. Right: quantification of mean fluorescence intensity. Ratio-paired (CXCR3, CCR4) or paired (CCR6) two-tailed student's T-test; **p<0.01, ***p<0.005. N=6-9 donors.
(C) Luminex quantification of cytokines in culture supernatants produced by CD4+ CAR-T after 24hr co-culture with irradiated CD19+ Raji or K562 tumor cells in absence of AhR inhibitor. Dotted lines indicate limits of detection. Ratio-paired two-tailed student's T-test; *p<0.05, **p<0.01, ***p<0.005, ****p<0.001. N=8 donors.
(D) Luminex quantification of cytokines in culture supernatants produced by CAR-T derived from CD4+ T_N after 24hr co-culture with irradiated CD19+ Raji or K562 tumor cells. Control-cultured CAR-T were restimulated in the presence of vehicle DMSO or 5μM CH-223191, and AhRi-cultured CAR-T were restimulated in the presence of vehicle DMSO.
(E) Luminex quantification of cytokines in culture supernatants produced by CD8+ CAR-T after 24hr co-culture with irradiated CD19+ Raji or K562 tumor cells in absence of AhR inhibitor. Ratio-paired two-tailed student's T-test; *p<0.05, **p<0.01, ***p<0.005, ****p<0.001. N=6 donors.

We further evaluated whether AhRi mediated similar effects on CAR-T produced from T_{MEM}. CD4+ T_{MEM} activated in the presence of AhR inhibitors similarly upregulated expression of T-bet and CXCR3 and downregulated CCR4 compared to control T-cells, but GATA-3 expression was unaffected [Figure 3.9A,B]. Like AhRi-cultured CD4+ T_N, AhRi CD4+ T_{MEM} produced lower levels of T_H2-characteristic cytokines, but did not produce less IL-10 or more IFNγ or IL-2 than control T-cells [Figure 3.9C]. Similarly, AhRi and control CAR-T derived from CD8+ T_{MEM} produced comparable levels of cytokines [Figure 3.9D]. Thus, AhR plays distinct roles in programming the effector functions of CD4+ T_N and T_{MEM}.

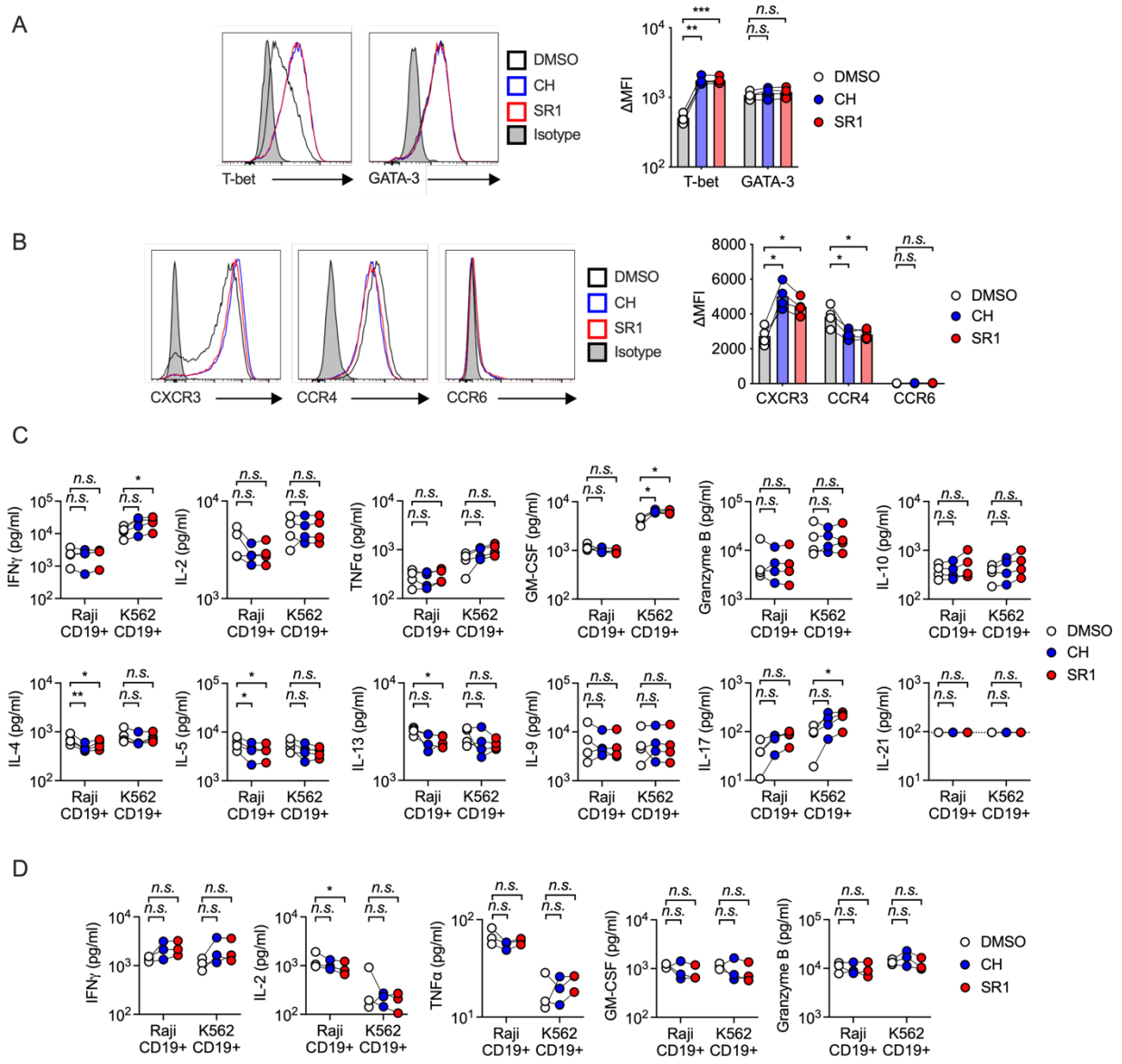

Figure 3.9. AhR inhibition does not substantially alter T_{MEM}-derived CAR-T cytokine production
(A-D) CD4+ (4 donors) and CD8+ T_{MEM} (3 donors) were activated with αCD3/CD28 beads with IL-2, transduced with a CD19-specific CAR and grown in the continuous presence of vehicle DMSO, 5μM CH-223191 or 5μM StemRegenin 1.
(A) Intracellular staining of CD4+ T-cells for T_H master regulator transcription factors on day 3. Left: representative histograms. Right: quantification of mean fluorescence intensity. One-way ANOVA of log-transformed values with Dunnett's test comparing CH and SR1 against DMSO; $^{**}p<0.01$, $^{***}p<0.005$.
(B) Staining of CD4+ T-cells for T_H subset-characteristic chemokine receptors on day 11. Left: representative histograms. Right: quantification of mean fluorescence intensity. One-way ANOVA of log-transformed values with Dunnett's test comparing CH and SR1 against DMSO; $^{*}p<0.05$.
(C) Luminex quantification of cytokines in culture supernatants produced by CD4+ CAR-T after 24hr co-culture with irradiated CD19+ Raji or K562 tumor cells in absence of AhR inhibitor. Dotted lines

indicate limits of detection. One-way ANOVA of log-transformed values with Dunnett's test comparing CH and SR1 against DMSO; *p<0.05, **p<0.01.
(D) Luminex quantification of cytokines in culture supernatants produced by CD8+ CAR-T after 24hr co-culture with irradiated CD19+ Raji or K562 tumor cells in absence of AhR inhibitor. One-way ANOVA of log-transformed values with Dunnett's test comparing CH and SR1 against DMSO; *p<0.05.

AhRi programs prolonged CD8+ CAR-T proliferation in response to subsequent antigen stimulation.

T-cells that have been extensively expanded *ex vivo* demonstrate weaker proliferative responses to antigen restimulation[36]. However, the high levels of IL-2 produced by AhRi CAR-T in response to tumor suggested that AhRi culture might instead enhance proliferation during subsequent antigen encounters. We profiled T-cell proliferative capacity by labeling CD19-specific control and AhRi CAR-T derived from T_N with CFSE dye, and restimulating labeled CAR-T by co-culture with irradiated CD19+ Raji or K562 tumor cells.

Control and AhRi CD4+ CAR-T proliferated equivalently following restimulation, diluting CFSE to similar extents 3 and 5 days after initiation of co-culture [Figure 3.10A]. Control and AhRi CD8+ CAR-T proliferated to the same extent through day 3, but AhRi CAR-T demonstrated greater CFSE dilution at 5 days, indicating increased proliferation later after restimulation [Figure 3.10B]. Cell cycle profiling of CAR-T at day 5 post-restimulation showed no differences between control and AhRi CD4+ CAR-T, but revealed elevated frequencies of AhRi CD8+ CAR-T in S or G2/M phases and less cells in G0/1 [Figure 3.10C], indicating AhRi CD8+ CAR-T were capable of sustaining proliferation following antigen restimulation for longer than control CAR-T. These data demonstrate that the increased expansion AhRi promotes during primary culture does not compromise subsequent proliferative responses to antigen stimulation, and, to the contrary, that AhRi culture confers CD8+ CAR-T with a capacity for prolonged proliferation.

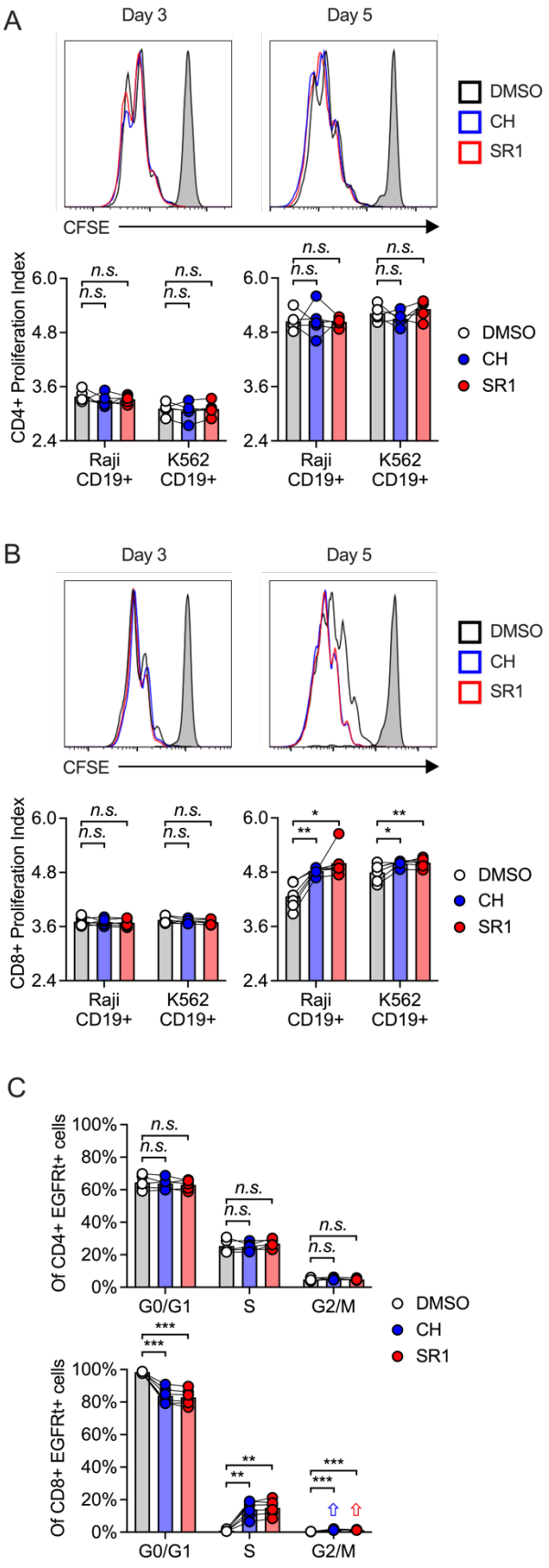

Figure 3.10. AhR inhibition promotes robust CAR-T proliferation following antigen stimulation

(A-C) CD4+ (5 donors) and CD8+ T_N (6 donors) were activated with αCD3/CD28 beads with IL-2, transduced with a CD19-specific CAR and grown in the continuous presence of vehicle DMSO, 5μM CH-223191 or 5μM StemRegenin 1. On day 11, CAR-T were labeled with CFSE dye and restimulated by co-culture with irradiated CD19+ Raji or K562 tumor cells in absence of AhR inhibitor.

(A) CFSE dilution by CD4+ CAR-T 3 and 5 days after restimulation. Top: representative histograms. Bottom: quantification of proliferation indices. One-way ANOVA with Dunnett's test comparing CH and SR1 against DMSO.

(B) CFSE dilution by CD8+ CAR-T 3 and 5 days after restimulation. Top: representative histograms. Bottom: quantification of proliferation indices. One-way ANOVA with Dunnett's test comparing CH and SR1 against DMSO; *p<0.05, **p<0.01.

(C) Quantification of restimulated CAR-T in Edu^{Low} $FxCycle^{Low}$ (G0/G1), Edu^{High} (S) and Edu^{Int} $FxCycle^{High}$ (G2/M) gates after intracellular staining for EdU incorporation over 2 hours and total DNA content at day 5 after restimulation. One-way ANOVA with Dunnett's test comparing CH and SR1 against DMSO; **p<0.01, ***p<0.005.

AhRi CAR-T mediate superior anti-tumor effects in a xenograft lymphoma model.

Given the enhanced function of AhRi CAR-T in response to tumor *in vitro*, we next investigated whether AhRi CAR-T mediated superior anti-tumor effects *in vivo*. NSG mice were injected intravenously with CD19+ Raji tumor cells to model disseminated Burkitt lymphoma, then treated 7 days later with CD19-specific control or AhRi CAR-T derived from T_N. CAR-T expansion *in vivo* was monitored by flow cytometry of peripheral blood, and tumor burden was assessed by bioluminescent imaging.

We first assessed the effects of AhRi on CD4+ CAR-T performance by treating mice with either $8x10^5$ or $1.6x10^6$ DMSO or CH CD4+ CAR-T. AhRi CD4+ CAR-T demonstrated enhanced expansion early after transfer and persisted at equivalent frequencies in the peripheral blood [Figure 3.11A]. This expansion was accompanied by modest early improvements in tumor control, but differences in tumor burden did not maintain statistical significance over time [Figure 3.11B]. The development of graft-versus-host disease after day 27 post CAR-T treatment precluded longer-term tumor control analysis. We next examined whether AhRi altered CD8+ CAR-T efficacy by treating tumor-bearing mice with $5x10^5$ DMSO or CH CD8+ CAR-T. While one donor exhibited enhanced peak AhRi CAR-T expansion [Figure 3.11C] and improved tumor control 55 days after treatment [Figure 3.11D], another demonstrated no improvement in CAR-T expansion or tumor control [Figure 3.11C-D], indicating AhRi conferred therapeutic benefit to CD8+ CAR-T in a donor-specific manner.

Given the marginal benefits that AhRi conferred to individual CD4+ and CD8+ CAR-T treatments, we asked whether combining AhRi CD4+ and CD8+ CAR-T would improve therapeutic efficacy to a greater extent. Tumor-bearing mice were treated with CD4+ and CD8+ CAR-T grown separately in either control or AhRi conditions and combined in a 1:1 CD4:CD8 ratio at infusion. While no difference was observed in CAR-T expansion or persistence [Figure 3.11E], AhRi CAR-T mediated enhanced tumor regression compared to control CAR-T [Figure 3.11F], suggesting AhRi during CAR-T production preserved subsequent T-cell function *in vivo*. These studies indicate that, in contrast to T-cells expanded by repeated antigen and cytokine stimulation[36,184], highly-expanded AhRi CAR-T exhibit enhanced anti-tumor functionality.

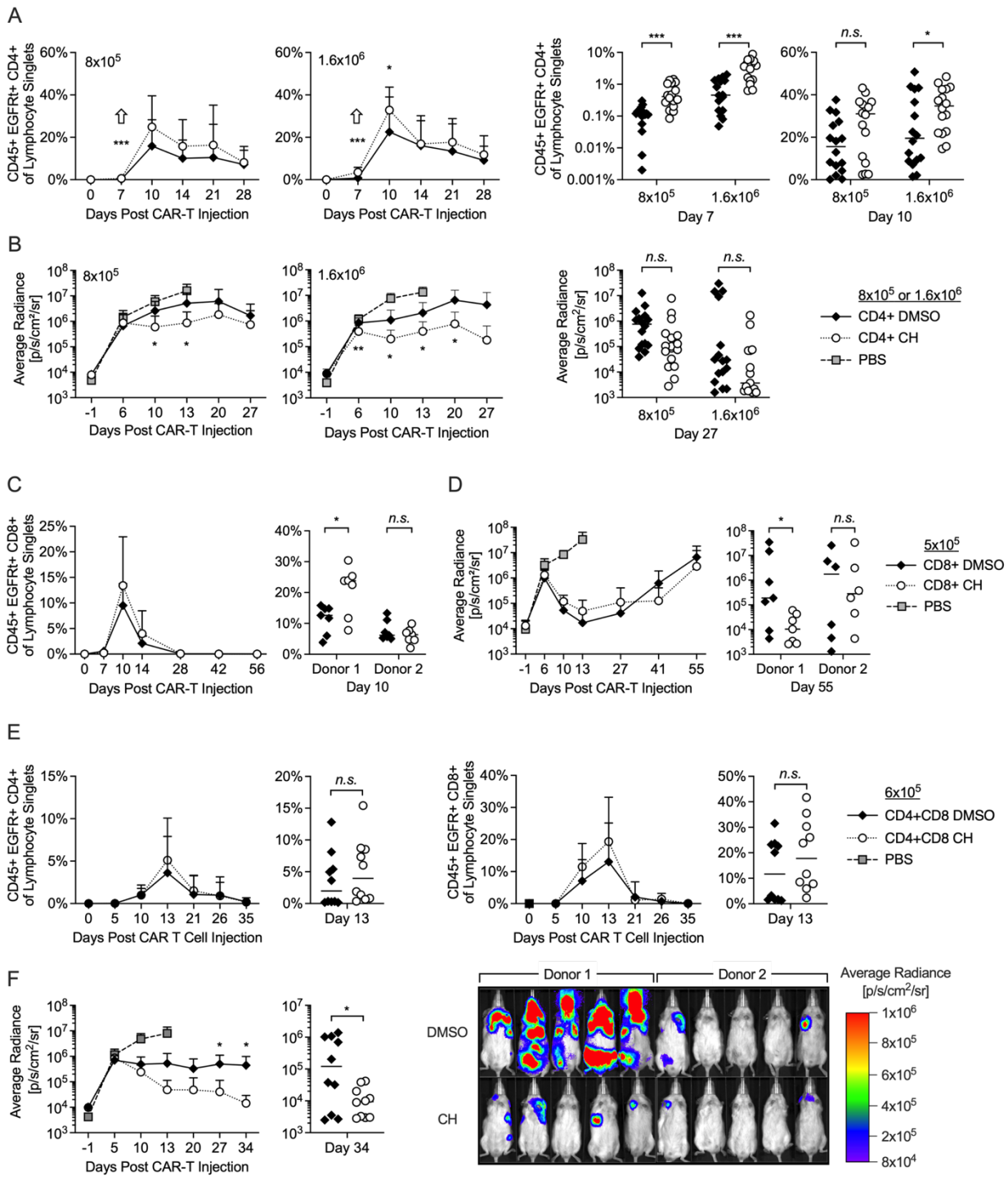

Figure 3.11. AhRi CAR-T mediate potent anti-tumor effects

(A-F) Disseminated Burkitt lymphoma was modeled by intravenous injection of $5x10^5$ CD19+ Raji tumor cells expressing firefly luciferase into NSG mice. 7 days later, tumor-bearing mice were treated with intravenous injection of PBS or (A-B) $8x10^5$ or $1.6x10^6$ CD4+, (C-D) $5x10^5$ CD8+ or (E-F) $6x10^5$ CD4+ and CD8+ CD19-specific CAR-T that had been cultured in vehicle DMSO or 5µM CH-223191. Tumor burden was measured weekly by intraperitoneal luciferin injection and

bioluminescent imaging, and CAR-T expansion was quantified over time by flow cytometry of peripheral blood. Mice were sacrificed when they met tumor euthanasia criteria or developed GvHD.
(A) CD4+ CAR-T expansion and persistence *in vivo*. Left: average frequencies of CD4+ CAR-T over time in peripheral blood of mice dosed with $8x10^5$ or $1.6x10^6$ cells. Right: frequencies of CD4+ CAR-T in peripheral blood in individual mice 7 and 10 days after CAR-T injection. Two-tailed student's T-test; *p<0.05, ***p<0.005. N=3 donors, 16 mice.
(B) Tumor burden in CD4+ CAR-T-treated mice. Left: average tumor radiance over time in mice dosed with $8x10^5$ or $1.6x10^6$ cells. Right: tumor radiance in individual mice 27 days after CAR-T injection. Mann-Whitney U test; *p<0.05, **p<0.01. N=3 donors, 16 mice.
(C) CD8+ CAR-T expansion and persistence *in vivo*. Left: average frequencies of CD8+ CAR-T in peripheral blood over time. Right: frequencies of CD8+ CAR-T in peripheral blood in individual mice 10 days after CAR-T injection. Two-tailed student's T-test; *p<0.05. N=2 donors, 14 mice.
(D) Tumor burden in CD8+ CAR-T-treated mice. Left: average tumor radiance over time. Right: tumor radiance in individual mice 55 days after CAR-T injection. Mann-Whitney U test; *p<0.05. N=2 donors, 14 mice.
(E) CD4+ and CD8+ CAR-T expansion and persistence *in vivo*. Left: average frequencies of CD4+ CAR-T in peripheral blood over time, and individual frequencies 13 days after CAR-T injection. Right: average frequencies of CD8+ CAR-T in peripheral blood over time, and individual frequencies 13 days after CAR-T injection. Two-tailed student's T-test. N=2 donors, 10 mice.
(F) Tumor burden in mice treated with CD4+ and CD8+ CAR-T. Left: average tumor radiance over time, and radiances of individual mice 34 days after CAR-T injection. Right: bioluminescent imaging of tumor burden in mice 34 days after CAR-T injection. Mann-Whitney U test; *p<0.05. N=2 donors, 10 mice.

Discussion

CAR-T therapy is an effective platform for treating hematologic malignancies, but efficacy can be compromised by the inability of *ex vivo* culture systems to robustly expand T-cells while maintaining their capacity to mount effective anti-tumor responses *in vivo*. Cell culture and engineering strategies that promote cellular states characteristic of quiescent T_{MEM}[43,46,47] or inhibit pathways that drive and support effector T-cell development[38,40–42,45] have demonstrated utility in enhancing tumor-specific T-cell therapeutic potency. However, few of these strategies facilitate T-cell expansion *ex vivo*, and supplementation with high levels of exogenous IL-2 to support proliferation can drive T-cell differentiation and limit function[185,186].

The aryl hydrocarbon receptor was originally described as a driver of regulatory T-cell and T_H17 development[117–119,122,125,126,128–130]; only more recently has AhR been implicated as an important mediator of T-cell dysfunction in tumor microenvironments[133,165,179–181,183,187]. The

finding that IL-2-induced tryptophan metabolism can activate AhR in T-cells and trigger features of exhaustion demonstrated that AhR activity also functions as an autoregulatory axis in activated T-cells[136]. Given that T-cell activation induces AhR expression[136], and that CD3/CD28 ligation and supplemental IL-2 are commonly utilized to expand tumor-specific T-cells *ex vivo*, we explored how inhibition of AhR activity during human CAR-T production affected T-cell transcription, growth, differentiation and antigen responses to tumor.

AhRi markedly enhanced T-cell transcription and production of IL-2 following *ex vivo* activation, prolonging proliferation and augmenting net expansion. However, in seeming contrast to IL-2's known roles driving effector differentiation and corresponding loss of function[36,54–57], highly-expanded AhRi CAR-T maintained expression of early T_{MEM} phenotypes at day 11, and robustly proliferated and produced abundant cytokine upon tumor encounter. Despite high levels of IL-2 in culture medium 3 days after activation, AhRi T-cells expressed lower levels of CD25 and active STAT3 and STAT5 than control T-cells, and only showed evidence of stronger IL-2 signaling after 7 days of culture. AhRi T-cells expressed higher levels of several transcripts associated with effective T-cell responses to tumor on day 3, including genes that limit reactive oxygen species accumulation[188] and the stemness-associated transcription factor *Tcf7*[189]. Moreover, AhRi T-cell expression of genes associated with glycolytic metabolism, cytotoxicity and commitment to T_H2, T_R1 or T_{RM} identities was diminished, indicating that AhRi attenuated effector differentiation early after activation.

STAT5 drives expression of cytotoxic molecules, glycolytic enzymes and coinhibitory receptors while diminishing expression of *Tcf7*[190], suggesting that modulation of IL-2 signaling by AhRi may underlie many of the observed transcriptional differences. Rapid expansion of tumor-infiltrating lymphocytes beginning with low supplemental IL-2 concentrations and progressing to high concentrations later in culture yielded robustly-expanded T-cell products that produced high levels of IFNγ and effectively killed target cells[54]; similar IL-2 signaling kinetics imposed by AhRi may contribute to maintenance of T-cell function following extensive expansion.

AhRi culture augmented T_C1-characteristic cytokine production and T_H1-characteristic T-bet, CXCR3, IFNγ and IL-2 expression in CAR-T derived from CD8+ and CD4+ T_N respectively. Our

finding that the addition of AhR inhibitor during restimulation of control-cultured T_N-derived CAR-T did not similarly alter cytokine production confirmed that augmented cytokine production by AhRi-cultured CAR-T reflected changes to T-cell state during primary culture. IL-2 is a well-described driver of T-bet and T_H1 polarization[129,191], but diminished CD25 expression and STAT3 and STAT5 activation were observed in AhRi T-cells at the same timepoint at which T-bet expression was elevated. *Tbx21* transcription can be limited by both constitutive STAT5 activity[190] and STAT5 deletion[191], suggesting that STAT5 signaling of variable duration or intensity could differentially regulate T-bet expression, or that other signals induced by IL-2 receptor ligation might modulate effects on T-bet expression.

AhRi may also enhance T-bet expression independently of IL-2: IFN signaling via STAT1 induces *Tbx21* transcription[192], and AhRi T-cells expressed elevated levels of many IFN response genes. While AhRi T-cells did not produce elevated IFNγ in culture medium or demonstrate increased STAT1 activation at day 3, it is possible that AhR regulates STAT1's transcriptional effects downstream of IFN binding. This potential regulatory function in T-cells would complement AhR's known role limiting type I IFN responses by regulating IFNβ transcription downstream of pattern recognition receptor engagement in fibroblasts via TIPARP induction[193]. Given the critical roles of IFNγ, TNFα and IL-2 production in immune responses to tumors, further elucidation of the mechanism(s) by which AhRi promotes T_H1/T_C1 development and function could inform development of additional strategies to enhance anti-tumor immunity.

AhRi culture did not alter CD4+ CAR-T proliferative responses to tumor over 5 days, but extended the magnitude and duration of CD8+ CAR-T proliferation. AhRi CD8+ CAR-T proliferation indices approached those of CD4+ CAR-T on day 5, and similar frequencies of cells remained proliferating. Differences in the relative amounts of IL-2 produced by restimulated cells may contribute to these observations: while AhRi increased CD4+ CAR-T production of IL-2 by an average of 1.7-fold, AhRi CD8+ CAR-T produced 3.2-fold more IL-2 than control CD8+ CAR-T, achieving concentrations as high as Raji-restimulated control CD4+ CAR-T. Increased AhRi CD8+ CAR-T proliferation in absence of an effect on CD4+ CAR-T may result from a larger relative increase in IL-2 production from control.

Consistent with improved *in vitro* function, AhRi CAR-T mediated superior tumor regression in NSG mice bearing disseminated Burkitt lymphoma xenografts. This result provides key confirmation that the improved *ex vivo* T-cell expansion driven by AhRi does not hasten loss of function longer-term, and that AhR is a critical mediator of many of the differentiation-promoting effects of IL-2 signaling that are detrimental to T-cell immunotherapy efficacy. We also found that AhRi could replace exogenous IL-2 to support CAR-T proliferation *ex vivo*, inviting further comparison of CAR-T expanded with IL-2 against AhRi CAR-T generated without IL-2. Use of inexpensive small molecule AhR inhibitors to replace supplemental IL-2 during commercial tumor-specific T-cell culture has the potential to both reduce the cost and augment the potency of tumor specific T-cell therapies.

In summary, AhR inhibition during T-cell culture increases IL-2 production and proliferation while maintaining early T_{MEM} phenotypes. AhRi-cultured CAR-T exhibit augmented T_H1 and T_C1 function and proliferate robustly in response to tumor *in vitro*, and mediate superior anti-tumor effects in tumor-bearing mice. Our data demonstrate that AhR inhibition during *ex vivo* T-cell culture is a promising strategy for the efficient generation of highly active cancer immunotherapy products.

Chapter 4

Concluding Remarks

The early clinical successes of chimeric antigen receptor T-cell therapy have sparked immense hope in the potential of this treatment platform to effectively and precisely kill any cancer that distinguishes itself from healthy tissue. However, basic challenges remain at this stage of development: manufacturing processes that rely on CD3/CD28 stimulation and IL-2 supplementation to produce CAR-T from often-suboptimal starting material can fail to generate T-cells sufficient in number or potency to effectively treat patients[184].

The paradigm of differentiation dictating T-cell activity has been well-established through studies documenting the efficacy of CAR-T expressing (or derived from subsets expressing) markers defining various stages of differentiation[29,30,36], and interventions that program T-cell qualities associated with less-differentiated cells have repeatedly been demonstrated to improve T-cell immunotherapy efficacy[38,40–43,45–47]. However, these interventions generally do not promote T-cell expansion *ex vivo*[184], working counter to the need to generate high doses of T-cells for effective adoptive transfer and demonstrating the need for additional innovation.

In much the same way that activation of other T_{MEM}-characteristic pathways can attenuate *ex vivo* T-cell differentiation during CAR production, we hypothesized that NOTCH signaling, which plays a key role in stem cell quiescence and self-renewal[92–106], might be able to limit differentiation and enhance CAR-T potency. However, NOTCH is also a well-described facilitator of CD8+ T_{EFF} differentiation[75–79], and plays a prominent role in the polarization of CD4+ T-cells toward specialized phenotypes that orchestrate pathogen-appropriate immune responses[81–91,144]. The divergent qualities of these T_H subsets strongly alter their performance as cancer immunotherapies[67–69], encouraging study of NOTCH-activated CAR-T through the lens of CD4+ polarization in order to understand any potential changes to CAR-T behavior.

In Chapter 2, we developed a cell-free culture system using readily GMP-adaptable reagents to activate NOTCH1 signaling during human CAR-T production. We found that N1 CD4+ CAR-T exhibited a less-differentiated phenotype and transcriptome at the end of culture, confirming that NOTCH activation in absence of other stromal cell or APC signals could limit T-cell differentiation. When we profiled N1 CD4+ CAR-T cytokine production, we found that NOTCH1 agonism augmented production of IFNγ, GzmB, IL-22 and IL-10, while suppressing

production of T_H2-characteristic cytokines. These cytokines did not fit any particular T_H subset-characteristic pattern, and N1 CD4+ CAR-T globally expressed lower levels of subset-characteristic chemokine markers, so we performed RNAseq to search for potential controllers of N1 CD4+ CAR-T function, and found transcriptional evidence of enhanced AhR and c-MAF activity. We examined the role of c-MAF using shRNAs and found that it drove IL-10, IL-4 and IL-17 production in N1 CD4+ CAR-T, but did not limit production of T_H1-associated cytokines as described in murine CD4+ T-cells[167,168]. Pharmacologic AhR inhibition, on the other hand, broadly disinhibited production of effector cytokines characteristic of many distinct T_H subsets while attenuating production of IL-22, IL-10 and GzmB. This unexpected result identified AhR as both a driver and a key autoregulator of cytokine production downstream of NOTCH, motivating the studies documented in Chapter 3.

We further found that NOTCH1 agonism enhanced CD4+ CAR-T proliferation upon subsequent CAR recognition of tumor, and that N1 CD4+ CAR-T expressed elevated levels of IL-2 signal transducers and genes associated with proliferation and growth following activation. Surprisingly, restimulation with titrated recombinant antigen revealed that N1 CD4+ CAR-T were also more sensitive to antigen, and that this effect was independent of CAR expression levels. The augmented proliferative response of N1 CD4+ CAR-T to tumor *in vitro* translated to expansion to markedly higher peak frequencies and strongly T_H1-skewed gene expression in tumor-bearing mice, and to enhanced helper function when co-transferred with control CD8+ CAR-T, enabling curative responses at low CAR-T doses. AhR and c-MAF inhibition during primary culture did not alter N1 CD4+ CAR-T proliferation upon restimulation *in vitro*, suggesting that these transcription factors did not program the enhanced proliferative and helper responses observed *in vivo*. NOTCH1 agonism was able to enhance CAR-T potency without compromising *ex vivo* expansion or transduction efficiency, increasing its appeal as for clinical translation to tumor-specific T-cell therapy production.

Thus, we confirmed that NOTCH signaling can be leveraged to restrict T-cell differentiation and improve CD4+ CAR-T anti-tumor efficacy, and demonstrated that this improvement is not the result of changes to polarity. We further identified c-MAF and AhR as important controllers of cytokine production downstream of NOTCH signaling, adding to the

described roles of master regulator transcription factors. Our results suggest that strong NOTCH signaling during CD4+ T-cell activation may induce c-MAF and AhR in order to drive IL-10 and limit effector cytokine production as autoregulatory measures to avoid excessive immune responses.

While we found that N1 CD4+ CAR-T displayed phenotypic and transcriptomic traits of T-cells described to proliferate robustly in response to tumor, we were unable to uncover a discrete mechanism by which NOTCH enhanced T-cell proliferation. Despite their improved expansion and helper activity *in vivo*, N1 CD4+ CAR-T did not produce more IL-2 than control CAR-T when restimulated, suggesting that other cell state changes determined their augmented proliferative capacity. Given the sensitivity that N1 CD4+ CAR-T exhibited to recombinant antigen over a short time scale, phosphoproteomic analysis of T-cell receptor signaling machinery may be better suited to interrogate cellular poise to respond to antigen.

While performing AhRi experiments with both N1 and control CD4+ CAR-T, we observed that AhR inhibition enhanced proliferation, maintained a minimally-differentiated phenotype and modified CD4+ CAR-T cytokine production by both types of cells, indicating that while NOTCH signaling enhanced AhR expression and activity, AhR was likely active during control CAR-T culture as well. We expanded our experiments and found that control CD8+ CAR-T growth was similarly improved by AhRi during culture, raising excitement that we might have stumbled upon a completely distinct strategy for enhancing production of T-cell therapies. AhR's known importance in T_{REG}, T_R1 and T_H17 development and function[118,119,122,125–130] again directed us toward study of AhRi's effects on CD4+ CAR-T polarization, and its emerging role as a metabolite-driven limiter of CD8+ T-cell function in the setting of malignancy [133–136,165,179–183] suggested that AhR was also likely to control CD8+ cytokine production during CAR-T culture.

In the dedicated AhRi experiments documented in Chapter 3, we found that CD3/CD28 activation rapidly and uniformly upregulates AhR expression in T-cells, and that AhR inhibition reduced expression of many genes associated with T_{EFF} differentiation. Intriguingly, AhRi strongly enhanced CD4+ and CD8+ T-cell proliferation, and we found that IL-2 production by T-cells was markedly increased. AhRi appeared to delay the kinetics of IL-2 signaling, however, likely contributing to the less-differentiated transcriptomic signature observed and enabling

maintenance of early T_{MEM} phenotypes at the end of culture. AhRi did not diminish levels of phosphorylated active AKT or P38 kinase, but did reduce active STAT3 and STAT5 levels, indicating that AhRi modulated IL-2 signaling and preserved phenotype during T-cell expansion in a manner distinct from other described cell conditioning strategies[41,42].

We further found that AhRi upregulated T-bet expression and drove T_H1 polarization of CD4+ T_N, and similarly enhanced T_C1 cytokine production by CAR-T derived from CD8+ T_N. AhRi CAR-T maintained elevated IL-2 secretion and proliferated robustly upon restimulation with tumor in absence of inhibitor, providing encouraging evidence that elevated IFNγ and TNFα were not signs of IL-2-driven T_{EFF} differentiation, which rapidly diminishes IL-2 production and proliferative capacities. These functional readouts are consistent with elevated expression of *Tbx21* without upregulation of many other T_H1-characteristic effector genes in AhRi CD4+ T-cells at day 3, and indicate that AhRi can prime T-cells for subsequent T_H1 function without driving overt differentiation during primary culture.

Despite exhibiting equivalent AhR and T-bet expression and increased proliferation during production, T_{MEM}-derived AhRi CAR-T did not display similar changes in cytokine production upon restimulation, suggesting that AhR may play a greater role in modulating less-differentiated T-cell cytokine production, or that AhRi expansion in the presence of supplemental IL-2 may begin to deliver too much function-limiting IL-2 signal to T_{MEM}-derived CAR-T. Given the capacity of AhRi to robustly expand bulk T-cells in absence of supplemental IL-2, further studies examining the function of CAR-T derived from more-differentiated T-cell subsets in the presence or absence of exogenous cytokine would offer helpful insight into how best to clinically translate AhRi usage.

To assess whether AhRi CAR-T maintained function long-term after extensive expansion *ex vivo*, we treated mice bearing lymphoma xenografts with T_N-derived CD4+ and CD8+ AhRi or control CAR-T. The individual activities of CD4+ and CD8+ AhRi CAR-T were not impressively enhanced compared to control cells, but critically demonstrated that AhRi-enhanced expansion *ex vivo* did not drive premature loss of T-cell function. In contrast, mice treated with combined AhRi CD4+ and CD8+ T-cells exhibited improved tumor control compared to control-treated animals, and mediated these effects in absence of strong changes in expansion *in vivo*. These

results indicate that AhRi durably enhances CAR-T function, and confirm that the robust IL-2-driven proliferation induced by AhRi during *ex vivo* culture does not compromise subsequent CAR-T performance. Our findings identified AhR as a valuable novel target for enhancing tumor-specific T-cell expansion and potency during culture, and invite further study into how AhRi might be combined with other culture interventions (including NOTCH1 agonism) to efficiently generate more effective immunotherapy products.

The work presented in this dissertation demonstrates that NOTCH and AhR transcriptional activity can be modulated to enhance production of highly active human CAR-T. Many challenges face the field of cancer immunotherapy and the CAR-T platform, including finding effective targets for specific tumor killing, forestalling T-cell exhaustion and overcoming immunosuppressive signals generated by tumors[2]. However, the ability to reliably manufacture healthy T-cells with potent anti-tumor activity is critical infrastructure that underpins all other adoptive therapy success, and every advance contributing to meeting this need builds toward better patient outcomes.

Bibliography

1. Wei J, Han X, Bo J, Han W. Target selection for CAR-T therapy. *J Hematol Oncol*. 2019;12(1):62.

2. Srivastava S, Riddell SR. Chimeric Antigen Receptor T Cell Therapy: Challenges to Bench-to-Bedside Efficacy. *J Immunol*. 2018;200(2):459–468.

3. Cornel AM, Mimpen IL, Nierkens S. MHC Class I Downregulation in Cancer: Underlying Mechanisms and Potential Targets for Cancer Immunotherapy. *Cancers*. 2020;12(7):1760.

4. Dhatchinamoorthy K, Colbert JD, Rock KL. Cancer Immune Evasion Through Loss of MHC Class I Antigen Presentation. *Front Immunol*. 2021;12:636568.

5. Driessens G, Kline J, Gajewski TF. Costimulatory and coinhibitory receptors in anti-tumor immunity. *Immunol Rev*. 2009;229(1):126–144.

6. Larson RC, Maus MV. Recent advances and discoveries in the mechanisms and functions of CAR T cells. *Nat Rev Cancer*. 2021;21(3):145–161.

7. Porter DL, Levine BL, Kalos M, Bagg A, June CH. Chimeric Antigen Receptor–Modified T Cells in Chronic Lymphoid Leukemia. *New Engl J Medicine*. 2011;365(8):725–733.

8. Brentjens RJ, Rivière I, Park JH, et al. Safety and persistence of adoptively transferred autologous CD19-targeted T cells in patients with relapsed or chemotherapy refractory B-cell leukemias. *Blood*. 2011;118(18):4817–4828.

9. Kalos M, Levine BL, Porter DL, et al. T Cells with Chimeric Antigen Receptors Have Potent Antitumor Effects and Can Establish Memory in Patients with Advanced Leukemia. *Sci Transl Med*. 2011;3(95):95ra73-95ra73.

10. Neelapu SS, Locke FL, Bartlett NL, et al. Axicabtagene Ciloleucel CAR T-Cell Therapy in Refractory Large B-Cell Lymphoma. *New Engl J Medicine*. 2017;377(26):2531–2544.

11. Schuster SJ, Svoboda J, Chong EA, et al. Chimeric Antigen Receptor T Cells in Refractory B-Cell Lymphomas. *New Engl J Medicine*. 2017;377(26):2545–2554.

12. Locke FL, Ghobadi A, Jacobson CA, et al. Long-term safety and activity of axicabtagene ciloleucel in refractory large B-cell lymphoma (ZUMA-1): a single-arm, multicentre, phase 1-2 trial. *Lancet Oncol*. 2018;20(1):31–42.

13. Maude SL, Laetsch TW, Buechner J, et al. Tisagenlecleucel in Children and Young Adults with B-Cell Lymphoblastic Leukemia. *New Engl J Medicine*. 2018;378(5):439–448.

14. Cohen AD, Garfall AL, Stadtmauer EA, et al. B cell maturation antigen-specific CAR T cells are clinically active in multiple myeloma. *J Clin Invest*. 2019;129(6):2210–2221.

15. Wang M, Munoz J, Goy A, et al. KTE-X19 CAR T-Cell Therapy in Relapsed or Refractory Mantle-Cell Lymphoma. *New Engl J Med*. 2020;382(14):1331–1342.

16. Turtle CJ, Hanafi L-A, Berger C, et al. CD19 CAR–T cells of defined CD4+:CD8+ composition in adult B cell ALL patients. *J Clin Invest*. 2016;126(6):2123–2138.

17. Turtle CJ, Hanafi L-A, Berger C, et al. Immunotherapy of non-Hodgkin's lymphoma with a defined ratio of CD8+ and CD4+ CD19-specific chimeric antigen receptor–modified T cells. *Sci Transl Med*. 2016;8(355):355ra116-355ra116.

18. Gardner RA, Finney O, Annesley C, et al. Intent-to-treat leukemia remission by CD19 CAR T cells of defined formulation and dose in children and young adults. *Blood*. 2017;129(25):3322–3331.

19. Grupp SA, Kalos M, Barrett D, et al. Chimeric Antigen Receptor–Modified T Cells for Acute Lymphoid Leukemia. *New Engl J Medicine*. 2013;368(16):1509–1518.

20. Kochenderfer JN, Dudley ME, Feldman SA, et al. B-cell depletion and remissions of malignancy along with cytokine-associated toxicity in a clinical trial of anti-CD19 chimeric-antigen-receptor–transduced T cells. *Blood*. 2012;119(12):2709–2720.

21. Maude SL, Frey N, Shaw PA, et al. Chimeric Antigen Receptor T Cells for Sustained Remissions in Leukemia. *New Engl J Medicine*. 2014;371(16):1507–1517.

22. Porter DL, Hwang W-T, Frey NV, et al. Chimeric antigen receptor T cells persist and induce sustained remissions in relapsed refractory chronic lymphocytic leukemia. *Sci Transl Med*. 2015;7(303):303ra139-303ra139.

23. Majzner RG, Mackall CL. Clinical lessons learned from the first leg of the CAR T cell journey. *Nat Med*. 2019;25(9):1341–1355.

24. Kaech SM, Wherry EJ. Heterogeneity and Cell-Fate Decisions in Effector and Memory CD8+ T Cell Differentiation during Viral Infection. *Immunity*. 2007;27(3):393–405.

25. Gerritsen B, Pandit A. The memory of a killer T cell: models of CD8+ T cell differentiation. *Immunol Cell Biol*. 2016;94(3):236–241.

26. Kaech SM, Wherry EJ, Ahmed R. Effector and memory T-cell differentiation: implications for vaccine development. *Nat Rev Immunol*. 2002;2(4):251–262.

27. Kumar BV, Connors TJ, Farber DL. Human T Cell Development, Localization, and Function throughout Life. *Immunity*. 2018;48(2):202–213.

28. Mahnke YD, Brodie TM, Sallusto F, Roederer M, Lugli E. The who's who of T-cell differentiation: Human memory T-cell subsets. *Eur J Immunol*. 2013;43(11):2797–2809.

29. Gattinoni L, Lugli E, Ji Y, et al. A human memory T cell subset with stem cell–like properties. *Nat Med*. 2011;17(10):1290.

30. Sommermeyer D, Hudecek M, Kosasih PL, et al. Chimeric antigen receptor-modified T cells derived from defined CD8+ and CD4+ subsets confer superior antitumor reactivity in vivo. *Leukemia*. 2016;30(2):492.

31. Paoli PD, Battistin S, Santini GF. Age-related changes in human lymphocyte subsets: Progressive reduction of the CD4 CD45R (suppressor inducer) population. *Clin Immunol Immunop*. 1988;48(3):290–296.

32. Utsuyama M, Hirokawa K, Kurashima C, et al. Differential age-change in the numbers of CD4+CD45RA+ DC4+CD29+ T cell subsets in human peripheral blood. *Mech Ageing Dev*. 1992;63(1):57–68.

33. Mackall CL, Fleisher TA, Brown MR, et al. Age, Thymopoiesis, and CD4+ T-Lymphocyte Regeneration after Intensive Chemotherapy. *New Engl J Medicine*. 1995;332(3):143–149.

34. Mackall CL, Fleisher TA, Brown MR, et al. Lymphocyte depletion during treatment with intensive chemotherapy for cancer. *Blood*. 1994;84(7):2221–8.

35. Fuks Z, Strober S, Bobrove AM, et al. Long term effects of radiation of T and B lymphocytes in peripheral blood of patients with Hodgkin's disease. *J Clin Invest*. 1976;58(4):803–814.

36. Gattinoni L, Klebanoff CA, Palmer DC, et al. Acquisition of full effector function in vitro paradoxically impairs the in vivo antitumor efficacy of adoptively transferred CD8+ T cells. *J Clin Invest*. 2005;115(6):1616–1626.

37. Kim EH, Suresh M. Role of PI3K/Akt signaling in memory CD8 T cell differentiation. *Front Immunol*. 2013;4:20.

38. Bowers JS, Majchrzak K, Nelson MH, et al. PI3Kδ Inhibition Enhances the Antitumor Fitness of Adoptively Transferred CD8+ T Cells. *Front Immunol*. 2017;8:1221.

39. Majchrzak K, Nelson MH, Bowers JS, et al. β-catenin and PI3Kδ inhibition expands precursor Th17 cells with heightened stemness and antitumor activity. *Jci Insight*. 2017;2(8):e90547.

40. Waart AB van der, Weem NMP van de, Maas F, et al. Inhibition of Akt signaling promotes the generation of superior tumor-reactive T cells for adoptive immunotherapy. *Blood*. 2014;124(23):3490–3500.

41. Klebanoff CA, Crompton JG, Leonardi AJ, et al. Inhibition of AKT signaling uncouples T cell differentiation from expansion for receptor-engineered adoptive immunotherapy. *Jci Insight*. 2017;2(23):e95103.

42. Gurusamy D, Henning AN, Yamamoto TN, et al. Multi-phenotype CRISPR-Cas9 Screen Identifies p38 Kinase as a Target for Adoptive Immunotherapies. *Cancer Cell*. 2020;37(6):818-833.e9.

43. Gattinoni L, Zhong X-S, Palmer DC, et al. Wnt signaling arrests effector T cell differentiation and generates CD8+ memory stem cells. *Nat Med*. 2009;15(7):nm.1982.

44. Chapman NM, Boothby MR, Chi H. Metabolic coordination of T cell quiescence and activation. *Nat Rev Immunol*. 2020;20(1):55–70.

45. Sukumar M, Liu J, Ji Y, et al. Inhibiting glycolytic metabolism enhances CD8+ T cell memory and antitumor function. *J Clin Invest*. 2013;123(10):4479–4488.

46. Buck MD, O'Sullivan D, Klein Geltink RI, et al. Mitochondrial Dynamics Controls T Cell Fate through Metabolic Programming. *Cell*. 2016;166(1):63–76.

47. Vodnala SK, Eil R, Kishton RJ, et al. T cell stemness and dysfunction in tumors are triggered by a common mechanism. *Science*. 2019;363(6434):eaau0135.

48. Klebanoff CA, Gattinoni L, Palmer DC, et al. Determinants of Successful CD8+ T-Cell Adoptive Immunotherapy for Large Established Tumors in Mice. *Clin Cancer Res*. 2011;17(16):5343–5352.

49. Besser MJ, Shapira-Frommer R, Itzhaki O, et al. Adoptive Transfer of Tumor-Infiltrating Lymphocytes in Patients with Metastatic Melanoma: Intent-to-Treat Analysis and Efficacy after Failure to Prior Immunotherapies. *Clin Cancer Res*. 2013;19(17):4792–4800.

50. Goff SL, Dudley ME, Citrin DE, et al. Randomized, Prospective Evaluation Comparing Intensity of Lymphodepletion Before Adoptive Transfer of Tumor-Infiltrating Lymphocytes for Patients With Metastatic Melanoma. *J Clin Oncol*. 2016;34(20):2389–2397.

51. Schwartz RH. T CELL ANERGY*. *Immunology*. 2003;21(1):305–334.

52. Curtsinger JM, Mescher MF. Inflammatory cytokines as a third signal for T cell activation. *Curr Opin Immunol*. 2010;22(3):333–340.

53. Kalia V, Sarkar S. Regulation of Effector and Memory CD8 T Cell Differentiation by IL-2—A Balancing Act. *Front Immunol*. 2018;9:2987.

54. Besser MJ, Schallmach E, Oved K, et al. Modifying interleukin-2 concentrations during culture improves function of T cells for adoptive immunotherapy. *Cytotherapy*. 2009;11(2):206–217.

55. Manjunath N, Shankar P, Wan J, et al. Effector differentiation is not prerequisite for generation of memory cytotoxic T lymphocytes. *J Clin Invest*. 2001;108(6):871–878.

56. van der Windt GJW, Everts B, Chang C-H, et al. Mitochondrial Respiratory Capacity Is a Critical Regulator of CD8+ T Cell Memory Development. *Immunity*. 2012;36(1):68–78.

57. Hinrichs CS, Spolski R, Paulos CM, et al. IL-2 and IL-21 confer opposing differentiation programs to CD8+ T cells for adoptive immunotherapy. *Blood*. 2008;111(11):5326–5333.

58. Hoffmann J-M, Schubert M-L, Wang L, et al. Differences in Expansion Potential of Naive Chimeric Antigen Receptor T Cells from Healthy Donors and Untreated Chronic Lymphocytic Leukemia Patients. *Front Immunol*. 2018;8:1956.

59. Alizadeh D, Wong RA, Yang X, et al. IL-15-mediated reduction of mTORC1 activity preserves the stem cell memory phenotype of CAR-T cells and confers superior antitumor activity. *Cancer Immunol Res*. 2019;7(5):canimm.0466.2018.

60. Singh H, Figliola MJ, Dawson MJ, et al. Reprogramming CD19-Specific T Cells with IL-21 Signaling Can Improve Adoptive Immunotherapy of B-Lineage Malignancies. *Cancer Res*. 2011;71(10):3516–3527.

61. Chen Y, Yu F, Jiang Y, et al. Adoptive Transfer of Interleukin-21-stimulated Human CD8+ T Memory Stem Cells Efficiently Inhibits Tumor Growth. *J Immunother*. 2018;41(6):274–283.

62. Luckheeram RV, Zhou R, Verma AD, Xia B. CD4+T Cells: Differentiation and Functions. *Clin Dev Immunol*. 2012;2012:925135.

63. Zhu J, Yamane H, Paul WE. Differentiation of Effector CD4 T Cell Populations*. *Annu Rev Immunol*. 2010;28(1):445–489.

64. Jiang T, Shi T, Zhang H, et al. Tumor neoantigens: from basic research to clinical applications. *J Hematol Oncol*. 2019;12(1):93.

65. Nishimura T, Iwakabe K, Sekimoto M, et al. Distinct Role of Antigen-Specific T Helper Type 1 (Th1) and Th2 Cells in Tumor Eradication in Vivo. *J Exp Medicine*. 1999;190(5):617–628.

66. Bowers JS, Nelson MH, Majchrzak K, et al. Th17 cells are refractory to senescence and retain robust antitumor activity after long-term ex vivo expansion. *Jci Insight*. 2017;2(5):e90772.

67. Muranski P, Boni A, Antony PA, et al. Tumor-specific Th17-polarized cells eradicate large established melanoma. *Blood*. 2008;112(2):362–373.

68. Martin-Orozco N, Muranski P, Chung Y, et al. T Helper 17 Cells Promote Cytotoxic T Cell Activation in Tumor Immunity. *Immunity*. 2009;31(5):787–798.

69. Lu Y, Wang Q, Xue G, et al. Th9 Cells Represent a Unique Subset of CD4+ T Cells Endowed with the Ability to Eradicate Advanced Tumors. *Cancer Cell*. 2018;33(6):1048-1060.e7.

70. Kopan R, Ilagan MaXG. The Canonical Notch Signaling Pathway: Unfolding the Activation Mechanism. *Cell*. 2009;137(2):216–233.

71. Radtke F, Wilson A, Mancini SJC, MacDonald HR. Notch regulation of lymphocyte development and function. *Nat Immunol*. 2004;5(3):247–253.

72. Radtke F, Wilson A, Stark G, et al. Deficient T Cell Fate Specification in Mice with an Induced Inactivation of Notch1. *Immunity*. 1999;10(5):547–558.

73. Sambandam A, Maillard I, Zediak VP, et al. Notch signaling controls the generation and differentiation of early T lineage progenitors. *Nat Immunol*. 2005;6(7):663–670.

74. Koyanagi A, Sekine C, Yagita H. Expression of Notch receptors and ligands on immature and mature T cells. *Biochem Bioph Res Co*. 2012;418(4):799–805.

75. Backer RA, Helbig C, Gentek R, et al. A central role for Notch in effector CD8+ T cell differentiation. *Nat Immunol*. 2014;15(12):1143–1151.

76. Maekawa Y, Minato Y, Ishifune C, et al. Notch2 integrates signaling by the transcription factors RBP-J and CREB1 to promote T cell cytotoxicity. *Nat Immunol*. 2008;9(10):1140–1147.

77. Cho OH, Shin HM, Miele L, et al. Notch Regulates Cytolytic Effector Function in CD8+ T Cells. *J Immunol*. 2009;182(6):3380–3389.

78. Kuijk LM, Verstege MI, Rekers NV, et al. Notch controls generation and function of human effector CD8+ T cells. *Blood*. 2013;121(14):2638–2646.

79. Mathieu M, Duval F, Daudelin J-F, Labrecque N. The Notch Signaling Pathway Controls Short-Lived Effector CD8+ T Cell Differentiation but Is Dispensable for Memory Generation. *J Immunol*. 2015;194(12):5654–5662.

80. Maekawa Y, Ishifune C, Tsukumo S, et al. Notch controls the survival of memory CD4+ T cells by regulating glucose uptake. *Nat Med*. 2014;21(1):55–61.

81. Auderset F, Schuster S, Coutaz M, et al. Redundant Notch1 and Notch2 Signaling Is Necessary for IFNγ Secretion by T Helper 1 Cells During Infection with Leishmania major. *Plos Pathog*. 2012;8(3):e1002560.

82. Maekawa Y, Tsukumo S, Chiba S, et al. Delta1-Notch3 Interactions Bias the Functional Differentiation of Activated CD4+ T Cells. *Immunity*. 2003;19(4):549–559.

83. Tran IT, Sandy AR, Carulli AJ, et al. Blockade of individual Notch ligands and receptors controls graft-versus-host disease. *J Clin Invest*. 2013;123(4):1590–1604.

84. Zhang Y, Sandy AR, Wang J, et al. Notch signaling is a critical regulator of allogeneic CD4+ T-cell responses mediating graft-versus-host disease. *Blood*. 2011;117(1):299–308.

85. Roderick JE, Gonzalez-Perez G, Kuksin CA, et al. Therapeutic targeting of NOTCH signaling ameliorates immune-mediated bone marrow failure of aplastic anemia. *J Exp Medicine*. 2013;210(7):1311–1329.

86. Kang JH, Kim BS, Uhm TG, et al. γ-Secretase Inhibitor Reduces Allergic Pulmonary Inflammation by Modulating Th1 and Th2 Responses. *Am J Resp Crit Care*. 2009;179(10):875–882.

87. Tu L, Fang TC, Artis D, et al. Notch signaling is an important regulator of type 2 immunity. *J Exp Medicine*. 2005;202(8):1037–1042.

88. Keerthivasan S, Suleiman R, Lawlor R, et al. Notch Signaling Regulates Mouse and Human Th17 Differentiation. *J Immunol*. 2011;187(2):692–701.

89. Bassil R, Zhu B, Lahoud Y, et al. Notch Ligand Delta-Like 4 Blockade Alleviates Experimental Autoimmune Encephalomyelitis by Promoting Regulatory T Cell Development. *J Immunol*. 2011;187(5):2322–2328.

90. Jiao Z, Wang W, Hua S, et al. Blockade of Notch Signaling Ameliorates Murine Collagen-Induced Arthritis via Suppressing Th1 and Th17 Cell Responses. *Am J Pathology*. 2014;184(4):1085–1093.

91. Bailis W, Yashiro-Ohtani Y, Fang TC, et al. Notch Simultaneously Orchestrates Multiple Helper T Cell Programs Independently of Cytokine Signals. *Immunity*. 2013;39(1):148–159.

92. Pan Y, Lin M-H, Tian X, et al. γ-Secretase Functions through Notch Signaling to Maintain Skin Appendages but Is Not Required for Their Patterning or Initial Morphogenesis. *Dev Cell*. 2004;7(5):731–743.

93. Vauclair S, Nicolas M, Barrandon Y, Radtke F. Notch1 is essential for postnatal hair follicle development and homeostasis. *Dev Biol*. 2005;284(1):184–193.

94. Yamamoto N, Tanigaki K, Han H, Hiai H, Honjo T. Notch/RBP-J Signaling Regulates Epidermis/Hair Fate Determination of Hair Follicular Stem Cells. *Curr Biol*. 2003;13(4):333–338.

95. Calvi LM, Adams GB, Weibrecht KW, et al. Osteoblastic cells regulate the haematopoietic stem cell niche. *Nature*. 2003;425(6960):841–846.

96. Arai F, Hirao A, Ohmura M, et al. Tie2/Angiopoietin-1 Signaling Regulates Hematopoietic Stem Cell Quiescence in the Bone Marrow Niche. *Cell*. 2004;118(2):149–161.

97. Kiel MJ, Yilmaz ÖH, Iwashita T, et al. SLAM Family Receptors Distinguish Hematopoietic Stem and Progenitor Cells and Reveal Endothelial Niches for Stem Cells. *Cell*. 2005;121(7):1109–1121.

98. Duncan AW, Rattis FM, DiMascio LN, et al. Integration of Notch and Wnt signaling in hematopoietic stem cell maintenance. *Nat Immunol*. 2005;6(3):314–322.

99. Zhang J, Niu C, Ye L, et al. Identification of the haematopoietic stem cell niche and control of the niche size. *Nature*. 2003;425(6960):836–841.

100. Searfoss GH, Jordan WH, Calligaro DO, et al. Adipsin, a Biomarker of Gastrointestinal Toxicity Mediated by a Functional γ-Secretase Inhibitor*. *J Biol Chem*. 2003;278(46):46107–46116.

101. Wong GT, Manfra D, Poulet FM, et al. Chronic Treatment with the γ-Secretase Inhibitor LY-411,575 Inhibits β-Amyloid Peptide Production and Alters Lymphopoiesis and Intestinal Cell Differentiation*. *J Biol Chem*. 2004;279(13):12876–12882.

102. Milano J, McKay J, Dagenais C, et al. Modulation of Notch Processing by γ-Secretase Inhibitors Causes Intestinal Goblet Cell Metaplasia and Induction of Genes Known to Specify Gut Secretory Lineage Differentiation. *Toxicol Sci*. 2004;82(1):341–358.

103. Es JH van, Gijn ME van, Riccio O, et al. Notch/γ-secretase inhibition turns proliferative cells in intestinal crypts and adenomas into goblet cells. *Nature*. 2005;435(7044):959–963.

104. Chapouton P, Skupien P, Hesl B, et al. Notch Activity Levels Control the Balance between Quiescence and Recruitment of Adult Neural Stem Cells. *J Neurosci*. 2010;30(23):7961–7974.

105. Ehm O, Goritz C, Covic M, et al. RBPJ -Dependent Signaling Is Essential for Long-Term Maintenance of Neural Stem Cells in the Adult Hippocampus. *J Neurosci*. 2010;30(41):13794–13807.

106. Imayoshi I, Sakamoto M, Yamaguchi M, Mori K, Kageyama R. Essential Roles of Notch Signaling in Maintenance of Neural Stem Cells in Developing and Adult Brains. *J Neurosci*. 2010;30(9):3489–3498.

107. Kondo T, Morita R, Okuzono Y, et al. Notch-mediated conversion of activated T cells into stem cell memory-like T cells for adoptive immunotherapy. *Nat Commun*. 2017;8(1):ncomms15338.

108. Kondo T, Ando M, Nagai N, et al. The NOTCH-FOXM1 Axis Plays a Key Role in Mitochondrial Biogenesis in the Induction of Human Stem Cell Memory-like CAR-T Cells. *Cancer Res*. 2019;canres.1196.2019.

109. Ikuta T, Tachibana T, Watanabe J, et al. Nucleocytoplasmic Shuttling of the Aryl Hydrocarbon Receptor. *J Biochem*. 2000;127(3):503–509.

110. Yao EF, Denison MS. DNA sequence determinants for binding of transformed Ah receptor to a dioxin-responsive enhancer. *Biochemistry-us*. 1992;31(21):5060–5067.

111. Swanson HI, Tullis K, Denison MS. Binding of transformed Ah receptor complex to a dioxin responsive transcriptional enhancer: Evidence for two distinct heteromeric DNA-binding forms. *Biochemistry-us*. 1993;32(47):12841–12849.

112. Ohtake F, Takeyama K, Matsumoto T, et al. Modulation of oestrogen receptor signalling by association with the activated dioxin receptor. *Nature*. 2003;423(6939):545–550.

113. Hankinson O. Role of coactivators in transcriptional activation by the aryl hydrocarbon receptor. *Arch Biochem Biophys*. 2005;433(2):379–386.

114. Yeste A, Mascanfroni ID, Nadeau M, et al. IL-21 induces IL-22 production in CD4+ T cells. *Nat Commun*. 2014;5(1):3753.

115. McBerry C, Gonzalez RMS, Shryock N, Dias A, Aliberti J. SOCS2-Induced Proteasome-Dependent TRAF6 Degradation: A Common Anti-Inflammatory Pathway for Control of Innate Immune Responses. *Plos One*. 2012;7(6):e38384.

116. Wilson SR, Joshi AD, Elferink CJ. The Tumor Suppressor Kruppel-Like Factor 6 Is a Novel Aryl Hydrocarbon Receptor DNA Binding Partner. *J Pharmacol Exp Ther*. 2013;345(3):419–429.

117. Poland A, Glover E, Kende AS. Stereospecific, high affinity binding of 2,3,7,8-tetrachlorodibenzo-p-dioxin by hepatic cytosol. Evidence that the binding species is receptor for induction of aryl hydrocarbon hydroxylase. *J Biol Chem*. 1976;251(16):4936–4946.

118. Mascanfroni ID, Takenaka MC, Yeste A, et al. Metabolic control of type 1 regulatory T cell differentiation by AHR and HIF1-α. *Nat Med*. 2015;21(6):638–46.

119. Apetoh L, Quintana FJ, Pot C, et al. The aryl hydrocarbon receptor interacts with c-Maf to promote the differentiation of type 1 regulatory T cells induced by IL-27. *Nat Immunol*. 2010;11(9):854–61.

120. Mezrich JD, Fechner JH, Zhang X, et al. An Interaction between Kynurenine and the Aryl Hydrocarbon Receptor Can Generate Regulatory T Cells. *J Immunol*. 2010;185(6):3190–3198.

121. Kerkvliet NI, Steppan LB, Vorachek W, et al. Activation of aryl hydrocarbon receptor by TCDD prevents diabetes in NOD mice and increases Foxp3+ T cells in pancreatic lymph nodes. *Immunotherapy*. 2009;1(4):539–547.

122. Hauben E, Gregori S, Draghici E, et al. Activation of the aryl hydrocarbon receptor promotes allograft-specific tolerance through direct and dendritic cell–mediated effects on regulatory T cells. *Blood*. 2008;112(4):1214–1222.

123. Lawrence BP, Denison MS, Novak H, et al. Activation of the aryl hydrocarbon receptor is essential for mediating the anti-inflammatory effects of a novel low-molecular-weight compound. *Blood*. 2008;112(4):1158–1165.

124. Holsapple MP, Morris DL, Wood SC, Snyder NK. 2,3,7,8-Tetrachlorodibenzo-p-Dioxin-Induced Changes in Immunocompetence: Possible Mechanisms. *Annu Rev Pharmacol*. 1991;31(1):73–100.

125. Gandhi R, Kumar D, Burns EJ, et al. Activation of the aryl hydrocarbon receptor induces human type 1 regulatory T cell–like and Foxp3+ regulatory T cells. *Nat Immunol*. 2010;11(9):846–853.

126. Quintana FJ, Basso AS, Iglesias AH, et al. Control of Treg and TH17 cell differentiation by the aryl hydrocarbon receptor. *Nature*. 2008;453(7191):65–71.

127. Veldhoen M, Hirota K, Christensen J, O'Garra A, Stockinger B. Natural agonists for aryl hydrocarbon receptor in culture medium are essential for optimal differentiation of Th17 T cells. *J Exp Medicine*. 2009;206(1):43–49.

128. Kimura A, Naka T, Nohara K, Fujii-Kuriyama Y, Kishimoto T. Aryl hydrocarbon receptor regulates Stat1 activation and participates in the development of Th17 cells. *Proc National Acad Sci*. 2008;105(28):9721–9726.

129. Quintana FJ, Jin H, Burns EJ, et al. Aiolos promotes TH17 differentiation by directly silencing Il2 expression. *Nat Immunol*. 2012;13(8):770–777.

130. Veldhoen M, Hirota K, Westendorf AM, et al. The aryl hydrocarbon receptor links TH17-cell-mediated autoimmunity to environmental toxins. *Nature*. 2008;453(7191):106–109.

131. Wei P, Hu G, Kang H, et al. An aryl hydrocarbon receptor ligand acts on dendritic cells and T cells to suppress the Th17 response in allergic rhinitis patients. *Lab Invest*. 2014;94(5):528–535.

132. Rothhammer V, Quintana FJ. The aryl hydrocarbon receptor: an environmental sensor integrating immune responses in health and disease. *Nat Rev Immunol*. 2019;19(3):1.

133. Campesato LF, Budhu S, Tchaicha J, et al. Blockade of the AHR restricts a Treg-macrophage suppressive axis induced by L-Kynurenine. *Nat Commun*. 2020;11(1):4011.

134. Mellor AL, Keskin DB, Johnson T, Chandler P, Munn DH. Cells Expressing Indoleamine 2,3-Dioxygenase Inhibit T Cell Responses. *J Immunol*. 2002;168(8):3771–3776.

135. Munn DH, Shafizadeh E, Attwood JT, et al. Inhibition of T Cell Proliferation by Macrophage Tryptophan Catabolism. *J Exp Medicine*. 1999;189(9):1363–1372.

136. Liu Y, Zhou N, Zhou L, et al. IL-2 regulates tumor-reactive CD8+ T cell exhaustion by activating the aryl hydrocarbon receptor. *Nat Immunol*. 2021;22(3):358–369.

137. Koch U, Lehal R, Radtke F. Stem cells living with a Notch. *Development*. 2013;140(4):689–704.

138. Chiba S. Concise Review: Notch Signaling in Stem Cell Systems. *Stem Cells*. 2006;24(11):2437–2447.

139. Mochizuki K, He S, Zhang Y. Notch and inflammatory T-cell response: new developments and challenges. *Immunotherapy*. 2011;3(11):1353–1366.

140. Minter LM, Turley DM, Das P, et al. Inhibitors of γ-secretase block in vivo and in vitro T helper type 1 polarization by preventing Notch upregulation of Tbx21. *Nat Immunol*. 2005;6(7):680–688.

141. Amsen D, Antov A, Jankovic D, et al. Direct Regulation of Gata3 Expression Determines the T Helper Differentiation Potential of Notch. *Immunity*. 2007;27(1):89–99.

142. Fang TC, Yashiro-Ohtani Y, Bianco CD, et al. Notch Directly Regulates Gata3 Expression during T Helper 2 Cell Differentiation. *Immunity*. 2007;27(1):100–110.

143. Mukherjee S, Schaller MA, Neupane R, Kunkel SL, Lukacs NW. Regulation of T Cell Activation by Notch Ligand, DLL4, Promotes IL-17 Production and Rorc Activation. *J Immunol*. 2009;182(12):7381–7388.

144. Auderset F, Schuster S, Fasnacht N, et al. Notch Signaling Regulates Follicular Helper T Cell Differentiation. *J Immunol*. 2013;191(5):2344–2350.

145. Amsen D, Blander JM, Lee GR, et al. Instruction of Distinct CD4 T Helper Cell Fates by Different Notch Ligands on Antigen-Presenting Cells. *Cell*. 2004;117(4):515–526.

146. Sun J, Krawczyk CJ, Pearce EJ. Suppression of Th2 Cell Development by Notch Ligands Delta1 and Delta4. *J Immunol*. 2008;180(3):1655–1661.

147. Park JH, Geyer MB, Brentjens RJ. CD19-targeted CAR T-cell therapeutics for hematologic malignancies: interpreting clinical outcomes to date. *Blood*. 2016;127(26):3312–3320.

148. Boulch M, Cazaux M, Loe-Mie Y, et al. A cross-talk between CAR T cell subsets and the tumor microenvironment is essential for sustained cytotoxic activity. *Sci Immunol*. 2021;6(57):eabd4344.

149. Purwar R, Schlapbach C, Xiao S, et al. Robust tumor immunity to melanoma mediated by interleukin-9–producing T cells. *Nat Med*. 2012;18(8):1248–1253.

150. Amsen D, Helbig C, Backer RA. Notch in T Cell Differentiation: All Things Considered. *Trends Immunol*. 2015;36(12):802–814.

151. Salter AI, Ivey RG, Kennedy JJ, et al. Phosphoproteomic analysis of chimeric antigen receptor signaling reveals kinetic and quantitative differences that affect cell function. *Sci Signal*. 2018;11(544):eaat6753.

152. Pont MJ, Hill T, Cole GO, et al. γ-Secretase inhibition increases efficacy of BCMA-specific chimeric antigen receptor T cells in multiple myeloma. *Blood*. 2019;134(19):1585–1597.

153. Hudecek M, Lupo-Stanghellini M-T, Kosasih PL, et al. Receptor Affinity and Extracellular Domain Modifications Affect Tumor Recognition by ROR1-Specific Chimeric Antigen Receptor T Cells. *Clin Cancer Res*. 2013;19(12):3153–3164.

154. Pelossof R, Fairchild L, Huang C-H, et al. Prediction of ultra-potent shRNAs with a sequential classification algorithm. *Nat Biotechnol*. 2017;35(4):350–353.

155. Dobin A, Davis CA, Schlesinger F, et al. STAR: ultrafast universal RNA-seq aligner. *Bioinformatics*. 2012;29(1):15–21.

156. Love MI, Huber W, Anders S. Moderated estimation of fold change and dispersion for RNA-seq data with DESeq2. *Genome Biol*. 2014;15(12):550.

157. Subramanian A, Tamayo P, Mootha VK, et al. Gene set enrichment analysis: A knowledge-based approach for interpreting genome-wide expression profiles. *P Natl Acad Sci Usa*. 2005;102(43):15545–15550.

158. Varnum-Finney B, Wu L, Yu M, et al. Immobilization of Notch ligand, Delta-1, is required for induction of notch signaling. *J Cell Sci*. 2000;113 Pt 23:4313–8.

159. Delaney C, Varnum-Finney B, Aoyama K, Brashem-Stein C, Bernstein ID. Dose-dependent effects of the Notch ligand Delta1 on ex vivo differentiation and in vivo marrow repopulating ability of cord blood cells. *Blood*. 2005;106(8):2693–2699.

160. Brodie T, Brenna E, Sallusto F. OMIP-018: Chemokine receptor expression on human T helper cells. *Cytom Part A*. 2013;83A(6):530–532.

161. Takeshita M, Suzuki K, Kassai Y, et al. Polarization diversity of human CD4+ stem cell memory T cells. *Clin Immunol*. 2015;159(1):107–117.

162. Radens CM, Blake D, Jewell P, Barash Y, Lynch KW. Meta-analysis of transcriptomic variation in T-cell populations reveals both variable and consistent signatures of gene expression and splicing. *Rna*. 2020;26(10):1320–1333.

163. Alam MS, Maekawa Y, Kitamura A, et al. Notch signaling drives IL-22 secretion in CD4+ T cells by stimulating the aryl hydrocarbon receptor. *Proc National Acad Sci*. 2010;107(13):5943–5948.

164. Josefowicz SZ. Regulators of chromatin state and transcription in CD4 T-cell polarization. *Immunology*. 2013;139(3):299–308.

165. Sadik A, Patterson LFS, Öztürk S, et al. IL4I1 Is a Metabolic Immune Checkpoint that Activates the AHR and Promotes Tumor Progression. *Cell*. 2020;182(5):1252-1270.e34.

166. Aschenbrenner D, Foglierini M, Jarrossay D, et al. An immunoregulatory and tissue-residency program modulated by c-MAF in human TH17 cells. *Nat Immunol*. 2018;19(10):1126–1136.

167. Gabryšová L, Alvarez-Martinez M, Luisier R, et al. c-Maf controls immune responses by regulating disease-specific gene networks and repressing IL-2 in CD4+ T cells. *Nat Immunol*. 2018;19(5):497–507.

168. Imbratta C, Hussein H, Andris F, Verdeil G. c-MAF, a Swiss Army Knife for Tolerance in Lymphocytes. *Front Immunol*. 2020;11:206.

169. Spolski R, Li P, Leonard WJ. Biology and regulation of IL-2: from molecular mechanisms to human therapy. *Nat Rev Immunol*. 2018;18(10):648–659.

170. Liberzon A, Birger C, Thorvaldsdóttir H, et al. The Molecular Signatures Database Hallmark Gene Set Collection. *Cell Syst*. 2015;1(6):417–425.

171. Alspach E, Lussier DM, Miceli AP, et al. MHC-II neoantigens shape tumour immunity and response to immunotherapy. *Nature*. 2019;574(7780):696–701.

172. Tran E, Turcotte S, Gros A, et al. Cancer Immunotherapy Based on Mutation-Specific CD4+ T Cells in a Patient with Epithelial Cancer. *Science*. 2014;344(6184):641–645.

173. Hunder NN, Wallen H, Cao J, et al. Treatment of Metastatic Melanoma with Autologous CD4+ T Cells against NY-ESO-1. *New Engl J Medicine*. 2008;358(25):2698–2703.

174. Groux H, O'Garra A, Bigler M, et al. A CD4+T-cell subset inhibits antigen-specific T-cell responses and prevents colitis. *Nature*. 1997;389(6652):737–742.

175. Gagliani N, Magnani CF, Huber S, et al. Coexpression of CD49b and LAG-3 identifies human and mouse T regulatory type 1 cells. *Nat Med*. 2013;19(6):739–746.

176. Roncarolo MG, Gregori S, Bacchetta R, Battaglia M, Gagliani N. The Biology of T Regulatory Type 1 Cells and Their Therapeutic Application in Immune-Mediated Diseases. *Immunity*. 2018;49(6):1004–1019.

177. Trifari S, Kaplan CD, Tran EH, Crellin NK, Spits H. Identification of a human helper T cell population that has abundant production of interleukin 22 and is distinct from TH-17, TH1 and TH2 cells. *Nat Immunol*. 2009;10(8):ni.1770.

178. McAleer JP, Fan J, Roar B, Primerano DA, Denvir J. Cytokine Regulation in Human CD4 T Cells by the Aryl Hydrocarbon Receptor and Gq-Coupled Receptors. *Sci Rep-uk*. 2018;8(1):10954.

179. Opitz CA, Litzenburger UM, Sahm F, et al. An endogenous tumour-promoting ligand of the human aryl hydrocarbon receptor. *Nature*. 2011;478(7368):197–203.

180. Holmgaard RB, Zamarin D, Munn DH, Wolchok JD, Allison JP. Indoleamine 2,3-dioxygenase is a critical resistance mechanism in antitumor T cell immunotherapy targeting CTLA-4. *J Exp Medicine*. 2013;210(7):1389–1402.

181. Wirth LJ, Burtness B, Mehra R, et al. IDO1 as a mechanism of adaptive immune resistance to anti-PD1 monotherapy in HNSCC. *J Clin Oncol*. 2017;35(15_suppl):6053–6053.

182. Munn DH, Sharma MD, Baban B, et al. GCN2 Kinase in T Cells Mediates Proliferative Arrest and Anergy Induction in Response to Indoleamine 2,3-Dioxygenase. *Immunity*. 2005;22(5):633–642.

183. Liu Y, Liang X, Dong W, et al. Tumor-Repopulating Cells Induce PD-1 Expression in CD8+ T Cells by Transferring Kynurenine and AhR Activation. *Cancer Cell*. 2018;33(3):480-494.e7.

184. Crompton JG, Sukumar M, Restifo NP. Uncoupling T-cell expansion from effector differentiation in cell-based immunotherapy. *Immunol Rev*. 2014;257(1):264–276.

185. Cieri N, Camisa B, Cocchiarella F, et al. IL-7 and IL-15 instruct the generation of human memory stem T cells from naive precursors. *Blood*. 2013;121(4):573–584.

186. Xu Y, Zhang M, Ramos CA, et al. Closely related T-memory stem cells correlate with in vivo expansion of CAR.CD19-T cells and are preserved by IL-7 and IL-15. *Blood*. 2014;123(24):3750–3759.

187. Hezaveh K, Shinde RS, Klötgen A, et al. Tryptophan-derived microbial metabolites activate the aryl hydrocarbon receptor in tumor-associated macrophages to suppress anti-tumor immunity. *Immunity*. 2022;55(2):324-340.e8.

188. Sukumar M, Cheng K, Gangaplara A, et al. Abstract 1527: Integrated computational and experimental analysis identifies the mitochondrial uncoupling protein 2 (Ucp2) as a key regulator of T cell anti-tumor function. *Immunology*. 2021;1527–1527.

189. Krishna S, Lowery FJ, Copeland AR, et al. Stem-like CD8 T cells mediate response of adoptive cell immunotherapy against human cancer. *Science*. 2020;370(6522):1328–1334.

190. Mo F, Yu Z, Li P, et al. An engineered IL-2 partial agonist promotes CD8+ T cell stemness. *Nature*. 2021;597(7877):544–548.

191. Liao W, Lin J-X, Wang L, Li P, Leonard WJ. Modulation of cytokine receptors by IL-2 broadly regulates differentiation into helper T cell lineages. *Nat Immunol*. 2011;12(6):551–559.

192. Afkarian M, Sedy JR, Yang J, et al. T-bet is a STAT1-induced regulator of IL-12R expression in naïve CD4+ T cells. *Nat Immunol*. 2002;3(6):549–557.

193. Yamada T, Horimoto H, Kameyama T, et al. Constitutive aryl hydrocarbon receptor signaling constrains type I interferon–mediated antiviral innate defense. *Nat Immunol*. 2016;17(6):687–694.